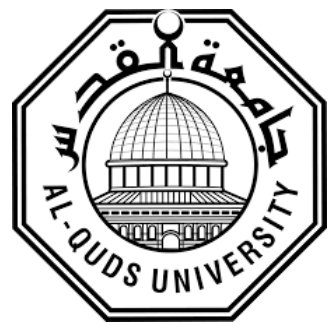


**Deanship of Graduate Studies  
AL-Quds University**



**Biological Samples Studies Using Broad Band Infrared  
Source**

**Aya Ali Ibrahim Thweib**

**M.Sc. Thesis**

**Jerusalem-Palestine**

**1439/2017**

# **Biological Samples Studies Using Broad Band Infrared Source**

**Prepared by:**  
**Aya Ali Ibrahim Thweib**

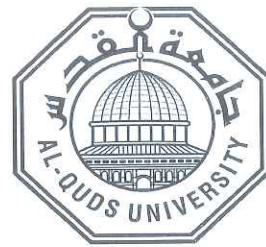
**B.Sc. Physics, Al-Quds University, Palestine.**

**Supervisor: Dr. Rushdi Ketaneh**

**Co-Supervisor: Prof. Mohammad Abu Taha**

**"A thesis submitted in partial fulfillment of the requirements  
for the degree of Master of Science in Physics at Faculty of  
Science and Technology, AL-Quds University."**

**Al-Quds University**  
**Deanship of Graduate Studies**  
**Department of Physics**



### **Thesis Approval**

#### **Biological Samples Studies Using Broad Band Infrared Source**

Prepared By: Aya Ali Ibrahim Thweib  
Registration No: 21120163

Supervisor: Dr. Rushdi Ketaneh  
Co-Supervisor: Prof. Mohammad Abu Taha

Master thesis submitted and accepted, Date: 20 December 2017

The names and signatures of the examining committee members are as follows:

- 1- Head of the Committee: Dr. Rushdi Ketaneh
- 2- Co-Supervisor: Prof. Mohammad Abu Taha
- 3-Internal Examiner: Dr. Amin Leghrouz
- 4-External Examiner: Dr. Hisham Hidmi

Signature.....  
A handwritten signature in blue ink, appearing to read "Rushdi Ketaneh".  
Signature.....  
A handwritten signature in blue ink, appearing to read "Mohammad Abu Taha".  
Signature.....  
A handwritten signature in blue ink, appearing to read "Amin Leghrouz".  
Signature.....  
A handwritten signature in purple ink, appearing to read "Hisham Hidmi".

Jerusalem – Palestine  
1439 AH/2017 AD

## **Dedication**

To my mother and father, who supported me in all stages of my life and I found them on my side whenever I needed them.

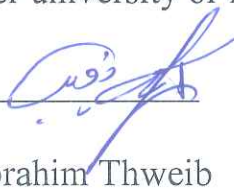
Your beloved daughter

Aya Ali Ibrahim Thweib

## **Declaration**

I hereby certify that this thesis, submitted for the degree of Masters, is the outcome of my own research, except where otherwise acknowledged, and that this thesis (or any part of the same) has not been submitted for a higher degree to any other university or institution.

Signed:



Aya Ali Ibrahim Thweib

Date: 20/12/2017

## **Acknowledgement**

First and foremost, all praise belongs to Almighty Allah, the Lord of the Universe, who has enabled me to accomplish and complete this work successfully. I would like to extend my sincere thanks and everlasting appreciation to my supervisors, Prof. Mohamed Abu Taha for his acceptance of the supervision and his continued follow-up of the thesis even after his retirement as I thank Dr. Rushdi Kittaneh for his constant support. I would also like to express my deepest appreciation to Dr. Zaidoun Salah, the head of the Culture Tissue Laboratory and the Medical Research Center and the labs technicians, Sharihan Erikat and Lina Qurea', for their endless cooperation. Also, I would never forget my students, Doaa' Slama, Duha Al wahsh, and Ayat Hassasneh who helped me alot in the project experiments. Finally, I would like to gratefully thank all my friends and colleagues, who played any role in the completion of this work and for every encouragement word I was given by them.

## **Abstract**

Nowadays, cancer treatment techniques are trying to be more directed with lesser side effects. One of these methods is using Infrared radiation as a co-factor or a main factor in treating cancer and all these methods are still under experimental investigation. Finding an inexpensive treatment for cancer with lesser side effect and with low treatment cost is the motivation of this project. An infrared source was established in research physics laboratory from inexpensive material by Abu-Taha and co-workers (2013) and used to radiate biological samples in this project (its electrical circuit is explained in details) which are: in-vitro and in-vivo different rat tissues and different types of cultured cancer cell line samples, these samples were exposed to IR radiation from the homemade source. The results were optimistic; for example cutaneous tissue were the most affected by heat, its temperature was increased by almost  $10^0\text{C}$  recording a temperature increase of more than  $40^0\text{C}$ . A contour plot was used to represent the heat distribution over the targeted tissue. Cancer samples proliferation was suppressed by heat. Using counting cells technique it was found that irradiating cancer samples for 60 minutes duration session affected the cells growth and for two hours duration session the cell's morphology was changed.

The primary results from this project indicate a successful performance of the homemade source and broad band infrared radiation in the medical field and it could be used as a potential technique in treating cancer by heat with low cost, less painful methods.

## Table of Contents

<b>Declaration .....</b>	<b>I</b>
<b>Acknowledgement .....</b>	<b>II</b>
<b>Abstract .....</b>	<b>III</b>
<b>Table of contents .....</b>	<b>IV</b>
<b>List of tables .....</b>	<b>VIII</b>
<b>List of figures .....</b>	<b>X</b>
<b>List of Appendices .....</b>	<b>XV</b>
<b>List of abbreviations .....</b>	<b>XVI</b>
<b>Chapter One: Introduction .....</b>	<b>1</b>
<b>    1.1 Historical background .....</b>	<b>1</b>
<b>    1.2 Problem statement .....</b>	<b>2</b>
1.3 Significance of the study.....	4
1.4 Objectives of the study.....	4
1.5 Hypothesis.....	4
1.6 Limitation of the study.....	4
1.7 Thesis plan.....	5
<b>Chapter Two: Literature review .....</b>	<b>6</b>
2.1 Introduction.....	6
2.2 Temperature distribution over biological tissue.....	6
2.3 Heat influence .....	7
2.4 Radiation mode.....	8
2.5 Effective penetration for treatment purposes.....	10
2.6 Cancer diagnosis using heat and IR radiation.....	11
2.7 Photoimmuno therapy (PIT).....	11
2.8 Summary .....	12
<b>Chapter three: Theoretical background .....</b>	<b>13</b>
3.1 Introduction .....	13
3.2 Electromagnetic spectrum (EMS).....	13
3.3 Infrared spectrum.....	14

3.3 Infrared Sources.....	17
3.3.1 Bi-spiral source.....	17
3.3.2 FeCr alloy sheet and Fe-Cr-Y source.....	18
3.4 Infrared detectors.....	19
3.5 Light interaction with matter.....	22
3.5.1 Introduction .....	22
3.5.2 Light absorption and scattering.....	23
3.5.3 Chromophores.....	25
3.5.4 Heating .....	26
3.5.5 Cancer treatment.....	27
3.5.6 Cancer diagnosis.....	27
3.5.7 Cancer Cells affected by heat.....	28
<b>Chapter four: Experimental system .....</b>	<b>29</b>
4.1 Introduction .....	29
4.2 study design.....	29
4.3 Trigger circuit.....	30
4.4 Characteristic study of IR source.....	31
4.5 Focusing tools.....	32
4.5.1 Aluminume tube wave guide.....	33
4.5.2 Gold mirror reflector.....	34
4.5.3 Hemispherical reflector.....	35
4.6 Tissue experiment.....	36
4.6.1 In-vitro experiment set up.....	36
4.6.2 In-vivo experimental set up.....	38
4.6.3 In-vitro cancer cell line set up.....	40
4.7 Study settings and materials.....	41
4.8 Data collections.....	43
4.9 potential limitations.....	44
4.10 Ethical considerations.....	44
<b>Chapter five: Results and discussion.....</b>	<b>45</b>

5.1 Introduction.....	45
5.2 Characteristics of IR radiation from two different sources.....	45
5.2.1 Bi-spiral source.....	45
5.2.1.1 Radiation Intensity Distance dependence.....	45
5.2.1.2 Radiation Intensity from Bi-spiral source Frequency dependence.....	47
5.2.1.3 Radiation Intensity from Bi-spiral source vs. Current.....	48
5.2.2 Characteristic of Fe-Cr-Y IR source.....	50
5.2.2.1 Radiation Intensity from Fe-Cr-Y source Distance dependence.....	50
5.2.2.2 Radiation Intensity from Fe-Cr-Y source vs. Current.....	51
5.2.2.3 Radiation Intensity from Fe-Cr-Y source Angle dependence.....	52
5.3 Effect of using focusing tools.....	55
5.3.1 Focusing Bi-spiral source radiation.....	55
5.3.1.1 Using an aluminum tube as a waveguide.....	55
5.3.1.2 Hemispherical shaped reflector.....	57
5.3.1.3 Plane front surface coated mirror.....	58
5.3.2. Fe-Cr-Y source.....	59
5.3.2.1 Hemispherical shaped reflector.....	59
5.3.2.2 Plane coated mirror.....	60
5.4 Heat distribution over biological samples.....	61
5.4.1 Rat samples.....	61
5.4.1.1 In-vitro trial with rat sample.....	61
5.4.1.2 Excised pieces.....	61
5.4.1.3 Whole rat body irradiated at specific area by Fe-Cr-Y source.....	64
5.4.1.4 Whole and excised rat body irradiated at specific area by Bi-spiral and Fe-Cr-Y source.....	68
5.4.2 In-vivo trial using rat sample.....	73
5.4.2.1 Upper part of skin.....	73
5.4.2.2 Abdomen muscle.....	77

5.4.2.3 Thigh muscle:.....	79
5.5 Cancer cell line samples.....	80
5.5.1 First stage results.....	81
5.5.1.1 MCF-7 cell line.....	81
5.5.1.2 KHOS cell line.....	85
5.5.1.3 Caco-2 cell line.....	88
5.5.2 Second stage results.....	92
5.5.2.1 MCF-7 cell line.....	92
5.6.2.2 MDA cell line.....	93
5.5.2.3 HT-29 cell line.....	95
5.5.2.4 HCT-116 cell line.....	97
<b>Chapter 6: Conclusions and Further work.....</b>	<b>101</b>
6.1 Introduction.....	101
6.2 Conclusions.....	101
6.3 Further work.....	102
<b>Appendices.....</b>	<b>104</b>
<b>References.....</b>	<b>109</b>
<b>الملخص.....</b>	<b>117</b>

## List of Tables

Table name	Page no
Table 5.1: Points temperature results irradiated by IR source of thigh muscle at 0.5 mm depth.	62
Table 5.2: Points temperature results of skin irradiated by IR source at depth 1.00 mm for the station hole.	63
Table 5.3: Points temperature results of skin irradiated by IR source at depth 1.00 mm for different holes.	63
Table 5.4: temperature-distance relationship of upper skin rat (in vitro)	66
Table 5.5: Recorded point temperature for upper skinned white rat using Bi-spiral source (the station point). (In vitro)	68
Table 5.6: Recorded points temperature for upper and bottom thigh muscle of a white rat using Fe-Cr-Y source (In vitro).	70
Table 5.7: Recorded points temperature for upper and bottom thigh muscle of a white rat using Fe-Cr-Y source (In vitro).	72
Table 5.8: Temperature-distance relationship of upper skin white rat for the first 11 min. (in vivo)	74
Table 5.9: Temperature-distance relationship of upper skin white rat after the pass of 11.77 min. of irradiation (in vivo)	76
Table 5.10: Temperature-distance relationship of abdomen muscle white rat (in vivo)	78
Table 5.11: Temperature-depth relationship of a thigh muscle	79
Table 5.12: Following up the development of culturing cancer cell line T-47D in treated media with IR irradiation	80
Table 5.13: temperature results of P1 after 2 <sup>nd</sup> irradiation session. (P1 was positioned directly under the thermal source)	82
Table 5.14: Photos of different areas of MCF-7 cell line that display IR radiation effect on them.	83
Table 5.15: Temperatures of two different places for bone cancer cell line.	86
Table 5.16: Photos of different areas of KHOS cell line that display IR radiation effect on them.	87
Table 5.17: Average temperature results of 10 points grid marked on 10 cm cell culture dish 1 <sup>st</sup> day irradiation session of Caco-2 cell line.	89

Table 5.18: Average temperature results of 10 points marked on 10 cm cell culture dish 2nd day irradiation session of Caco-2 cell line.	91
Table 5.19: Results are summarized in the following table:	95
Table 5.20: summarizes the procedures and the results HCT-116 cell line:	97
Table 5.21: Following up the changes HCT-116 cell line growth after different IR radiation duration sessions.	100

## List of Figures

Figure 3.1: Comparison of wavelength, frequency and energy for the electromagnetic spectrum.	13
Figure 3.1: Main vibrational modes for molecules	16
Figure3.2: A Bi-spiral Source	17
Figure 3.3: FeCr alloy sheet and Fe-Cr-Y source	18
Figure 3.5: Physical dimensions of a simplified heating conductor	19
Figure 3.4: Schematic presentation of pyroelectric effect	20
Figure 3.5: a) Schematic of a Thermocouple. b) Schematic of basic iron-constantan thermocouple circuit	21
Figure 3.6: Depth of light penetration into the skin, at various wavelengths	23
Figure 4.1: Schematic showing turning on constructed source.	29
Figure 4.2: A schematic and a photograph of MOSFET with a sketch of the clipping circuit used to trigger the lock in amplifier with 0.3 V reference signal.	30
Figure 4.3: Investigating Fe-Cr-Y source set up	31
Figure4.4: Investigating Fe-Cr-Y source intensity vs. angle	31
Figure 4.5: A schematic of the radiation behavior without using a reflector or a waveguide tools.	32
Figure4.6: Photograph of different wave guides. 1) Aluminume tube wave guide. 2) Gold mirror wave guide. 3) Hemispherical wave guide.	33
Figure 4.7: A photo of Al tube wave guide in front of the Bi-spiral source	33
Figure 4.8: A schematic of the radiation behavior along the Al tube wave guide.	34
Figure 4.9: 1) A photo of flat mirror placed behind the FeCr alloy stripe source. 2) A schematic of the radiation behavior when incident on flat mirror reflector.	34
Figure 4.10: A schematic of two different hemispherical reflectore, a and b.	35
Figure 4.11: A photo of Hemispherical wave guide behind the Bi-spiral source.	35
Figure4.12: A schematic of the radiation behavior when beam collides with the inner surface of hemispherical reflector.	36
Figure 4.13: a) Plexiglass plates. b) Tissue sample was stretched over plexiglass plate; 1) the holder. 2) The plexiglass plate	37
Figure 4.14: A schematic of the plexiglass plate with grid holes	37
Figure 4.15: A schematic of the plexiglass plate with one column of holes	37
Figure 4.16: Photo showing experimental setup for IR tissue absorption in vivo.	38
Figure 4.17: Photo showing direct IR absorption by rat's shaved skin.	38

Figure 4.18: Photo showing in-vivo IR absorption by rat's belly muscle.	38
Figure 4.19: Photo showing in-vivo IR absorption set up by different depths through thigh muscle.	39
Figure 4.20: The thermocouple probe was inserted into needle to reach different depths in thigh tissue.	39
Figure 4.21: A photo of 10cm cell culture dish marked in different ways to monitor temperature; a) marked as grid. b) marked as separated area.	40
Figure 4.22: A photo of in-vivo cancer cell line in an open hood from different direction.	40
Figure 4.23: A photo showing cancer cell line setup inside the incubator; a) the used equipment. b) Probing media temperature of the sample inside the incubator.	41
Figure 5.1: IR Intensity vs. distance fitting.	46
Figure 5.2: A schematic represent PD and PI.	47
Figure 5.3: Conceptual diagram comparing the structure of CW with pulsed light of various pulse durations.	47
Figure 5.4: IR intensity versus frequency for Bi-spiral source	48
Figure 5.5: IR intensity versus current for Bi-spiral source	49
Figure 5.6: IR intensity measurements dependence distance fitting for Fe-Cr-Y source	51
Figure 5.7: IR intensity fitting versus average current.	52
Figure 5.8: Schematic showing intensity angle dependence set up.	53
Figure 5.9: Dependence of IR intensity on the angle between the vertical axis to the foil and detector.	53
Figure 5.10: polar diagram for Bi-spiral source.	53
Figure 5.11: Dependence of IR intensity on the angle between the vertical axis to the foil and detector	54
Figure 5.12: IR intensity versus distance for Bi-spiral source with and without focusing Al tube waveguide element	55
Figure 5.13: IR intensity measurements dependence distance power fitting for Bi-spiral source with Al tube wave guide	56
Figure 5.14: Bi-spiral source intensity versus frequency with and without hemispherical reflector at different frequencies.	57
Figure 5.15: IR intensity versus distance for Bi-spiral source without and with using plane front coated mirror.	58
Figure 5.16: IR intensity measurements dependence distance power fitting for Bi-spiral source with plane front coated mirror placed behind	58
Figure 5.17: IR intensity versus distance for Fe-Cr-Y source with and without using a hemispherical shaped reflector.	59

Figure 5.18: IR intensity measurements dependence distance power fitting for Fe-Cr-Y source with hemispherical reflector.	59
Figure 5.19: IR intensity versus distance for Fe-Cr-Y source with and without using plane coated mirror reflector.	60
Figure 5.20: IR intensity measurements dependence distance power fitting for Fe-Cr-Y source with and without plane coated mirror reflector.	60
Figure 5.21: A photo of rat's thigh sectioned muscle.	61
Figure 5.22: A photo of the set up using gold coated mirror.	64
Figure 5.23: Temperature distribution over upper part of skin tissue (in vitro).	65
Figure 5.24: measured points temperature dependent distance (in vitro)	66
Figure 5.25: Wire frame plot for temperature distribution through the shaved marked skin (in-vitro).	67
Figure 5.26: Temperature distribution over inner side of skin tissue (in vitro) using Fe-Cr-Y source	69
Figure 5.27: Temperature-Distance for points at same horizontal distances from the IR source, but at different depths.	71
Figure 5.28: Temperature-Distance for points at the same horizontal distances from the IR source, but at different depths.	72
Figure 5.29: Temperature distribution over upper part of skin tissue for the first 11 minutes (in vivo).	73
Figure 5.30: Measured temperature versus distance (in vivo) along 11.77 min session duration.	74
Figure 5.31: Temperature distribution over upper part of skin tissue after the pass of 11.77 minutes from irradiation (in vivo).	76
Figure 5.32: Measured temperature versus distance (in vivo) after 11.77 min of radiation	77
Figure 5.33: Temperature distribution over abdomen muscle	78
Figure 5.34: Marked 10cm cell culture dish	81
Figure 5.35: a photo of colorectal adenocarcinoma cell line arrangement	88
Figure 5.36: a photo of MCF-7 cell line before irradiation and at the end of sessions	92
Figure 5.37: a photo of MDA cell line before irradiation and at the end of sessions	93
Figure 5.38: a photo of untreated MDA cell line	94
Figure 5.39: Photos of MDA cell line after 2 hrs sessions of irradiation two times	94
Figure 5.40: a photo of control colorectal adenocarcinoma cell line plate.	95
Figure 5.41: Flow chart summarizing the procedure of HT-29 trial.	96

Figure 5.42: a photo of HCT-116 cell line	97
Figure 5.43: Flow chart summarizing the procedures and results of radiating HCT-116 cell line by IR radiation after 24 hours.	98
Figure 5.44: Photos show the changes in HCT-116 cell line after 2 hrs of irradiation	98
Figure 5.45: a photo of the change in HCT-116 cell line after duration 30 min of irradiation	99

## **List of Appendices**

A: Bi-spiral source output depending on distance	104
B: Bi-spiral source output depending on current and frequency	106
C: Fe-Cr-Y Source output depending on distance	107
D: Fe-Cr-Y Source output depending on degree	108

## List of abbreviations

CaCo2	Colon cancer cell line
CW	Continuous wave
EMS	Electromagnetic spectrum
FIR	Far infrared
FTIR	Fourier transform infrared
LLLT	Low level laser therapy
mAb	Monoclonal antibody
MIR	Mid infrared radiation
NEP	Noise equivalent power
NIR	Near infrared radiation
NIRS	Near infrared radiation spectrum
OPT	Occupied Palestinian Territory
PDT	Photodynamic therapy
PIT	Photoimmun therapy
PW	pulse wave
PZT	Lead Zirconium Titanate
RDS	Resistance between source and drain
TAT	Thermoacoustic tomography
TBI	Traumatic brain injury
T-47D	Breast cancer cell line
PD	Pulse duration
VGSth	Gate threshold voltage
WHO	World Health Organization
PAT	Photoacoustic tomography
IR	Infrared
emf	Electromotive force
DC	Duty cycle
HT-29	colorectal adenocarcinoma cell line
MDA	Breast cancer adenocarcinoma cell line
MCF-7	Breast cancer cell line
STDEV	Standar deviation
PI	Pulse interval
T-47D	Cancer cell line, tissue type mammary gland
HCT-116	Colon cance

# **Chapter One**

## **Introduction**

### **1.1 Historical background**

One of the oldest treatments techniques was healing with sunlight, it is known to be an ancient treatment for some skin diseases called in the civilization of the Pharaohs and ancient Indian 3500 years ago "heliotherapy". Ibn al-Bitar wrote in his book "Mufradat Al-Adwiya" a prescription contains a substance extracted from a particular plant combining with exposing to sunlight for vitiligo treatment around 1100 AD. Two centuries ago the spark of sunlight entering the medical field had been started; when Downes and Blunin 1877 suggested that sunlight could eliminate the anthrax germ. Not only sunlight had some positive observation in dermatology field, but also according to Palm from Edinburgh in 1890 sunlight had a role in treating rickets. Also, Herodotus in 525 BC claimed that the ancient Egyptians gained their skull hardness from exposing their shaved head to sun radiation since the day of their birth. (Hönigsmann, 2013), It is clear that phototherapy or "heliotherapy" had a strong existence in the ancient civilization regardless of its scientific stability.

The role of light in medicine was returned strongly in the beginning of the 20<sup>th</sup> century; experiments were done using photosensitizers and visible light to treat skin cancer. This technique is known nowadays as Photodynamic therapy (PDT). Von Tappeiner and colleagues performed the first trial to treat patients with skin cancer using the photosensitizers around 1920s (Hönigsmann, 2013), but one of its side effects was making treated patients sensitive to the light for some time (American cancer society, 2015). From the previous phototherapy is a type of treatment using electromagnetic radiation which includes visible and invisible light, infrared and ultraviolet (Putowski et al, 2016). To avoid PDT side effects professor Kobayashi and his colleagues developed a new technique called monoclonal antibody (mAb) that will only be activated if the sensitizer identify a certain cancer cell protein exists on its surface (Tichauer, 2014).

Synchronizing the previous treatment techniques other oriented treatments were investigated intensively; hyperthermia and thermal therapy in 1893, which is applying heat to the patient in

different ways for treatment purpose (Luk, Hulse, and Phillips, 1980; Bischof, 2006). Low level laser therapy (LLLT) was introduced in 1967 (Hashemite et al, 2010).

Infrared radiation involves a photobiological responses in cutaneous tissue, this interaction could be photothermally and/or chemothermally (non-thermally) stimulated (Anderson and Parrish, 1981; Tanaka et al, 2012; Obayashi et al, 2015). Infrared therapeutic effect was investigated in diverse fields; to relieve neck pain (Chen et al, 2013), for lowering blood pressure and waist circumference using sauna Far infrared (Beever, 2010). Accelerating wound healing process (Dash and Selvi, 2013), for treating Traumatic brain injury (TBI) (Henderson and Morries, 2015), Infrared can be used as an adjacent agent to chemotherapy (Obayashi et al, 2015), and to radiotherapy (Luk, Hullse, and Phillips, 1980; Kaur et al, 2011)

Near Infrared (NIR) penetration power intensities were estimated through tissue. If the source power ranged between 6-15 W, it is considered high power and is called Phototherapy (Henderson and Morries, 2015). In other words if the sample will suffer a thermal damage, its temperature should increase by  $0.16^{\circ}\text{C}/\text{mV}$  (Stadler et al, 2004), otherwise it is called low level laser therapy (LLLT) with powers ranging between 50-200 mW (Henderson and Morries, 2015)

## 1.2 Problem statement

Light spectrum is a gift from ALLAH which is essential for our existence and our daily lives issues, widely spread in all aspects of life e.g.; pharmacy, industry, military, food, health, etc.

Utilizing from this miracle by studying light interaction with tissue makes it possible to find new potential methods to treat and diagnose diseases with low cost. The second large intense radiation on earth is infrared (Keyes, 1980), it is non-ionizing radiation (National Cancer Institution, 2015).

According to the National Cancer Institution the burden of Cancer in the United States in 2016,” an estimated 1,685,210 new cases of cancer will be diagnosed in the United States and 595,690 people will die from it. While in the Occupied Palestinian Territory (OPT) “In the period 1999–2009, a total of 59,627 deaths were analyzed with a yearly average of 5,421

deaths (3,019 males and 2,401 females), the most common cause of death out of all cancer types was lung cancer among males (22.8 %) and breast cancer among females (21.5 %) followed by prostate cancer for males (9.5 %) and by colon cancer for females (11.4 %)” (Abu-Rmeileh et al, 2016). These numbers are nominated to increase according to World Health Organization (WHO, 2016) in both developed and less developed countries.

The traditional treatments of cancer are: surgical, chemotherapy, and radiotherapy (American cancer society, 2017). The type of cancer and its location determined the best way to treat it, but what is difficult to be treated by sectioning in surgical process, chemotherapy or radiotherapy are used to complete the treatments process (Obayashi, 2015). The last two mentioned treatments are not only have many side effects and hazard on normal cells, but also some kind of cancer cells which cannot be cured by them completely will regrow with greater resistance to conventional cancer treatments (Tichauer, 2014). So, new treatment methods must be explored. In this study we suggest irradiation with broad infrared radiation.

A broad band Infrared source was constructed by Buss in 2009 and reused in this investigation by pointing it directly to biological tissues. The reactions between Infrared irradiation and biological tissue will result in IR absorption which will lead to molecular vibrations causing the sample temperature to increase. In order to study temperature distribution on normal tissue, white rat tissue sample is used; in-vivo and in-vitro. Different tissue types of Rat samples were examined by measuring their temperature through the radiation session by thermocouples. Also, different types of cancer cell line in-vitro were irradiated by the same source and its temperature is being measured by thermocouple probes and recorded on data studio program, its morphology was observed by inverted microscope and its growth rate was estimated by counting technique. Infrared radiation with all its portions has tremendous activity nowadays in medical issues especially in cancer treatment and diagnosis.

There are many studies about how heat affects cancer cell, but heating cancer cell using Broad band IR source are not explored extensively. Also temperature dispersed over the tissue is very important to be studied since it is a critical point for determining the dose and duration of treatment or diagnosis (Bischof, 2006).

### **1.3 Significance of the study**

The research was established in order to find potential new low cost methods for treating cancer, using Fe-Cr-Y miniature IR sources. It was proved that heat affects cancer cell growth many years ago (Luk, Hulse, and Phillips, 1980). The advantages of using broad band miniature IR source beside its inexpensive costs, it is considered to be a local hyperthermia method, and low intensity radiation source.

### **1.4 Objectives of the study**

1. Investigate the possibility to use homemade, low cost, miniature IR source for absorption study by biological tissues.
2. Study the effect of increasing the temperature on biological samples (rat tissue and cancerous cell line) up to  $\sim 42^{\circ}\text{C}$ .
3. Study the temperature distribution over the samples radiated by IR radiation.
4. Investigate the possibility to diagnose different cancer cell samples from their heat absorption.

### **1.5 Hypothesis**

1. The ability of using miniature infrared source to perform experiments on different biological samples.
2. Non-invasive, inexpensive techniques can be applied in medicine.
3. Temperature affects the growth of cancerous cell.
4. Cancer cell line species can be identified according to their absorption of IR radiation.

### **1.6 Limitation of the study**

1. The population of the study was small.
2. The shortage in anesthesia materials and an expert for applying it.
3. The inverted microscope camera was not always available for documenting each trial.

4. Only two thermocouple probes were available which prevented taking measurements for more than two points at the same time.

## **1.7 Thesis plan**

The thesis is organized as follows: First chapter introduced phototherapy through history and its developments through decades in a briefly narrative form followed by the study significance and objectives. Chapter two introduced a collection of previous studies of different subjects such as temperature distribution over biological samples, heat influence, radiation mode, effective treatment and photo immunotherapy. In chapter three a detailed explanation of electromagnetic radiation and its effect on biological samples is presented, also there were explanations of the principle of the used tools in the experiment. The motivation of finding an potentially inexpensive treatment for cancer in this study demanded critical steps to undergo a scientific procedures which was introduced in chapter four, also showed the experimental system; each trial included with figure for more clarity and the potential limitations that faced the experiment: firstly; the need to study the properties of the Fe-Cr-Y source which was established by Buss in 2009 in research physics lab at Al-Quds university. Secondly; investigate the physical effects on healthy normal cells irradiated by the Fe-Cr-Y source using in-vitro and in-vivo techniques on rats by monitoring the samples temperature. Thirdly; exposing cancer samples to IR radiation and monitoring samples temperature and cells morphology. Finally after viewing the results and discussing them in chapter five; it was the conclusions and some suggestions of what could be done to develop and improve the study introduced in chapter six.

## **Chapter Two**

### **Literature review**

#### **2.1 Introduction**

This chapter reviews some areas in the medical field where IR radiation is used and discusses the possibility of using IR sources as a diagnostic and treatment tool for cancer. Based on studies that have been examined by the researcher shows there is a strong desire and a demanding need to find new ways that are characterized as a noninvasive techniques, with low side effects, low cost and relatively with quick results in cancer diagnosis and treatment which attracted many researchers in the last two decades.

In this review, the advantages of using PW (pulse wave) as an effective power for treatment and temperature influence will be investigated. Also, some treatments attempt targeting cancer cell and diagnose the disease using IR radiation and heat will be summarized. So it is important in this survey to review studies dealt with different IR wave lengths to assess their penetration to biological tissue whether the conditions of the experiments were "in vitro or in vivo" according to the experimental results.

#### **2.2 Temperature distribution over biological tissue**

An experiment was done by Stadler in (2004) where two groups of black and white mice tissues were exposed to CW (continuous wave) laser 830 nm in order to study the change in skin temperature by irradiating them with different power with fluencies of  $0.0\text{-}5.0 \text{ J/cm}^2$ . Each group contained 12 mice. In the black group the surface temperature was reported to increase by  $4.44^\circ\text{C}$  after delivering  $5 \text{ J/m}^2$ , the surface initial temperature was  $29.0^\circ\text{C} \pm 1.0^\circ\text{C}$  monitored using a thermal camera and two other thermocouples were localized 1mm depth measured an increment in temperature by  $3.21^\circ\text{C}$  from an initial of  $31.00^\circ\text{C} \pm 1.30^\circ\text{C}$  while the temperature increment was lower in the white group. Similarly, Kim and Jeong in (2014) studied the temperature distribution over the surface of a porcine skin and at different depths from the thigh of the animal; the measurements were taken after 24 hours of postmortem. The

samples were exposed to a continuous radiation (CW) of wavelength of 1064 nm and intensity of  $3.14 \text{ W/cm}^2$ . The surface temperature was increased from  $26^\circ\text{C}$  to  $40^\circ\text{C}$  as observed by an Infrared Camera after 12 seconds, the examined depths were 0.1, 0.2, 0.3, 0.4, and 0.5 cm and each one temperature was measured by T-thermocouple and they were respectively; 38, 34, 31, 30, and  $29^\circ\text{C}$ . According to Kim and Jeong no thermal damage was observed below  $40^\circ\text{C}$ . The difference between Stadler and (Kim and Jeong) experiments results was because Stadler experiment was done *in vivo* while (Kim and Jeong) was done *in vitro* because living tissue differs from postmortem one. (Henderson and Morries, 2015)

### 2.3 Heat influence

The phenomenon that confirmed whether the Fe-Cr-Y source that was used in the experiment to irradiate some biological samples and some cancer cell lines with board band infrared radiation has thermally damage or non-thermally damage for biological tissue was heat; below  $40^\circ\text{C}$  no thermal damage was recorded (Niemz, 2004; Kim and Jeong, 2013). Any change in the heat inside the tissue will cause a temperature change (Niemz, 2004), and so, temperature was measured by thermocouple to record the change that the source could influence the samples; since temperature can be an indication for the samples conditions.

Luk, Hulse, and Phillips (1980) conducted a review of literature extended for more than 100 years. They concluded that many scientists who combined hyperthermia technique with surgical or radiation cancer treatment found positive effect on patients health. Hyperthermia in Mise and coworkers in (1990) experiment showed a positive influence of heat in treatment; the researchers heated tumor cells and anti-tumor effector cells using a water bath to raise the temperature of samples to  $42^\circ\text{C}$  for 30 minutes, by comparing the growth of treated tumor cells with untreated one it was clear from the experimental results that after 10 days of growth the treated cancer cells mean diameter (mm) was decreased. There are other types of hyperthermia; Luk, Hulse, and Phillips mentioned (1980) that Hall and co-workers used perfusion which is pouring through an organ liquid temperature ranges between  $(41.5 - 45)^\circ\text{C}$  to treat 32 patients suffering from carcinoma of the urinary bladder and the results were

promising; the cancer of 26 patients were almost regressed and 4 of cancer patients were completely regressed.

Lepock (2002) clarify some of the effect of hyperthermia on mammalian cells after exposure to temperature 40-41  $^{\circ}\text{C}$  the cell growth decreases, the signal pathways changes, it will become more sensitive to other stresses and acquiring thermo tolerance. Exposing for more temperature up to 45  $^{\circ}\text{C}$  will extensively cause denaturation of protein. Also it was showed in Kalamida et al. (2015) that the growth of different cancer cell lines e.g. (T98G, U87MG, DU145, PC3, H1299, and MCF7) incubated at 40 $^{\circ}\text{C}$  was regressed compared to those incubated at 37 $^{\circ}\text{C}$ . In (2013) Kim and Jeong was able to raise the temperature of a sectioned porcine skin from 26-40  $^{\circ}\text{C}$  during low level laser therapy (LLLT), the beam characteristics were 1064 nm, 3.14 W/cm $^2$ . Other experiments were done to investigate LLLT thermal effect. A 915 nm laser was used with different powers and duration 3W for 3min, 3W for 5min, 3W for 7min, 4W for 3min, ...., 5W for 7min, irradiated a KP4 and MIA-PaCa2 cell lines (pancreatic cancer cells), the samples were cultured in 96-well plates and incubated at 25 $^{\circ}\text{C}$ . As the power and duration increases the percentage of apoptosis increases, the temperature of the cell media increased almost 11 $^{\circ}\text{C}$  only. Obayashi (2015) claimed in his experiment that neither the power was high nor was the duration enough to raise the media temperature to 42 $^{\circ}\text{C}$  in order to describe the effect of LLLT to be thermally damage to tissue, but it did make gemcitabine which is a chemotherapy medication used to treat pancreatic cancer more effective.

## 2.4 Radiation mode

Finding a way for discovering the radiation depth of biological tissue is of great importance for both treatment and diagnosis purposes in medicine. The introduction for this is the absorption and scattering processes of electromagnetic radiation within biological tissue. Electromagnetic pulses can reveal much information about the tissue optical properties when it is radiated by the electromagnetic energy (Ku et al., 2005).

One of the scientific argument: is whether the radiation mode (pulse or continuous) is more penetrating through biological tissue. According to Hashmi et al. (2010), pulse radiation (PW) is known to penetrate much more than continuous radiation (CW) and its power density that

had been delivered is more than few ( $\text{mW/cm}^2$ ) for greater than 5 cm beneath skin. This information was confirmed by studies as mentioned in Henderson and Morries (2015) review: for ex vivo samples from sheep and human skin the power measurements showed a decrease in the delivered power on 2 mm depth, but the decrease in PW mode was less than CW mode. Also, a drop of power was found at 3 cm of lamb skull, tissue, and brain. Even for in vivo human tissue, NIR radiation pulse setting of 10 Hz was recorded at depth 25-30 mm of human hand.

Imaging field in medicine utilized from the ability of different wavelength to penetrate different depths of tissue; such as thermoacoustic tomography (TAT) and photoacoustic tomography (PAT). TAT uses radiofrequency or microwave band while PAT uses visible light or (NIR) in order to reach deeper tissue up to 5 cm which could be a potential diagnostic tool for breast cancer (Ku et al., 2005). Tomography benefit from the phenomenon of therapeutic window for NIR within wavelength ranges between 700 and 900 nm, where absorption is low in comparison with scattering (Hawrysz and Sevick-Muraca, 2000).

Also, treatment sessions outcomes in pulsed wave (PW) mode is more effective than continuous wave (CW) mode in some areas for a couple of reasons; less tissue damage caused from heating, and PW suits the biological system frequency and the photo dissociation of nitric oxide (Hashmi et al., 2010). Hashmi et al. (2010) explored a33 articles to clarify the differences between pulse and continuous mode 9 of them compared CW with PW directly, were 6 of them agreed that PW is better than CW and two conflict these conclusions, meanwhile one of them did not find a difference between CW and PW. For instance PW is better in wound healing, pain relief and decreasing neurological deficits. However Almeida-Lopes et al. (2008) claimed that pulse and continuous mode had the same effect on repairing the rat tibia. In this experiment an infrared laser was operated with 830 nm wavelength, 100 mW and beam diameter 0.06 mm and PW (10Hz). The radiation dose was divided over three sessions within 72 hours duration. The examined energies were between (2J -10J) and the effective one including both modes were between 4J and 8J with fluency between (70-280) $\text{J/cm}^2$  were enough for increasing the tissue preparation. However, for 10J the CW caused damage for the treated tissue. AL-Witan and Zhang (2004) found that the wound healing percentage using CW is higher than PW 100 Hz of 635 nm given 3 times weekly with

duration 18.7 min in order to achieve  $1 \text{ J/cm}^2$  fluency. It should be noted that the chosen wave at the border of IR window has less penetration of tissue. Ezzati, Bayat and Khoshvaghti, (2009) results were contrary to previous results about wound healing in a third-degree burn; a Pulse 890 nm wavelength in LLLT with  $11.7 \text{ J/cm}^2$  is a promising technique. A 74 rat had third-degree burns in two spots on their interior skin (thoracic) (distal and proximal). The proximal spot was the control one. A comparison was done to figure out which technique is the best; CW or PW or 0.2% nitrofurazone. Similarly, the previous researchers in (2010) found the same results for 67 rats treated from second-degree burns with the same methodology.

Ando et al. (2011) performed a comparison between PW at 10 Hz and CW laser with an 810 nm in treating TBI (Trauma brain injury) confirmed that mice exposed to PW had the best healing results. After 4 weeks from the exposure the brain lesion area became smaller than the control one.  $36 \text{ J/cm}^2$  delivered to 1 cm diameter spot illuminated for 12 minutes.

## **2.5 Effective penetration for treatment purposes.**

According to Henderson and Morries (2015), low-power NIR cannot deliver energy to 1 cm depth of tissue. In order to get an affective result in treatment with low level light therapy (LLLT) two factors must be fulfilled; penetration level and irradiance intensity(Hashmi et al., 2010). Furthermore Henderson and Morries (2015) inferred that pulsing at 10 Hz delivered 2.4% of the surface energy using 810 nm wavelength reached the depth of 3 cm and for 980 nm light at 10–15 W almost 1.22% of the energy penetrated 3 cm, the effective NIR sources power were 6, 10, and 15 W. It was clear in Henderson and Morries (2015) studies on power attenuation through multiple types of sheep and human tissues (ex vivo and in vivo) that effective power was over 6 W and pulse mode was more effective in delivering higher power for deeper structure of tissue. But whether if the radiation was pulse or continuous, its power densities must be  $\geq 10 \text{ W/cm}^2$  in order to have a thermal affect on the biological tissue with a duration more than 1  $\mu\text{s}$  (Niemz, 2004).

## **2.6 Cancer diagnosis using heat and IR radiation**

One of the potential methods for breast cancer diagnosis is photoacoustic tomography (PAT) which depends on the ability of visible and near infrared radiation penetration of tissue, according to Ku et al. (2005) there were many studies started from 1999 that explored the ability of photoacoustic imaging in detection of tumors; Ku et al. (2005) used a short pulse laser to image deep objects into mastectomy specimens and was able to detect a 5 cm blood object.

Fourier transform infrared (FTIR) is a powerful analytical tool which was used by Colagar, Chaichi, and Khadjavand (2011) to distinguish between normal and cancer gastric tissue samples that were sectioned and fixed in formalin from 4 patients. The primary results suggested that the normal samples were more absorbing than cancerous tissue.

Kalamida et al. (2015) study proved that a group of cancer cell lines are thermo-sensitive: H1299 lung carcinoma, MCF 7 breast adenocarcinoma, U87MG glioblastoma, DU145 and PC3 prostate carcinoma viability was determined by investigating their proliferation (ki67 index), and apoptosis (Caspase 9: which is a protein activated during programmed cell death (McDonnell et al, 2003). After 3 days of incubating into different temperatures (34°C, 37°C and 40°C) using a confocal microscopy; this suggests that some cancer cells may be identified as more heat-sensitive and may help diagnose them for better treatment.

## **2.7 Photoimmunotherapy (PIT)**

Tichauer (2014) summarized two factors that made cancer treatment diverse and difficult:

1. "Every tumor is genetically unique".
2. The tumor structure made it difficult to reach all its parts by traditional treatment.

The basic of PIT is targeting specific cell membrane by injecting photosensitive agents that will only combine with the targeted cells and it will only be activated using near infrared radiation directed to the targeted cells (Mitsunaga et al., 2012; Tichauer, 2014; Sato, Choyke, and Kobayashi, 2014; Sato et al., 2015).

Breast cancer (Mitsunaga et al., 2012), gastric cancer (Sato, Choyke, and Kobayashi, 2014), ovarian cancer (Sato et al., 2015), and many other researches exploring all other types of cancer and how it will response to PIT.

## **2.8 Summary**

This chapter provided the readers with a brief review of other potential cancer treatment and diagnosis methods. The selected articles dealt with studies talk about temperature spread over biological tissue, heat influence, LLLT and PIT, also discussed the best mode for radiation, its potential duration and power. It is concluded that IR radiation is worth studying to improve and adapt new methods for cancer diagnosis and possible treatment.

## Chapter three

### Theoretical background

#### 3.1 Introduction

Light spectrum is a gift from ALLAH. It is essential for our existence and our daily life issues in several fields e.g.; pharmacy, industry, military, food, health, etc. Optical spectroscopy is a developing science widely spread based on the interaction between light and matter. One of its branches is infrared spectroscopy which had been found by experiments. Infrared radiation is non-invasive method, safe on biological samples and accessible. Any living body is an Infrared radiator; Smith (2002) ensured that anybody with finite temperature is a radiation source, these advantages led to several researches in the medical fields and therapeutic areas to benefit from Infrared radiation.

#### 3.2 Electromagnetic spectrum (EMS)

Bakshi and Gods (2009) mentioned that EMS contains regions of different frequencies. It goes from Low frequencies which are used for modern radio communication to gamma radiation at the highest frequency end. Banwell (1972) clarified that shorter wavelengths have more energy. See Figure 3.1.

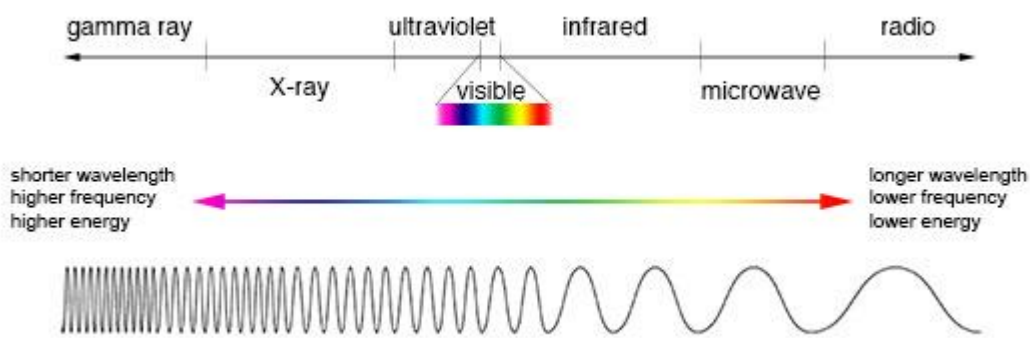


Figure 3.1: Comparison of wavelength, frequency and energy for the electromagnetic spectrum. (Credit: NASA's Imagine the Universe)

### 3.3 Infrared spectrum

On 11<sup>th</sup> February 1800 Sir Frederick William Herschel, a German-born British astronomer, discovered infrared light and named it ‘calorific rays’. He was a clever man who noticed that the temperature of different visible light differs, using a prism to separate the visible light into its components and measured its temperature with thermometers, he found that the temperature increases from violet to red, then he measured the temperature beyond the red colored beam where this area had the highest temperature, which known nowadays to be "Infrared"(Lifepixel, 2014).Infra is a Latin prefix meaning ‘below’ (BioSmart Technologies, 2014). "Infrared (IR) light is electromagnetic radiation with longer wavelengths than those of visible light, extending from the nominal red edge of the visible spectrum at 740 nanometers (nm) to 1 mm"(Boundless, 2014), with frequency ranges from approximately 300 GHz to 400 THz. Abu-Sharkh (2014) clarified that in biophysics IR spectroscopy is known to be a non-destructive method for probing materials on molecular level for its ability to be absorbed by them. IR spectroscopy is used to probe molecular vibrations (Caltech, 2014), as a way to study and characterize matter (Mehta and Akul, 2008). Also, Infrared region is known to be a "heat radiation" or therapeutic window (Niemz, 2004; BBC, 2014).These characteristics facilitated new applications for IR spectrum in the medical field e.g.; monitoring temperature(Hollis, 2002), for treating muscle stiffness, headaches (Wiki, 2014), increasing blood circulation without hard work also, it stimulate the production of collagen (building block for human tissue) (active forever, 2014),it is a potential tool for diagnosing tumors (Ku et al., 2005; BBC, 2014), and targeting cancer (Bischof J. C., 2006).

Going through more details will help understanding Infrared radiation; Plank (1900) suggested that absorbed or emitted energy can take the form of electromagnetic radiation.

$$\Delta E = h\nu ; \text{ where } h: \text{Planks constant.}$$

$$h=6.63\times10^{-34} \text{ joule.s/molecule. } \nu: \text{Frequency.}$$

This absorbed or emitted energy is either rotational one; where molecule rotates about its center of gravity or vibrational; where variety of displacement from their equilibrium position or electronic energy occurs (Banwell, 1972).

The energy needed for the transition processes to be done from higher energy to lower are: Electronic, vibrational and rotational. Rotational and vibrational excitation occurs at internal energy level (Richard, Rachael, and Zijuan, 2014).

The infrared portion of the electromagnetic spectrum is usually divided into three regions; near-, mid- and far- infrared with wavelengths range ( $\mu\text{m}$ ) respectively; (0.78-3), (3-250), (250-1000) named after their relation to the visible spectrum wavelength (Abu Sharkh, 2014).

- Far-infrared (FIR), the lower part of this range may also be called microwaves. FIR is being absorbed strongly by water at Earth's atmosphere. (Bondless, 2014) According to Levin (1975) FIR contains a pure rotational transition of light molecules.
- Mid-infrared (MID), hot objects (black-body radiators) can radiate strongly in this range, and human skin at normal body temperature radiates strongly at the lower end of this region. This radiation is absorbed by molecular vibrations, where different atoms in a molecule vibrate around their equilibrium positions differently. This range is sometimes called the fingerprint region, since the mid-infrared absorption spectrum of a compound is very specific for that compound (Bondless, 2014), making MIR spectrum the most widely used for investigating structure and chemical bonds. (Richard, Rachael, and Zijuan, 2014)
- Near-infrared (NIR, this region has the highest frequencies; it can be detected directly by some types of photographic film, and by many types of solid state image sensors for infrared photography and videography. It deserved to be called Therapeutic window ranges between (600-1200) nm. It is widely used for treating higher depth through biological tissue (Niemz, 2004).

"Molecular spectroscopy is the study of the interaction of electromagnetic waves and matter. When infrared 'light' or radiation hits a molecule, the bonds in the molecule absorb the energy of the infrared and respond by vibrating. This absorbed or emitted energy is either rotational one; where molecule rotates about its center of gravity or vibrational (Banwell, 1972). There are six main movements that describe the vibrating molecules shown in Figure 3.2.

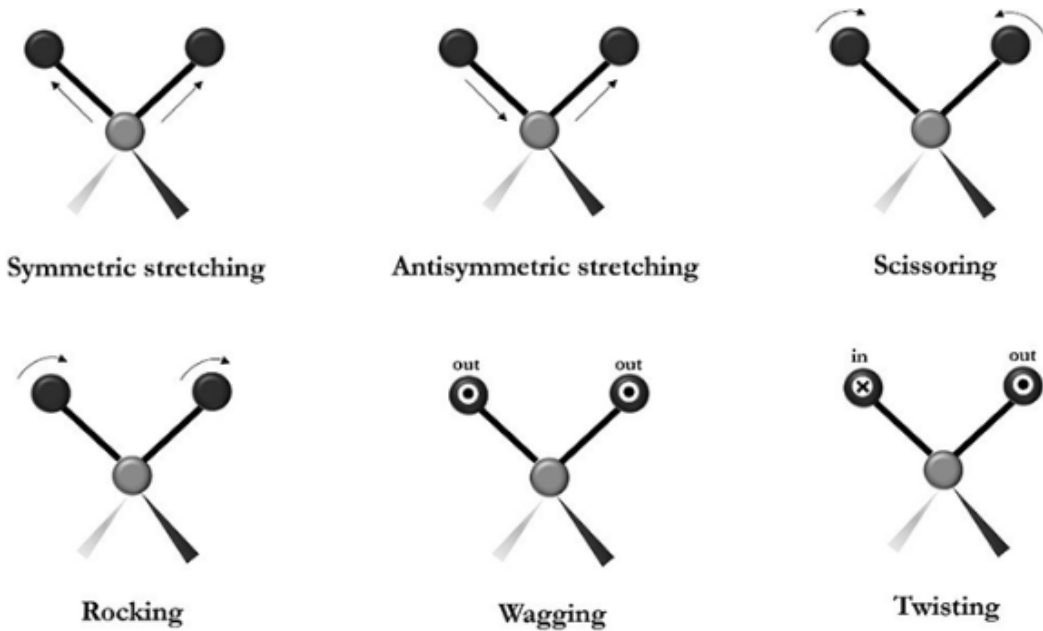


Figure 3.2: Main vibrational modes for molecules (Da Silva et al., 2017).

This study investigated whether these vibrations were enough to increase the biological tissue temperature and to create heat that would be able to affect the proliferation of cancer cell lines using broad band IR "Fe-Cr-Y source".

### **3.3 Infrared Sources**

About 80% of the sun's rays radiate IR spectrum (BioSmartTechnologies, 2014). As said previously anybody with finite temperature is a source of Infrared radiation. Any object will radiate infrared if its temperature is above 0 Kelvin (Hamamat, 2004). In the present work two pulsed sources were used in the experiment; a Bi-spiral and FeCr alloy stripes source.

#### **3.3.1 Bi-spiral source:**

This IR source acquired its name from the shape it is constructed in. It is constructed in a form of spiral supported by four legs as shown in Figure 3.3. This source is after Laine et al., 1997. Its diameter is 2 mm, it emits a broad band radiation in the range 750-15000 nm when operated at dull red~900°C. Its material is nickel-chrome alloy. It can be operated by a power function generator in the two frequency mode in which it is assumed to be self cooled between pulses.



Figure3.3: A Bi-spiral Source

### 3.3.2 FeCr alloy stripes source:



Figure 3.4: FeCr alloy sheet and Fe-Cr-Y source

This is the homemade source in its most simple form which is called Fe-Cr-Y. It is a sheet of FeCr alloy. This alloy is composed of Fe-Cr-Al steel containing “yttrium” at the following percentages: (Fe72.8/Cr22/Al 5/Y0.1/Zr 0.1) with foil thickness 25  $\mu\text{m}$ . The most versatile of the alloys that is suitable for use over wide range temperatures up to 1300°C. The “yttrium” Y can be used up to (0.3%) is the key to its longer high temperature life, having greater oxidation resistance. The optimum temperature for our experiment was  $\sim 900$  °C, or when filament is heated to dull red, the melting point of the alloy is  $\sim 1380$  °C. Foils are electrically heated followed by self-cooling process, in order to use them correctly to get the infrared radiation they must be electrically heated to about 900-1000°C (AZO, 2016).

The intensity of different dimensions of FeCr alloy stripes were studied by Buss (2009), which theoretically can be explained; to have an ideal thermal emitters its cross section area should decrease allowing its electrical resistance R of a rectangular conductor, but since the sheet thickness cannot be reduced then rectangular emitter area is increased by increasing its length or its width is decreased (Ott T., 2015). See Figure 3.5 and equation 1.

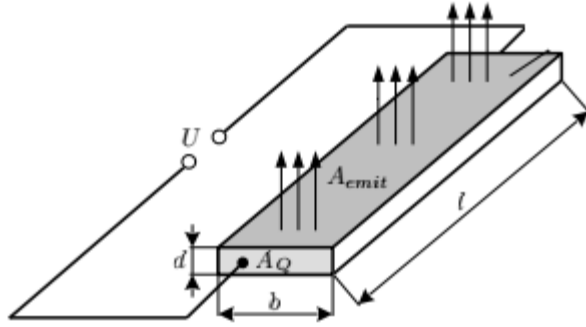


Figure 3.5: Physical dimensions of a simplified heating conductor (Ott T., 2015).

$$R = \rho \frac{l}{A_Q} = \rho \frac{l}{db} \dots\dots (1)$$

$\rho$ : specific electrical resistance.  $l$ : The conductor length.  $A_Q = d \times b$ . The cross sectional area.  $d$ : thickness.  $b$ : width.  $A_{emit}$ : emitting area.

As mentioned in the description of the IR sources, both are two sided radiator and this is a point that can be used to enhance the radiation intensity by reflecting the radiation beams toward targets using simple tools that are going to be mentioned in chapter 4.

There are three types of reflections that might occur to light and they are: internal reflection, specular (regular) reflection from polished surfaces, and diffuse reflection from rough surfaces (Khoshhesals, 2012), to enhance the reflectivity of some metals or tools it might be coated with a thin layer or mixed with metal flakes such as; Aluminume, nickel, and thin oxide coating (Wake and Brady, 1993).

### 3.4 Infrared detectors

An infrared detector reacts with infrared (IR) radiation (Wiki, 2014). Several characteristics should be considered in choosing detector type, e.g. beam wavelength, cooling method, response time, and the noise equivalent power (NEP) which is a measure of the performance of a detector (Buss, 2009), that represents the quality of incident light equal to the intrinsic noise level of a detector, signal-to-noise ratio (S/N) is 1.

There are two types of Infrared detectors which are thermal and quantum.

1. Thermal detectors: response to IR energy, some of their advantages are; low cost, don't need cooling, sensitive, robust under severe environmental conditions; ambient temperature and atmospheric changes while their main disadvantage is slow in response.
2. Quantum detectors: are faster, have higher detection and its photosensitivity depends on wave length, so it needs to be cooled except for NIR measurements (Hamamatsu, 2004; Fuji, 2014).

In this study a pyroelectric and thermocouple detectors are used; both of them are thermal detectors that operate at room temperature. The pyroelectric detector does not depend on wavelength of the received beam, instead it depends on the window material used.

1. Pyroelectric detector: consists of a PZT (Lead Zirconium Titanate) having the pyroelectric effect. The element surface is always electrified, but it is neutralized by ions in the air. When light enters the element and is absorbed, the element temperature increases, resulting in a change in the spontaneous polarization state leading to changes in voltage. It is necessary to use an optical chopper for measurement of still objects; otherwise it is not needed if the source is alternating.

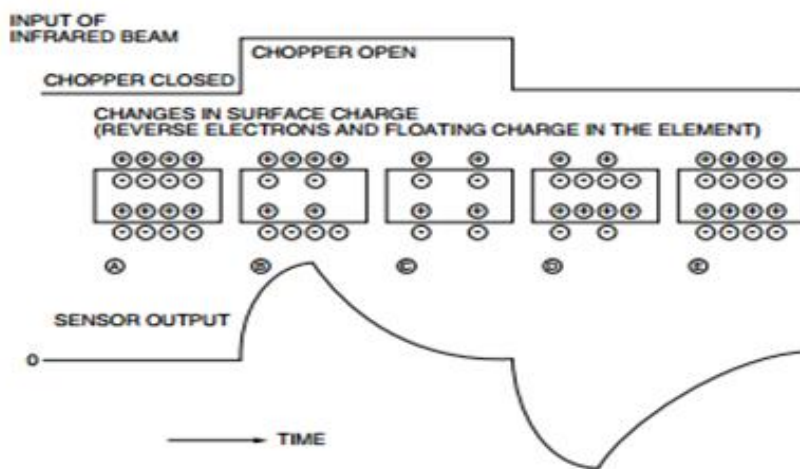


Figure 3.6: Schematic presentation of pyroelectric effect (Hamamatsu, 2004).

2. Thermocouple detector: It is a device used extensively for measuring temperature. It is a simple, widely used component (Beckwith and Lienhard, 1993; Duff and Towey, 2010).

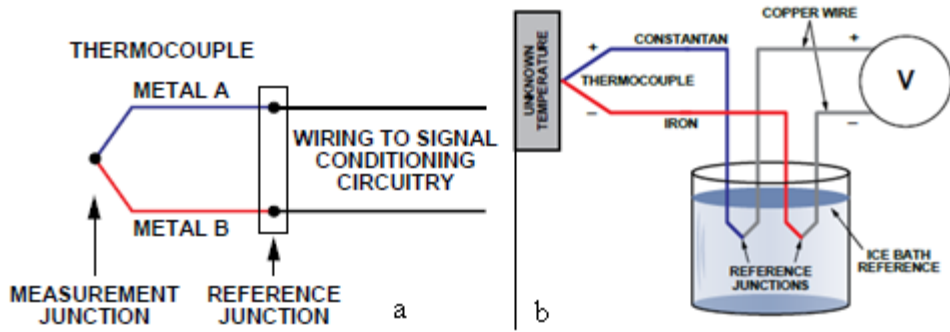


Figure 3.7: a) Schematic of a Thermocouple. b) Schematic of basic iron-constantan thermocouple circuit (Duff and Towey, 2010).

A thermocouple was shown in Figure 3.7, consists of two wires of dissimilar metals joined together at one end, called the *measurement* (“hot”) junction. The other end, where the wires are not joined, is connected to the signal conditioning circuitry traces, typically made of copper. This junction between the thermocouple metals and the copper traces is called the *reference* (“cold”) junction (Duff and Towey, 2010).

The working principle of thermocouple is based on three effects, discovered by Seebeck, Peltier and Thomson. They are as follows:

1. Seebeck effect: "states that when two different or unlike metals are joined together at two junctions, an electromotive force (emf) is generated at the two junctions. The amount of emf generated is different for different combinations of the metals."
2. Peltier effect: "when two dissimilar metals are joined together to form two junctions, emf is generated within the circuit due to the different temperatures of the two junctions of the circuit."
3. Thomson effect: "when two unlike metals are joined together forming two junctions, the potential exists within the circuit due to temperature gradient along the entire length of the conductors within the circuit" (Beckwith and Lienhard, 1993).

In order to get an accurate absolute-temperature reading, the reference junction must be known by putting it into an ice bath (Duff and Towey, 2010). So, in order to have emf through the circuit, a difference in temperature must sustain, results from the differences in metals

which are joint at the measurement junction. The total emf or the current flowing through the circuit can be measured easily by the suitable device.

The device for measuring the current or emf is connected within the circuit of the thermocouple. It measures the amount of emf flowing through the circuit due to the two junctions of the two dissimilar metals maintained at different temperatures.

The voltage or current output obtained from thermocouple circuit gives the value of unknown temperature directly (Beckwith and Lienhard, 1993).

Thermocouple is capable of measuring temperature in the range of (-200°C to +2500°C.), it is immune to shock and vibration and suitable for use in hazardous environments, also it is characterized with its fast response and no self-heating (Duff and Towey, 2010).

## **3.5 Light interaction with matter**

### **3.5.1 Introduction**

When light reaches the skin; interactions take place, interaction effects are due to absorption and excitation by photons (Foder, Elman and Ullmann, 2011). The interaction depends on the building blocks of the matter and the wave length of the incident light wave which may results in (reflection, refraction or absorption partially or totally of the wave ... etc.) (Flammer, mozaffarieh and Bebie, 2013).

Kemp (1987) mentioned that not all frequencies of Infrared spectrum are absorbed by the sample. In order for a molecule to absorb infrared radiation; change in its dipole moment must be sustained. If the molecule is polar, it will interact with the electric field of the spectrum and fluctuate during vibrational motion, otherwise absorption will not occur. In other words; if the frequency of the radiant IR spectrum matches the frequency of the molecule, then absorption occurs, and the amplitude of vibration of the molecule will change (Richar, Rachae and Zijuan, 2014).

### 3.5.2 Light absorption and scattering

When light is absorbed by tissue, its energy is transformed into chemical, thermal or mechanical energy which can be used to direct or selective cell death in therapeutic application (Niemz, 1999). Skin affected by light is of several degree of absorption of electromagnetic wave radiation (Flammer, mozaffarieh and Bebie, 2013). The relatively low absorption of near infrared light in biological tissue compared with visible and mid infrared spectrum allows the light to penetrate the skin and skull layers to sample the brain tissue beneath (Hollis, 2002). So scattering dominates over absorption (Heelspurs, 2015), at the end of Near Infrared spectrum, penetration is limited by the absorption of water. Absorption processes are important for diagnosis (serve as fingerprint of molecule) and therapeutic applications which are “light source illuminator to produce physical effects on tissue for treatment purposes” (Shanthi, 2013).

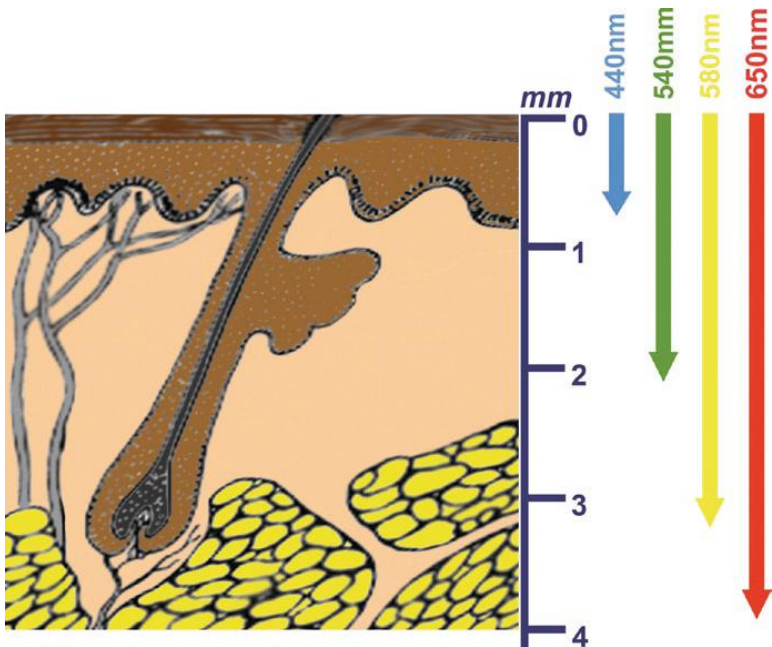


Figure3.8: Depth of light penetration into the skin, at various wavelengths (Shanthi, 2013).

Absorption is an observable quantity since it can be estimated by temperature and this can help in solving the ambiguity of optical tissue interactions (Okada et al., 1996). Many models were proposed to describe these interactions (Matcher, Cope, and Deply, 1997). Experiments in vivo and ex vivo were done to find the suitable model and their results were stimulated by

Monte Carlo program in order to find a good matches between the experimental and theoretical results using selected boundary conditions. These models will always be developed as long as more optical tissue interactions are known (Gheong, Prahl, and Welch, 1990).

Scattering arises from the microscopic variations and inhomogeneities of the refractive index (Shanthi, 2013), which is produced when an electric field of an incident beam forces the medium charge particles to oscillate, and re-emit the beam with frequency equals to the incident one which do not matches natural vibrations of tissue molecules(Hollis, 2002; Niemz, 2004). Also scattering processes are important in both diagnosis depends on the size, morphology, and structure of the components in tissues. While therapeutic applications provide useful feedback during therapy. The scattering process is affected by the size and the structure of the tissue, Ralyleigh and Mie explained the process: Rayleigh limit occurs when the scatterers are much smaller than the wavelength of light and Mie scattering occurs when the size of the scatterers is comparable to the wavelength. The angular distribution of scattering is described by the scattering phase function,  $P(\theta)$  which gives the probability of a photon to be scattered at an angle  $\theta$ , with respect to the initial direction of incidence and the scattered waves will interfere with the incident wave, modifying its phase and hence the velocity of the light through the medium, as a result of scattering, the velocity of light in all matter is less than that *in vacuo* (Shanthi, 2013).

Absorption and scattering process synchronize light intensity reduction; in absorption phenomenon photons are being transformed into thermal energy, while scattering photons would change their direction (Cope, 1991). Banwell (1972) explained that as the beam penetrates longer distance in a sample the absorption increases which is called Path Length of Sample. Multiple scattering processes through tissue make it very difficult to predict its physical path length between the beam entrance and exit from the tissue using NIRS and optical imaging techniques, overcoming this dilemma has a great influence in understanding the optical properties of tissue (Okada et al., 1996). This relation can be expressed in terms of the Beer\_Lambert law which relates the attenuation of light to the properties of the material through which the light is traveling. In biology and physics, they are normally written as in equation (2):

$$T = \frac{I}{I_0} = e^{-\Sigma \ell} = e^{-\sigma \ell N} \dots\dots (2)$$

where  $\mathbf{T}$  is the attenuated beam,  $\Sigma$  is the linear attenuation coefficient,  $I_0$  and  $I$  are the intensity (power per unit area) of the incident radiation and the transmitted radiation, respectively,  $\sigma$  is the attenuation cross section,  $\ell$  length and  $N$  is the concentration (number of atoms per unit volume) of the attenuating medium (Banwell, 1972). But in biological tissue where the medium is turbid, the Beer\_Lambert law is inefficient (Hollis, 2002; Shanthi, 2013). There is another relation that describes the relation between radiation intensity of light and distance called inverse square law.

$$I = c/x^2 \dots\dots (3)$$

$I$  is the radiation intensity,  $c$  is a proportionality constant,  $x$  is the distance travelled (Pidwirny, 2006).

### 3.5.3 Chromophores:

The components of tissue which are responsible for absorbing light are called Chromophores (Fodor, Lucian, and Ullmann, 2011). Types of Chromophores include the following:

#### 1. Hemoglobin

It is present in red blood cells forming 40-45% of it. The majority is carrying out oxygen to cells tissue and returning with carbon dioxide to lungs, known as the most chromophores in biological tissue for near infrared radiation. Specific absorption of NIR is in the range of 650–1050 nm (Cope, 1991).

#### 2. Water

According to Marieb (1995) water forms 60 \_ 80 % of our bodies which made it a very active chromophore. Water has low absorption over NIR. Beyond 0.9  $\mu\text{m}$  absorption rises sharply with increasing wavelength (Heelspurs, 2015).

### 3. Lipids

Lipids can be found in subcutaneous tissue and around internal organs. Lipids are not even spread through the tissue of body e.g. lipid forms 11.6% of brain. Most fat in our body is neutral fats of the form triglycerides. Another fat is Phospholipids, which are the main component of cell membranes (Hollis, 2002).

#### 3.5.4 Heating:

The thickness of the targeted tissue, the wave length of the incident beam and chromophores control the absorption process (Niemz, 2004), which is responsible for heating the tissue making targeted tissue temperature to increase higher than surrounding. Increasing temperature may cause irreversible changes to DNA, RNA and some proteins. These changes will end up with denaturation and coagulation for them (Fodor, Lucian, and Ullmann, 2011).

Heat therapy has multiple forms: microwave radiation, laser, water bath (Mise et al, 1990), and perfusion; "blood combined with melphalan" (Luk, Hulse and Phillips, 1980). According to Kenge, lakhssassi, and Vaillancourt (2012) alternative frequency wave heating source is more effective in increasing the dermis temperature than continuous frequency wave source.

In medicine, bioheat transfer has important applications which are thermal therapies and cryopreservation. Heat therapy is divided into two types (Bischof, 2006):

1. Hyperthermia, describes treatment sessions including temperature ranging (42°C -45°C) extended for hours (Bischof, 2006). Many researchers found that hyperthermia might have the ability to decrease the rate of tumors developing for immunogenic therapy (Luk, Hulse and Phillips, 1980).
2. Thermal therapy, describes treatment sessions with temperature greater than 50°C for couple of minutes (Bischof, 2006).

In order to declare a sufficient protocol or adopt model for heat therapy, many factors must be investigated combining biophysical properties with biology (Bischof, 2006). An effective selective destruction of tumor tissue using thermal therapy must be based on a carefully planning side by side with technology improving (Luk, Hulse, and Phillips, 1980). Temperature is a major factor that controls thermal therapy outcomes (Bischof, 2006).

### **3.5.5 Cancer treatment:**

Cancer is a disease in which cells grow and divide uncontrollably (Abasalt, Mohammad, and Tahereh, 2011). It is important to find alternative treatments other than surgical resection, radiation and chemotherapy to treat benign cancer. These treatments are clinically difficult to be dose controlled since it affects the normal tissue in a bad way (Luk, Hulse, and Phillips, 1980). The side effects of the traditional treatments for cancer motivated researchers toward low-energy IR radiation treatment (Tichauer, 2014; American cancer society, 2017).

Thermal therapies are a promising alternative treatment (Bischof, 2006), and this is because high temperature can damage and kill cancer cells, usually with minimal injury to normal tissues (Luk, Hulse and Phillips, 1980; Van der Zee, 2002). On the other hand Kenge, lakhssassi, and Vaillancourt (2012) clarify that many researches agreed that heat therapy is less effective in treating cancer alone, in agreement with results obtained by Luk, Hulse and Phillips (1980).

Hyperthermia is almost always used with other forms of cancer therapy, such as radiation and chemo therapies. Hyperthermia may make some cancer cells more sensitive to radiation or harm other cancer cells that radiation cannot damage. When hyperthermia and radiation therapy are combined, they are often given within an hour of each other. Hyperthermia can also enhance the effects of certain anti cancer. The effectiveness of hyperthermia treatment is related to the temperature achieved during the treatment, as well as the length of treatment and cell and tissue characteristics (Luk, Hullse, and Phillips, 1980; Van der Zee, 2002; Hildebrandt et al., 2002; Kaur et al., 2011).

### **3.5.6 Cancer diagnosis:**

Some cancer diseases are difficult to be diagnosed at early stages of the cancer, e.g. gastric cancer (Di Mario et al. 2006). Finding new methods to detect cancerous tissues led them to therapeutic targets. Infrared has become a reality, due to huge clinical studies and developing Infrared spectroscopy instruments. This method is non-destructive for biological samples like ultraviolet, x-rays and gamma rays (Parker, 1971; Neumann, 2002). IR has the ability to

distinguish between normal and tumor tissue, since tumor tissues absorbs more infrared radiation than healthy one, this can be displaced by photograph making use of infrared cameras. This device is called thermo gram (Bitesize, 2014). It is important to find new novel diagnostic techniques to diagnose the disease in its earlier stages similar to "biochemical finger print" of the tissue (Abasalt, Mohammad and Tahereh, 2011). In most cases, by the time of tumor detecting; it would be spread widely in the body (Obayashi, 2015), and an early stage diagnosis is vital for successful treatment.

### **3.5.7 Cancer Cells affected by heat:**

Hyperthermia mechanisms are not well known yet, but there are some indications such as protein denaturation and damaging DNA by radiation causes growth stop (Lepock, 2002). Also, changes in the membrane permeability and distortion in the cell shape is sustained (Bischof, 2006). According to Kalamida et al. (2015) temperature above  $41^{\circ}\text{C}$  is a toxic temperature for cancer cells and is used for suppressing their growth. Cancer cells are affected by radiation faster than normal cells because their cells tend to divide more quickly and they grow out of control (American Cancer Society, 2014). Cancer cells are more sensitive to heat because they cannot adapt themselves with physiological stresses of heat and this make them more affected to heat-induced death than normal cells (Icnirp, 2012), by damaging proteins and structures within cells (Hildebrandt et al., 2002). If the absorbed heat by tissue was in large amounts it can cause burns or tissue damage (National Cancer Institute, 2014).

## **Chapter four**

### **Experimental system**

#### **4.1 Introduction:**

This chapter describes the research methodology used to fulfill the aims introduced in chapter 1 quantitatively. Using Fe-Cr-Y source which was powered by an electrical circuit (see details: Buss, 2009). In this work a broad band infrared radiation will be allowed to fall on biological samples and to achieve this goal several steps were taken to ensure the results reliability.

#### **4.2 study design:**

The source is attached to an electrically pulsed circuit. This allows it to radiate pulsed broad band infrared radiation. The complete experimental circuit used to run the IR source is shown in Figure 4.1.

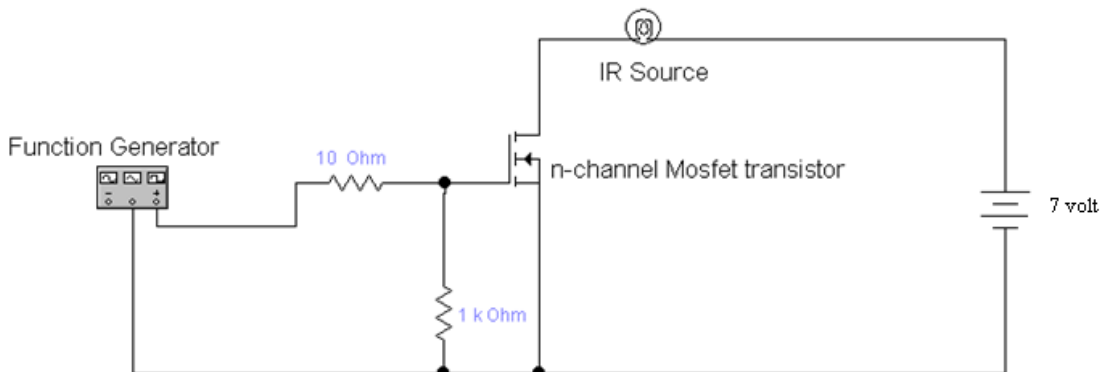


Figure 4.1: Schematic showing turning on constructed source.

A power function generator model TFG-8101 was used to power the IR source in pulse mode, in conjunction with a DC power supply model GPS-1850 to supply enough current to turn on the source. MOSFET transistor was used as a switch to control high currents passing through source, when the current source is applied the switching MOSFETs will be turned on and when the current source is disconnected the switching MOSFETs will be turned off. So, its main purpose is to drive current from power supply. As a closed switch; it's RDS (resistance

between source and drain) is very small, this allows current to pass without consuming energy or increasing in the transistor temperature. Its maximum gate threshold voltage ( $V_{GS\text{th}}$ ) is 4V (Buss, 2009).

### 4.3 Trigger circuit:

The function of this electronic simple circuit is to limit the voltage across the lock in amplifier from the function generator which must be 0.5V. This circuit is called the clipping circuit and consists of four carbonic resistors and two diodes connected as in Figure10, when the voltage from the function generator exceeds 0.7 V it will give us voltage of 0.7 V, with the load resistors this voltage is limited to 0.3V (Buss, 2009).

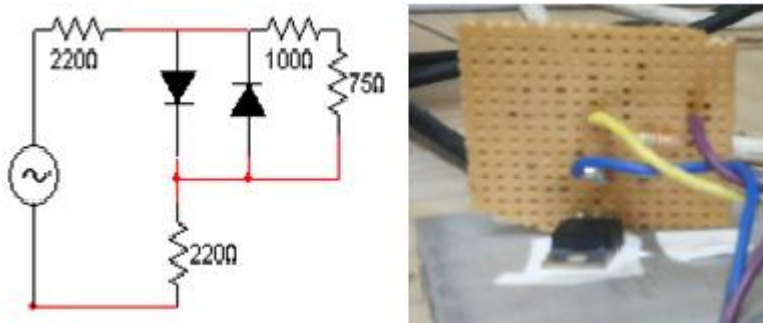


Figure 4.2: A schematic and a photograph of MOSFET with a sketch of the clipping circuit used to trigger the lock in amplifier with 0.3 V reference signal.

Since the IR source material is heated electrically by high current (more than 2 Amp), this will be dissipated in the form of heat, to avoid circuit damage a heat sink is used to dissipate the excess heat through the sinker.

#### 4.4 Characteristic study of IR source

The Fe-Cr-Y source characteristics were studied extensively as mentioned in ch.3. A Lock-in amplifier from Scitec Instruments Ltd (2017) is used for recovering signals that are buried in noise compared to a reference signal of the same frequency. This reference square signal was directly taken from the function generator to the reference socket of the Lock-in amplifier. Input signal from a pyroelectric detector which collected IR source radiation is fed into the input part of the phase sensitive detector.

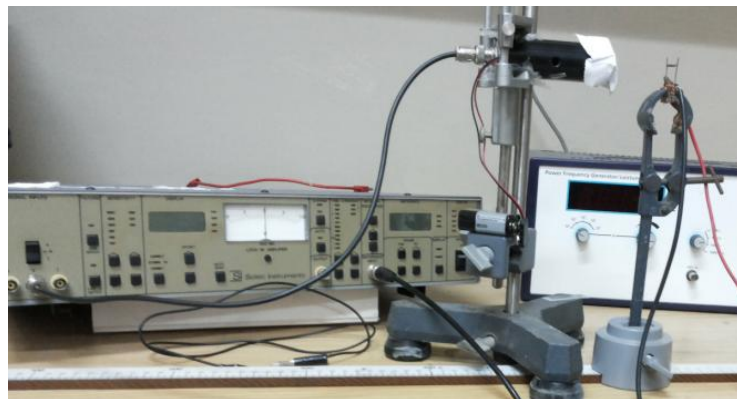


Figure 4.3: Investigating Fe-Cr-Y source set up

As shown in Figure 4.3 the constructed source is facing the detector window. IR source position can be changed along the guiding meter stick without loss of alignment.



Figure 4.4: Investigating Fe-Cr-Y source intensity vs. angle

This arrangement allows studying energy distribution at different angles with respect to source angle.

## 4.5 Focusing tools

The IR source is a two sided emitting source, i.e. it emits in the forward and backward the same amount of radiation, see Figure 4.5.

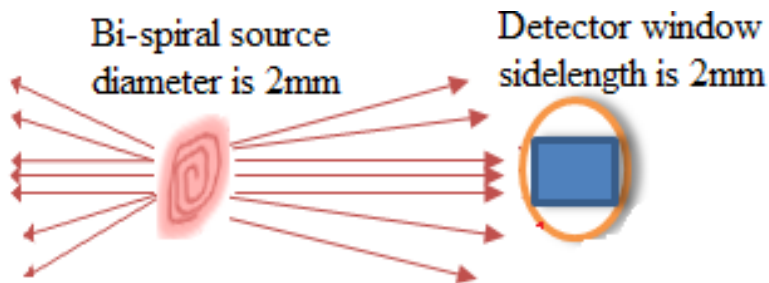


Figure 4.5: A schematic of the radiation behavior without using a reflector or a waveguide tools.

Focusing light from IR source can be employed to focus the forward beam or double the intensity by collimating the backward beam into forward direction. Wave guides are simple tools with different geometry have the ability to reflect infrared radiation; it is used to enhance the source radiant intensities. Since the IR radiation is highly attenuated along the skin depth; increasing the intensity delivered to the biological tissue will increase as well as the absorbing process and it will lead to higher thermal effect by making a heat zone (Wake and Brady, 1993).

The used focusing tools are presented in the following photo Figure 4.6.

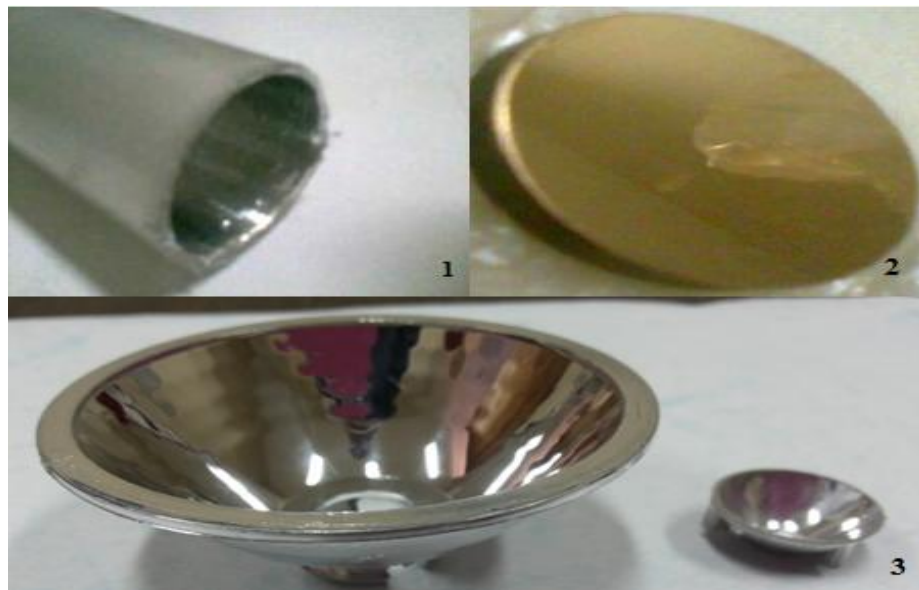


Figure4.6: Photograph of different wave guides. 1) Aluminume tube wave guide. 2) Gold mirror wave guide. 3) Hemisherical wave guide.

#### 4.5.1 Aluminume tube wave guide:

An Aluminume tube length 80 mm and diameter 15 mm was used infront of the source in order to direct forward infrared radiation by reflecting the broad beam into several angles along the tube. As shown in the following Figures.



Figure 4.7: A photo of Al tube wave guide in front of the Bi-spiral source

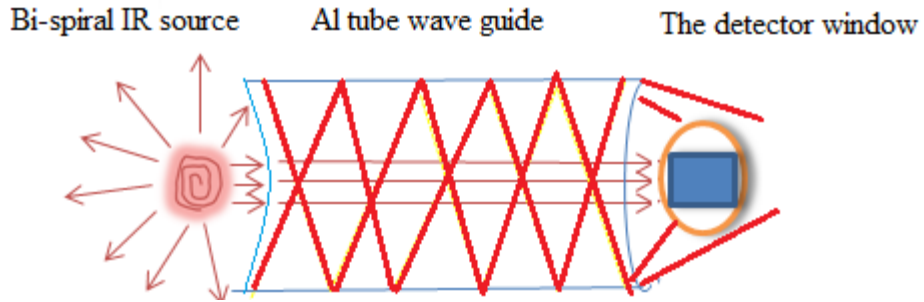


Figure 4.8: A schematic of the radiation behavior along the Al tube wave guide.

The red beams are the reflected ones from the inner surface of the Al tube.

#### 4.5.2 Gold mirror reflector:

A 30 mm diameter flat and front coated mirror with gold is used to enhance the infrared radiation source by reflecting the backward beam of the other side of the source in the forward direction towards the detector window. As shown in Figure 4.9.

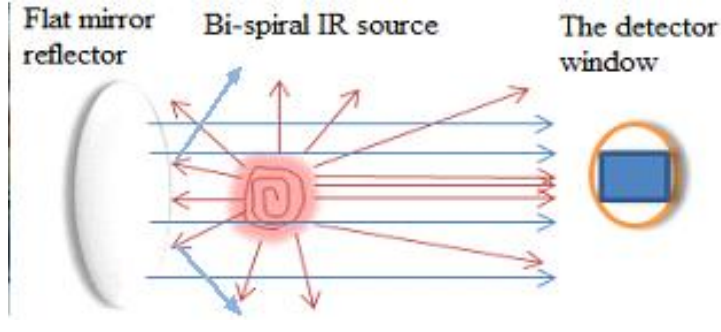


Figure 4.9: 1) A photo of flat mirror placed behind the FeCr alloy stripe source. 2) A schematic of the radiation behavior when incident on flat mirror reflector.

The blue beams are the reflected one from the surface of the flat mirror.  
Note: not all reflected beams will return back with  $90^0$  within the detector window.

#### 4.5.3 Hemispherical reflector:

Two different sizes of hemispherical mirrors were taken from torches to investigate their effectiveness to enhance infrared radiation focusing in the forward direction. Their dimensions are: First, the bigger one diameters are (45 and 12) mm and its depth is 22mm. Secondly, the smaller one diameters are (20 and 8) mm and its depth is 6 mm, see Figure 17. They were positioned behind the infrared source in order to reflect the source backward radiation towards the detector window, see Figures 4.10, 4.11 and 4.12.

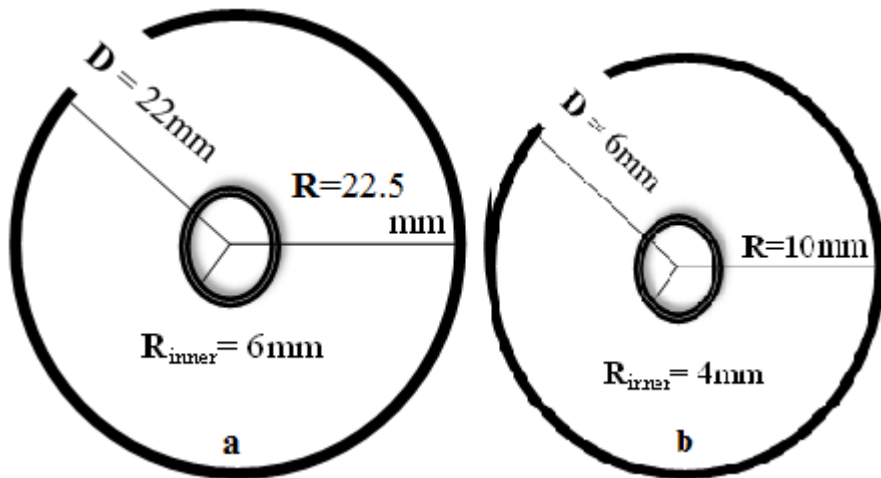


Figure 4.10: A schematic of two different hemispherical reflectors, a and b.



Figure 4.11: A photo of Hemispherical wave guide behind the Bi-spiral source.

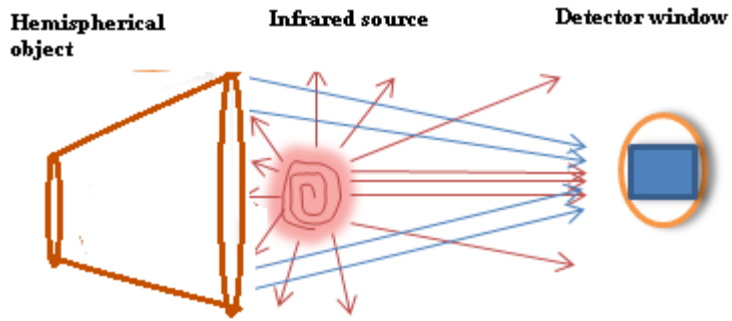


Figure4.12: A schematic of the radiation behavior when beam collides with the inner surface of hemispherical reflector.

The blue beams are the reflected ones from the hemispherical inner surface.

## 4.6 Tissue experiment

Tissue sample was taken from white rats. The rats are raised in controlled conditions. Two versions of experiments used; in-vitro and in-vivo. In the case of in-vitro trial; formalin and ether were used to end the rat's life and for in-vivo experiment; Ketamine was used to anesthetize the rat, vernier caliper was used with accuracy 0.01mm to measure the samples dimensions.

### 4.6.1 In-vitro experiment set up:

Samples were taken from either skin or thigh and stretched over a plexiglass plate. The arrangements allow easy measurements of temperature distribution from the other side by inserting thermocouples through holes 1 mm diameter drilled in the plexiglass plate, as presented in Figure 4.13.

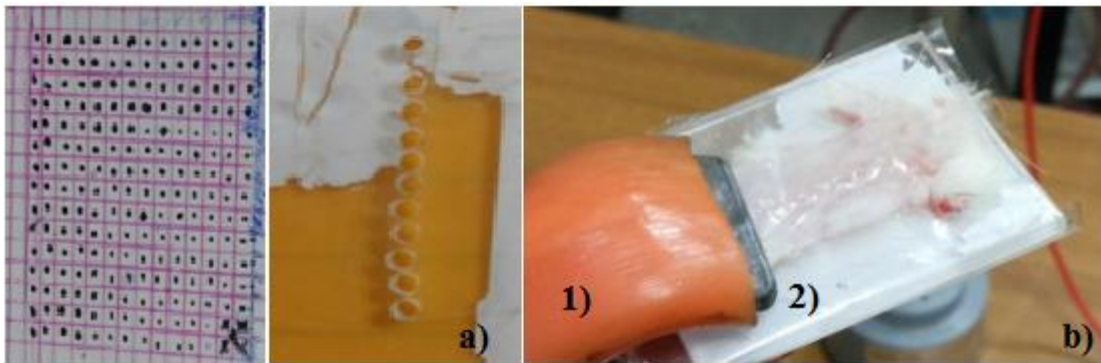


Figure 4.13: a) Plexiglass plates. b) Tissue sample was stretched over plexiglass plate; 1) the holder. 2) The plexiglass plate

The grid plexiglass holes are separated horizontally by 3 mm and by 2 mm vertically between the holes as in Figure 4.14. For one column plexiglass holes, they are separated from the first hole respectively; 4, 9, 11.5, 14 and 16.5 mm, see Figure 4.15.

Two thermocouple probes were used to measure temperature; one was fixed on a point of tissue directly under the IR source and the other is manually moved over different marked points.

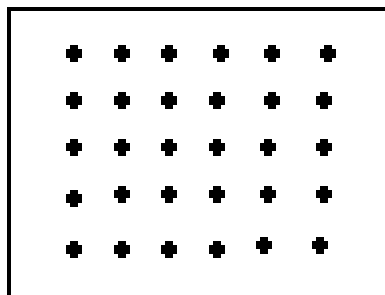


Figure 4.14: A schematic of the plexiglass plate with grid holes

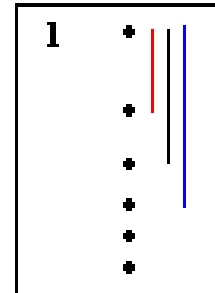


Figure 4.15: A schematic of the plexiglass plate with one column of holes

#### **4.6.2 In-vivo experimental set up:**

White rats were used in order to study the temperature distribution over the belly shaved skin and at 1mm depth of skin; which is the rat's skin thickness. Also, the belly upper muscle was examined and its thigh temperature depth. These areas were marked and temperature was taken for these spots using a thermocouple type k which was connected to Pasco Interface 750 and the data was recorded using Data Studio program.

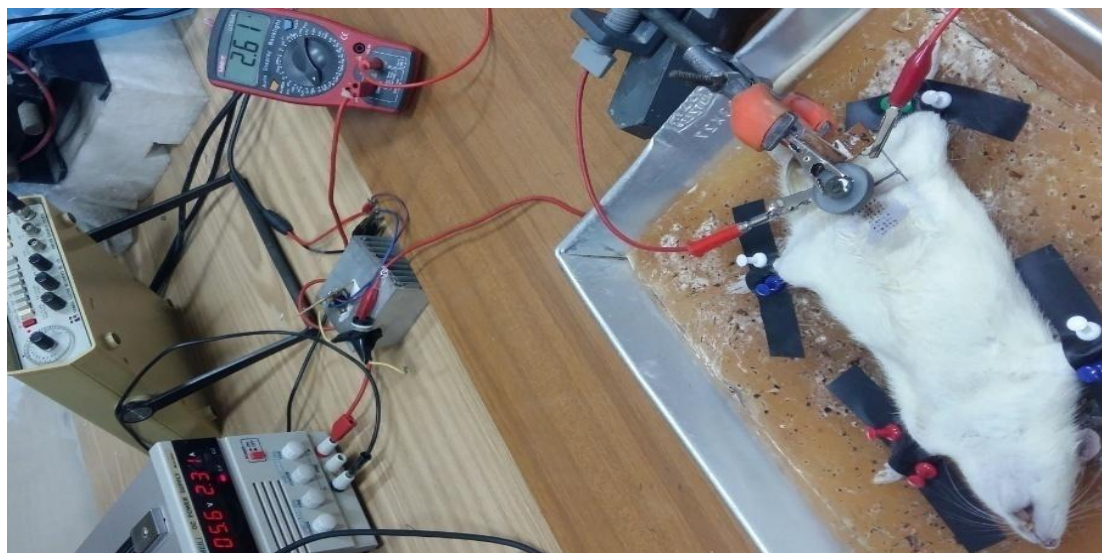


Figure 4.16: Photo showing experimental setup for IR tissue absorption in vivo.



Figure 4.17: Photo showing direct IR absorption by rat's shaved skin.

Figure 4.18: Photo showing in vivo IR absorption by rat's belly muscle.

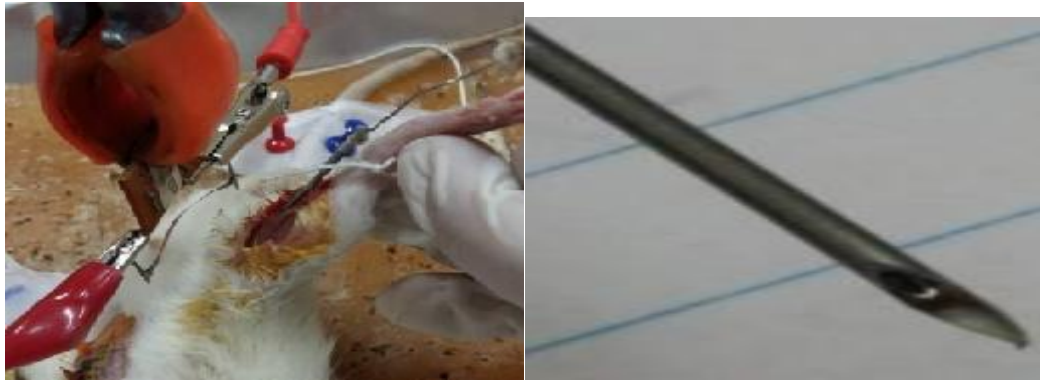


Figure 4.19: Photo showing in-vivo IR absorption set up by different depths through thigh muscle.

Figure 4.20: The thermocouple probe was inserted into needle to reach different depths in thigh tissue.

To explore the temperature distribution through thigh muscle at different depths using thermocouple probe, it was insert into a hollow needle as in figure 4.20. The needle length was 3 cm and the distance that was probed 1.7 cm, the rat temperature was 31°C before irradiation. It should be mentioned that the depth is horizontally increasing not vertically; since the rat thigh will not exceed 1.5 cm, the idea of inserting the thermocouple probe inside a hollow metal needle was performed in Kim and Jeong experiment (2013)

#### 4.6.3 In-vitro cancer cell line set up:

Cancer cell lines were cultured in a 10cm cell culture dish and incubated in humidity chamber at 37 °C with 5% CO<sub>2</sub>.

First stage was measuring temperature for cancer cell line at marked points within 10 minutes duration in an open hood out from the incubator. Thermocouple type k was used to measure temperature and data was recorded by Data Studio program.

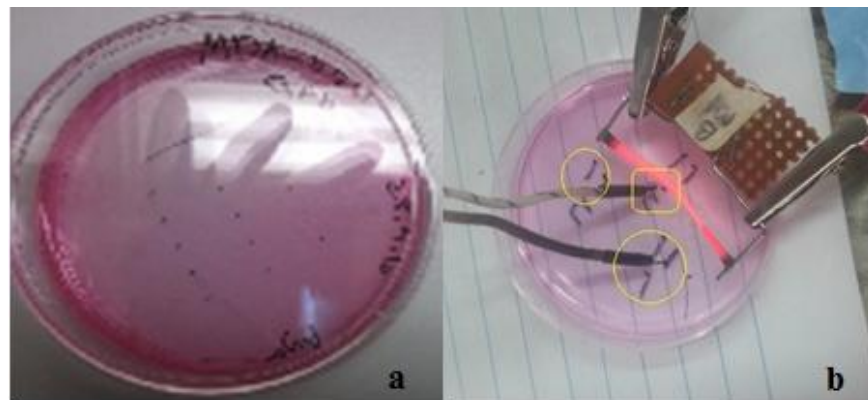


Figure 4.21: A photo of 10cm cell culture dish marked in different ways to monitor temperature; a) marked as grid. b) marked as separated area.

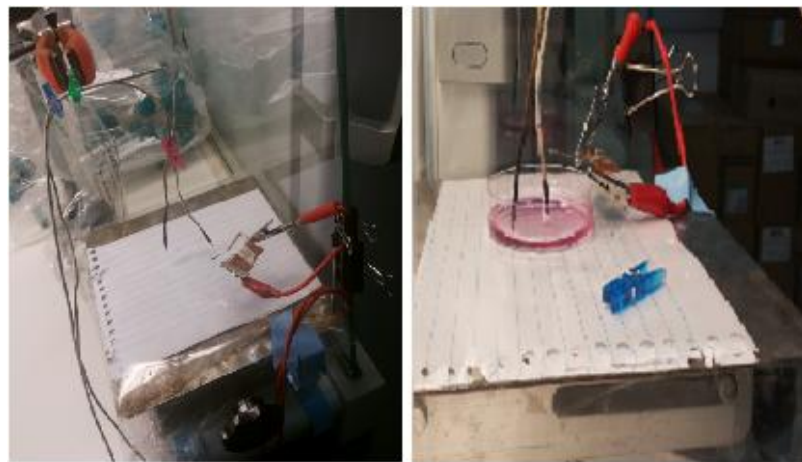


Figure 4.22: A photo of in-vivo cancer cell line in an open hood from different direction.

Before radiation sessions and after the end of session cancer cell line condition was examined using an inverted microscope.

Second stage: was monitoring temperature and its effect over the growth of the cancer cell line. The experiment was done inside the incubator.



Figure 4.23: A photo showing cancer cell line setup inside the incubator; a) the used equipment. b) Probing media temperature of the sample inside the incubator.

## 4.7 Study settings and materials

### 1. IR sources studying characteristics:

The Fe-Cr-Y source circuit was constructed in 2009 by Buss from FeCr alloy strip to radiate broad band infrared and it is used to study its ability to affect biological sample tissue, its intensity characteristics with distance, current and frequency were studied using thermal detector “Pyroelectric detector” connected to Lock-in amplifier; the studied frequency was in the range of 10 to 20 Hz. Its characteristics were compared with another thermal source (Bi-spiral source) made in Keel University by Laine and co-workers (1997). The experiment was done in LASER physics research laboratories of Al-Quds University.

## **2. Rat tissue temperature study:**

Investigating point temperature distribution over an excised white rat tissue, over dead rat tissue (not excised tissue), and for white rat living tissue; the experiments were held in LASER physics research laboratories of Al-Quds University. The targeted tissue were skin surface, back side of the skin; its thickness is 1 mm, and muscles tissue; belly surface and for different depths of the rat thigh; the muscles are directly exposed to radiation after removing the skin. Six controlled white rats were used, supplied from physiology laboratory in Al-Quds University. Ketamine was used to anesthetize a 174.3 gm white rat; one mg of Ketamine was dissolved in 10 mg of saline and was given to the rat by injecting it under the skin in the abdomen. It is useful for short procedures and is inexpensive (Kurdi, Theerth, and Deva, 2014), the rest of them were death using formalin and ethanol. The electrical arrangements for Fe-Cr-Y source were almost the same for all experiments and they were: 12 Hz frequency and voltage ranged from 5.00 to 6.00 volts and the current oscillated between (2.21-2.70) Ampere. While the electrical arrangements for Bi-spiral source were: current 0.3 Ampere, AC voltage 1.69 volts and frequency was 12 Hz.

## **3. Cancer cell lines temperature study:**

Breast cancer cell lines including MCF7, MDA cells were grown in RPMI media (from tissue culture lab in Al-Quds University which is under supervision of Dr. Zaidoun Salah, supplemented with 10% FBS, 1% glutamine, and 1% penicillin/streptomycin. Colon cancer cell lines including Caco-2, HT-29 and HCT-116 cells were grown in DMEM/F12 media supplemented with 5% horse serum, 1% glutamine, 1% Penicillin/Streptomycin KHOS cancer cell line is referred to as bone cancer. Cells were incubated in humidity chamber on 37 °C with 5% CO<sub>2</sub>.

The sample was exposed to the IR radiation to investigate the influence of radiation on the cell proliferation.

Some trials were done in tissue culture lab, where irradiation sessions were done in an open hood. The source placed ≈ 2.00 cm away from the sample and the electrical arrangements of the experiments were: frequency 13 Hz, voltage ranged between 4.90 to 6.80 volts and current oscillated between 2.31 and 2.51 Ampere. Temperature of the media was monitored by two

thermocouples for certain positions (as in figure 4.22) one of them is connected to channel A and the other one to channel B where the last one is relatively nearer to the IR source. The total session duration for all trials did not exceed 10 minutes and after two sessions or less duration the sample was returned back into incubator for couple of minutes.

Other trials were held at the Medical research center in Al-Quds University. The irradiation sessions were done in a suitable environment of cancer cells *in vivo* into incubator. The electrical arrangements for the following experiments were; I (1.97-2.26) Ampere, voltage 7.00 volts and the frequency was 11 Hz. Cancer cell line initial temperature before irradiation was 28°C. Temperature of the media was monitored by two thermocouples at certain positions

#### **4.8 Data collections:**

The first data collection was about the source characteristics:

The source intensity was investigated with distance, frequency, current and time using phase detector device which displayed the results. Data was manually collected, and displayed by data studio and origin program.

The second data collection was "in-vivo rat temperature":

Thermocouple props were touching the rat skin at the start of irradiation and temperature results were collected and displayed each 0.1 second using Pasco Data Studio program which has some other statics options such as maximum value, minimum value, mean value, standard deviation and others.

The third data collection was "in-vitro cancer cell line":

In spite of the experiment place, the data had been collected and displayed using Data Studio program, were thermocouple probes were touching the cell line in the plate when the irradiation started.

Statistical analysis: Data are expressed as the mean ± standard deviation.

#### **4.9 potential limitations:**

There were some obstacles during the implementation of the experiment:

1. Help was requested from biological department and it was offered by Mr. Raed Rizq.
2. Supplying anesthesia. 20 mm of ketamine was donated by hospital.
3. Help was requested from tissue culture laboratory and help was offered by the lab technician.
4. The population of the samples was limited due to poor laboratory resources.

#### **4.10 Ethical considerations**

Ethical considerations of the study have been addressed by implementing the following measures:

1. Ethical approval was obtained from ethical committee of Al-Quds University, Institutional Review Board (IRB).
2. Texts belonging to other authors and used in any part of this study have been fully referenced with Harvard Referencing System.

## **Chapter five**

### **Results and discussion**

#### **5.1 Introduction**

The results of the experiments were presented and discussed in this chapter: Firstly, the results of studying the characteristics of the thermal sources used were presented. Secondly, the results of the effect of thermal sources radiation on biological tissue were presented, namely temperature effect. Finally, the effect of broad band irradiation on the growth of different cell lines is investigated.

#### **5.2 Characteristics of IR radiation from two different sources**

In this section IR radiation from two types of sources will be studied.

Radiation intensity from a Bi-spiral type source (Laine et al., 1997) is studied against distance, current, and frequency. Fe-Cr-Y source is of greater interest; since it is very simple and inexpensive one.

The behavior of radiation intensity is expected to follow a decay according to the inverse square law, see (equation 3, section 3.5.2); so as the distance separation horizontally between the infrared source and detector increases the intensity of radiation will decrease. The fitting is going to be shown later.

##### **5.2.1 Bi-spiral source:**

Characteristics study of this source output intensity against distance and frequency.

###### **5.2.1.1 Radiation Intensity Distance dependence:**

Since the power supply is not a constant current source, the current ranged between 1.90 mA to 2.16 mA and frequency was 12 Hz; hence the current and frequency is manually selected each time. Hashmi et al. (2010) confirmed that low pulse frequencies are more effective with biological tissue treatments as it allows more penetration. Also, the pulse width or ON time is

higher at low frequencies than high frequencies; 12 Hz has a time width of 43 ms than higher frequency. The initial distance separating the source from the detector window was 20mm. The Bi-spiral source intensity radiation kept full for the first 20 mm separation measurements i.e. current and frequency kept constant while distance between source and detector changed, then it started to decrease inversely proportional to the distance squared, and was fitted using origin program, see Figure 5.1.

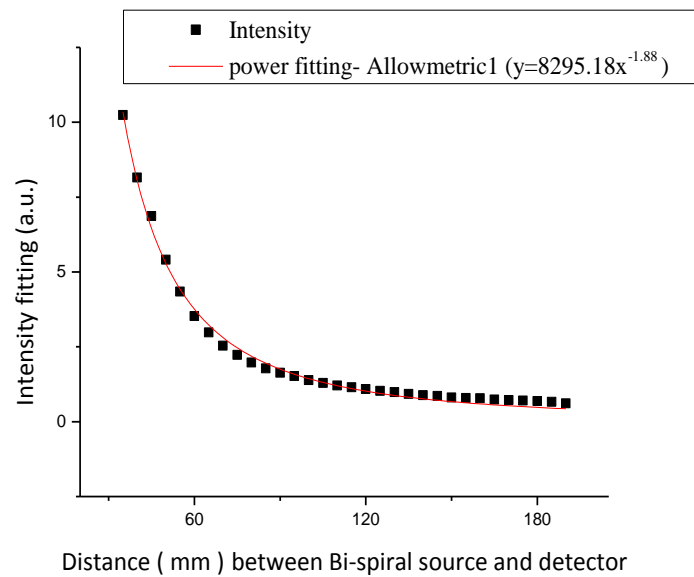
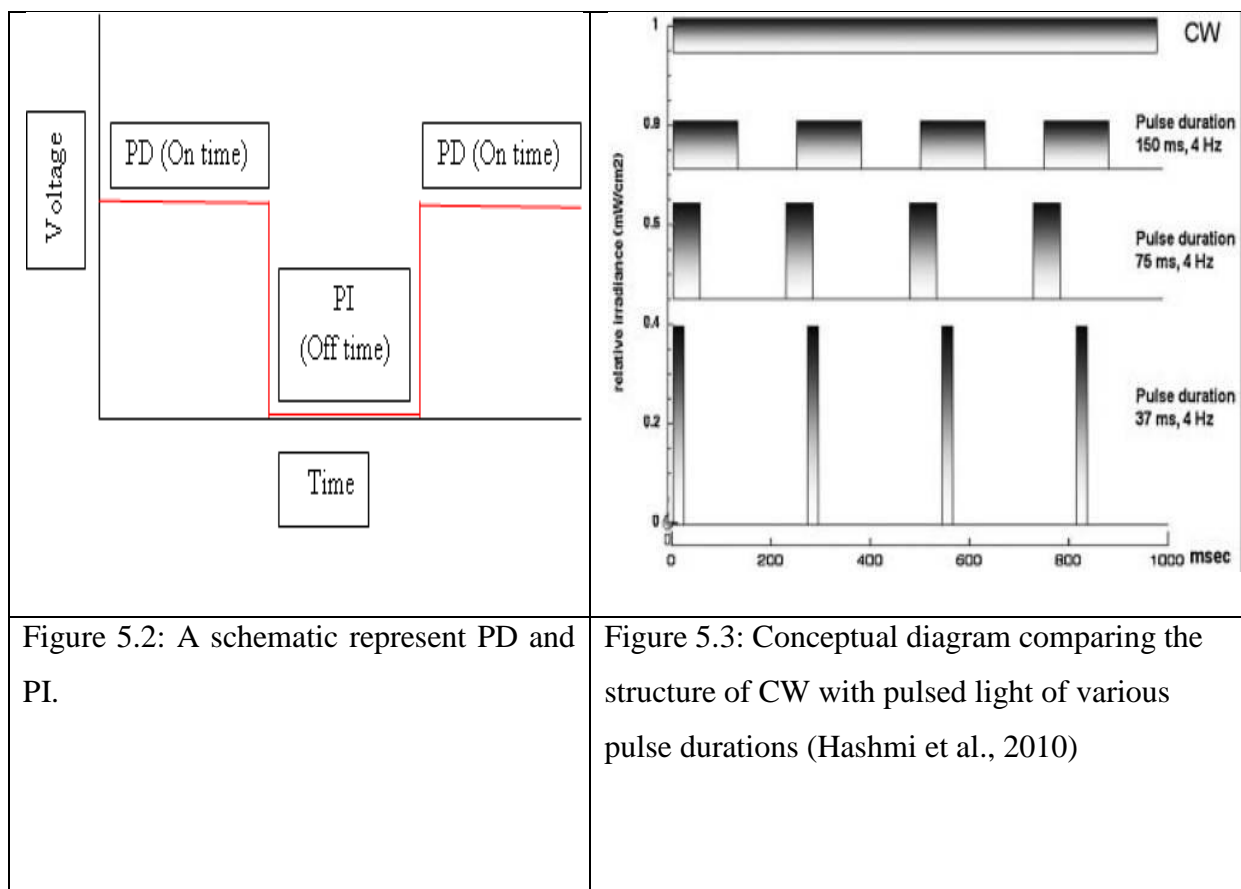


Figure 5.1: IR Intensity vs. distance fitting.

The fitting showed that the power of  $\mathbf{x}$  in the inverse square law, See equation 3, to be (-1.88) which reasonably close to the (-2.00) expected.

### 5.2.1.2 Radiation Intensity from Bi-spiral source Frequency dependence:

The delivered intensity from the IR source to the detector depends on the power generator frequency. In the following experiment the distance between detector and source were kept constant at 40 mm. It is expected for IR intensity to decrease as the frequency increases; since its pulse width or ON time or Pulse duration (PD) (Hashmi et al., 2010) will decrease. As the radiation time for one cycle is decreased, the delivered IR intensity for detector of one cycle is also decreased. PD and pulse interval (PI) or off time can be controlled by increasing or decreasing its time using function generator, see Figure 5.2.



Using Oscilloscope the PD for some frequencies were taken; frequencies are: (11.5, 12, 13, and 13.5) Hz and their PD respectively; (44, 42, 38, and 35) ms, but for the same frequency, as shown in Figure 5.3.

The attenuation of the Bi-spiral source radiation intensity as frequency increases above 13 Hz was found to be similar to that of Buss (2009) results, see Figure 5.4.

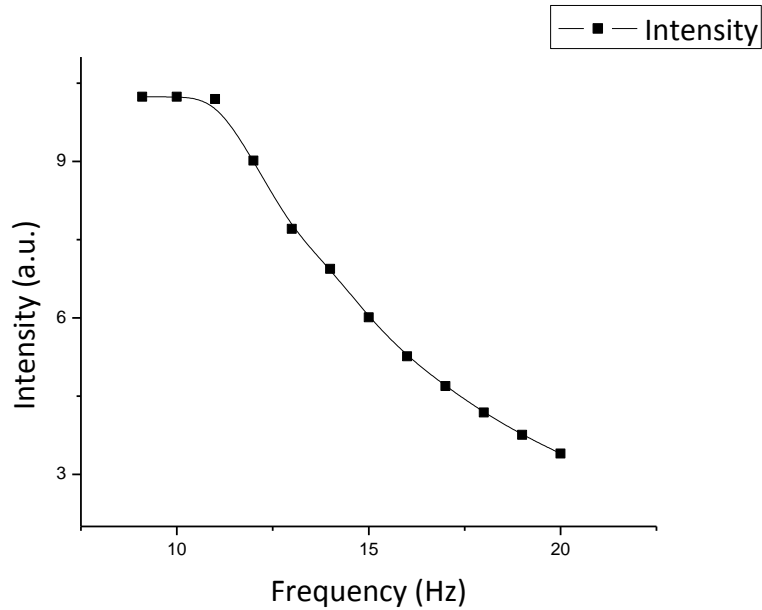


Figure 5.4: IR intensity versus frequency for Bi-spiral source

### 5.2.1.3 Radiation Intensity from Bi-spiral source vs. Current:

The delivered IR intensity from Bi-spiral source to the detector dependency on the current drawn by source was investigated. Bi-spiral source was connected to a power generator 1 W/I and it started emitting IR radiation when its foil color gives a dull red or at 900°C (Laine et al., 1997), before this value the foil was not able to radiate enough electromagnetic waves that can be detected by the Pyroelectric detector; Ott et al. (2015) explained that high radiation power is related to high operating temperature of the thermal emitter; because changing current to investigate its effect on the thermal source intensity did not supply enough range of points to be drawn at constant frequency, current was changed by changing the frequency of the power generator, and this meant that the relation is intensity dependent frequency and not directly with current. The distance between the Bi-spiral source and the pyroelectric detector window was kept constant at 40 mm but increasing the alternative current without changing frequency was not possible. Figure 5.5 showed a decrease in the IR

intensity radiation as current increased related to the increment in the frequency; according to the alternative current equation 4,

$$i(t) = I_0 \sin(\omega t) \quad \dots \quad \text{where } \omega \text{ is the angular frequency.}$$

$$\omega = 2\pi f \quad \rightarrow \quad i(t) = I_0 \sin((2\pi f)t) \quad (4)$$

From the previous equation the current changes are related to the changes in the frequency value. So as frequency increases the current is increased and the intensity of the radiation source will decrease for each PD. These results were unexpected and till now the behavior of intensity dependent current cannot be explained, although the explanation might be referred to the pulse duration of the frequencies between 9-20 Hz.

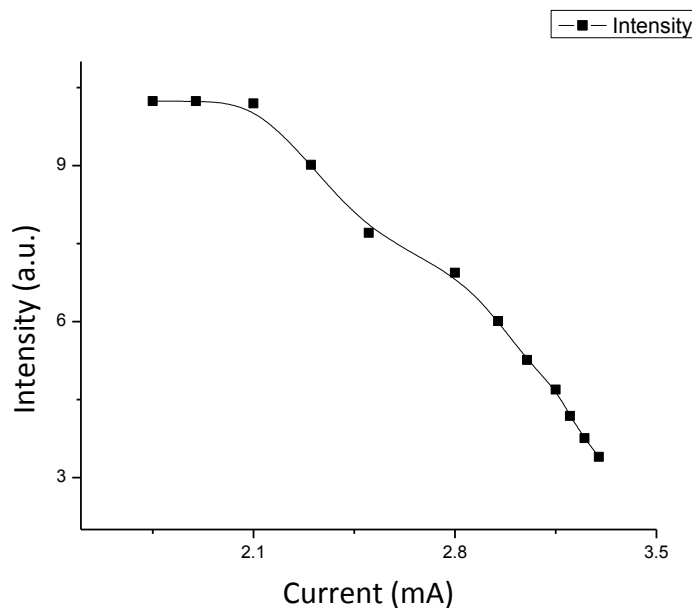


Figure 5.5: IR intensity versus current for Bi-spiral source

### **5.2.2 Characteristic of Fe-Cr-Y IR source:**

The second type of source used in this study is very simple to construct. This type of source was the subject of a research by (Buss, 2009). Since radiation characteristics are dependent on dimensions of source material, the characteristics study will be repeated. Source strip dimensions were taken using vernier caliper with accuracy  $\pm 0.01$  mm, stripe length is 2.70 cm, 0.18 cm width and 0.08 mm thickness. The source turned on to reach the dull red point when only current passes along it exceeded 2.00 Amps, temperature recorded by thermocouple type k to be  $\sim 1000^{\circ}\text{C}$ , the foil resistance ( $R$ ) before running the experiment was 3.50 ohm, the rate Power ( $P_r$ ) of energy transfer to thermal energy along the foil is 23.1 Watt at  $I = 2.57$  Amps depending on the power law:  $P_r = I^2 R \dots\dots (5)$  The source radiated on frequency equals to 10 Hz, PD around 50 ms, Off time or Pulse Interval (PI) equals to PD, and its Duty cycle (DC) would be around 0.5; these parameters are necessary to verify the source according to Hashmi (2010).

**DC =  $f \times PD$ ;** it is a unitless fractional number.

#### **5.2.2.1 Radiation Intensity from Fe-Cr-Y source Distance dependence:**

The output intensity from the IR source was found to depend on the horizontal distance between the detector and the source. The source was powered with 6.00 volts allowing an average current of 2.57 A to pass through the FeCr alloy stripe. It can be seen from Figure 36 that the stripe high radiation intensity enabled the detection of maximum emitted intensity for 16.00 cm far away from the detector window. While the Bi-spiral gave maximum intensity only at 3.50 cm, but the Bi-spiral source IR intensity decay with respect to distance is smoother than the Fe-Cr-Y source because of its uniform bi-spiral shape; e.g. it's rolled gave more uniformly shape for the pulse (Laine, et al., 1997), this note can also be recognized from Figure 5.6.

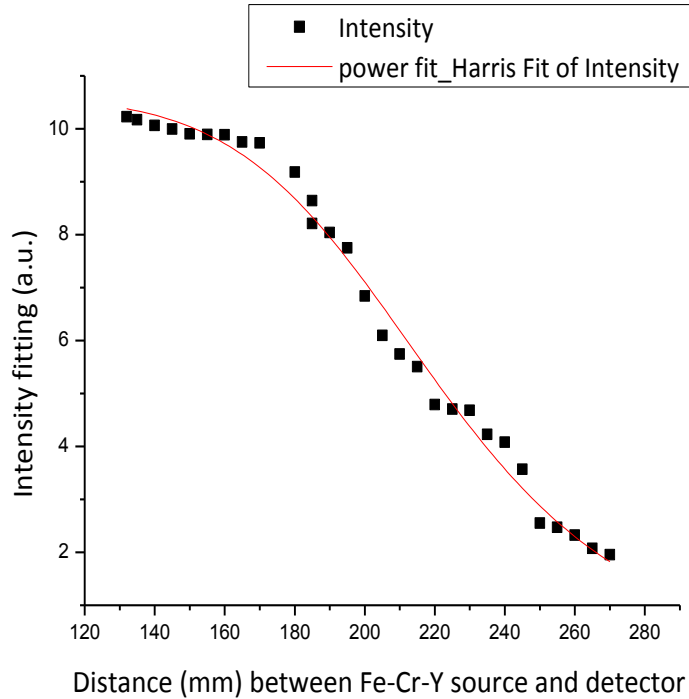


Figure 5.6: IR intensity measurements dependence distance fitting for Fe-Cr-Y source

An ideal thermal emitter has highly electrical resistance (Ott et al., 2015), but according to Laine, et al. (1997) it is not a problem to use a foil stripe with low resistance as a pulse source but that would decrease the electric circuit options in order to keep the device from failure; this is why the electric circuit limited the changing current and frequency investigations.

### 5.2.2.2 Radiation Intensity from Fe-Cr-Y source vs. Current:

In order to study the dependence of Fe-Cr-Y source radiation intensity on changing the passing current through the FeCr alloy strip, the applied frequency kept at 11.5 Hz and the separation distance between the source and the detector window was 1.80 cm. The amplitude was increased in order to increase the current passing through the electrical circuit; Figure 5.7 represents the change in the Fe-Cr-Y source intensity at different current values.

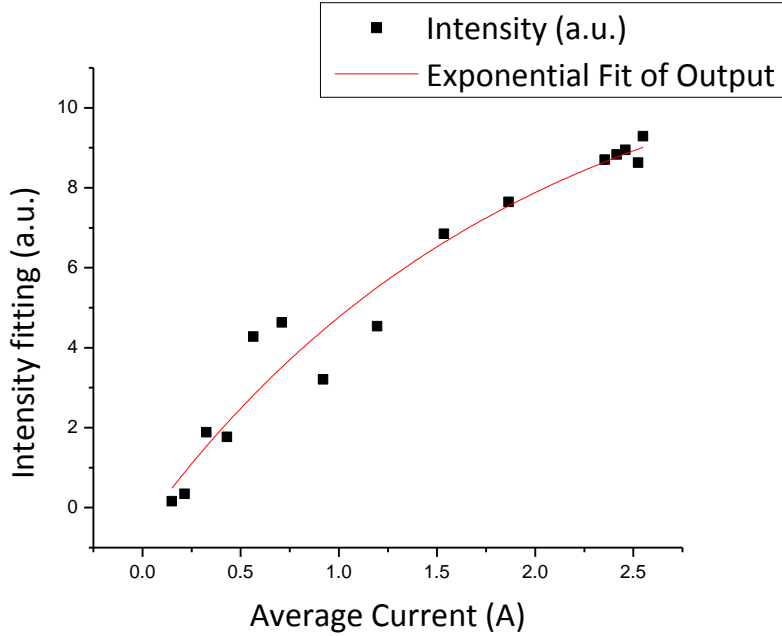


Figure 5.7: IR intensity fitting versus average current.

The rate power of the thermal energy dissipated through the FeCr alloy strip was increased by increasing the current at constant frequency as in equation 5, section (5.2.2) and this caused an increasing in the radiation intensity which was detected by the pyroelectric detector.

### 5.2.2.3 Radiation Intensity from Fe-Cr-Y source Angle dependence:

In this experiment the previous conditions of the intensity of Fe-Cr-Y source distance dependence kept the same except for the horizontal distance separated was 10.00 cm. The IR sources in all previous experiments faced the detector window perpendicularly to each other normal plane. The sensitivity of the detector would change if its angle of view was changed; the IR source has a specific dimension as mentioned earlier. This meant that radiation was expected to be spread over a range of angles around the source. The angle of the window plane detector was changed with respect to the IR stripe source normal. The detector was fixed on the rotating angle disk and the source was fixed  $7.9 \text{ cm} \pm 0.1 \text{ cm}$  away, see Figure 5.8.

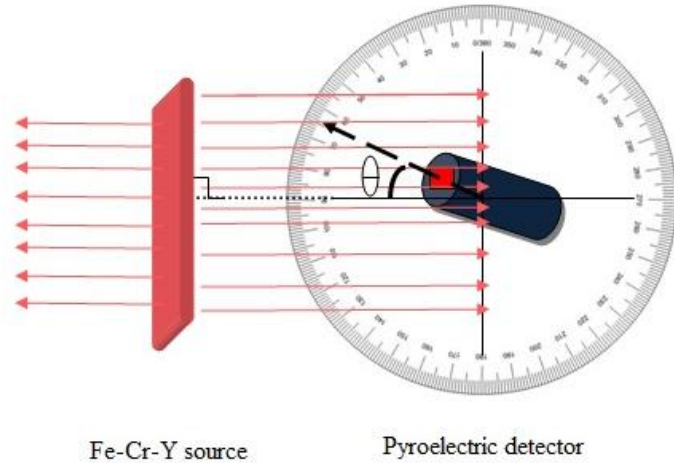


Figure 5.8: Schematic showing intensity angle dependence set up.

The results were introduced by a polar diagram and compared with Laine and Abu-Taha (1997) work, see Figure 5.9 and 5.10.

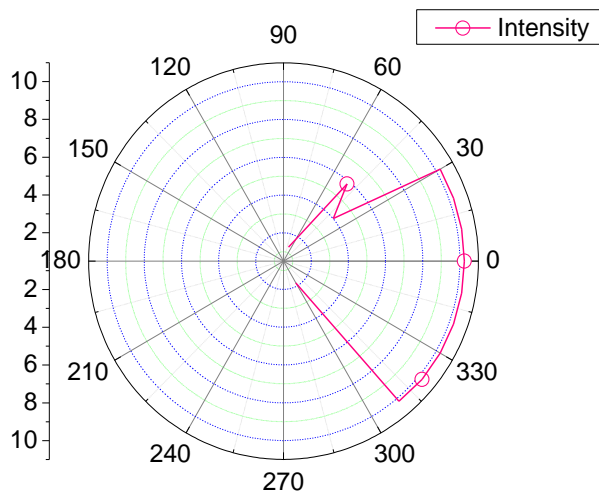


Figure 5.9: Dependence of IR intensity on the angle between the vertical axis to the foil and detector.

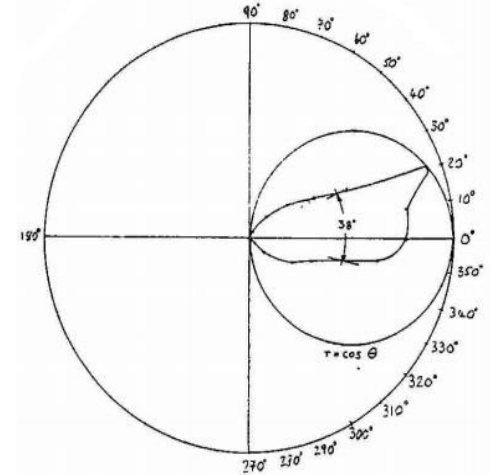


Figure 5.10: polar diagram for Bi-spiral source (Laine and Abu Taha, 1997 by private communication)

It is clear from the plotted data that the ability of Fe-Cr-Y source to perform in a full intensity for a quite a wide range of degree is greater than Bi-spiral source.

Another comparison with angle dependence was done but in different technique; where this time thermal source was fixed on the rotary disk. The idea of this technique is to imitate the clinical situation where the sample is at fixed distance from the rotating radiated IR source. Comparing the second technique of detecting IR radiation with respect to angel with Laine and Abu-Taha plotting, Figure 5.10 will reveal the superiority of the Fe-Cr-Y source against the Bi-spiral source, see Figure 5.11.

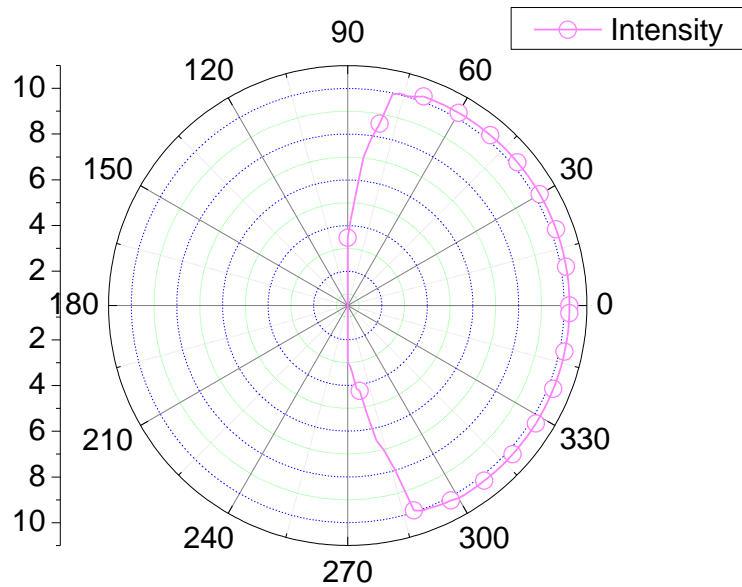


Figure 5.11: Dependence of IR intensity on the angle between the vertical axis to the foil and detector

The Fe-Cr-Y source performance was impressive; for the first few centimeters the Lock-in amplifier signal was very stable with maximum intensity for couple of minutes; each new separating distance was monitored for three minutes to investigate the longest distance that can the pyroelectric detector detect a full intensity of the IR emitter source radiation. For the first 11.0 cm separation between Fe-Cr-Y source and the detector, the intensity was full then it returned to behave as expected according to the inverse square law.

### 5.3 Effect of using focusing tools

Since both types of sources emit from front and back surfaces there is possibility to enhance emitted power from the IR source without increasing the current of the circuit or increasing the power rate of the source only by enhancing the forward source radiation by reflecting tools like plane front coated mirrors and metal waveguides.

#### 5.3.1 Focusing Bi-spiral source radiation:

##### 5.3.1.1 Using an aluminum tube as a waveguide:

This waveguide was used with Bi-spiral source. It is an aluminum tube with internal polished surface. It was placed between the source and the detector window, i.e. focusing the forward radiation. It has a length of 58.00 mm and internal diameter of 16.50 mm.

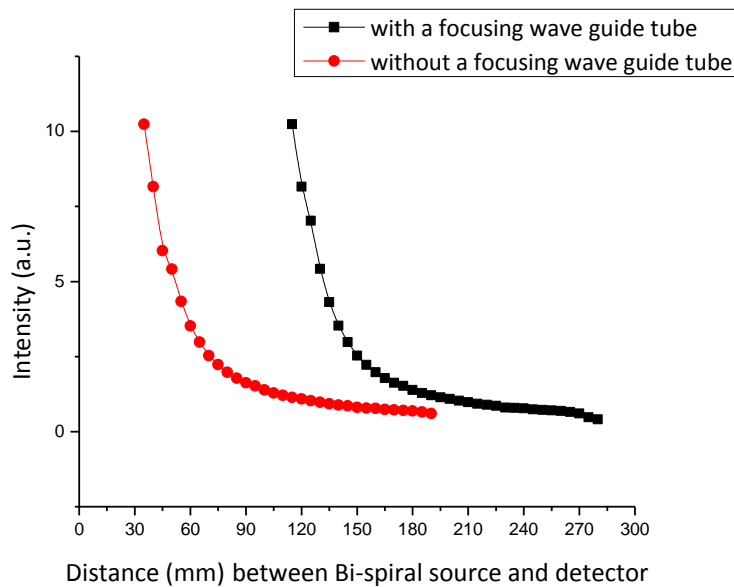


Figure 5.12: IR intensity versus distance for Bi-spiral source with and without focusing Al tube waveguide element.

Figure 5.12, shows that intensity values are shifted to longer distances from the source with the same behavior. Al tube can be used to deliver radiation to longer distances without being

attenuated. It is clear from comparing the previous figure results that the Al tube waveguide did not enhance the radiation intensity, but it provided an extra length for applications where samples are difficult to be reached.

Comparison of the two figures 4.5 and 4.8 shows that waveguide tube allows all radiation from the source to be guided toward the pyroelectric detector. It can be noticed from figure 5.12 that both of the plots have identical curves, but with different positions! On the other hand the aluminum tube is useful for limiting the exposed area from IR radiation.

The power fitting for IR intensity dependence distance for the Bi-spiral source equals (-4.48) exceeding the expected value (-2.00), as shown in Figure 5.13.

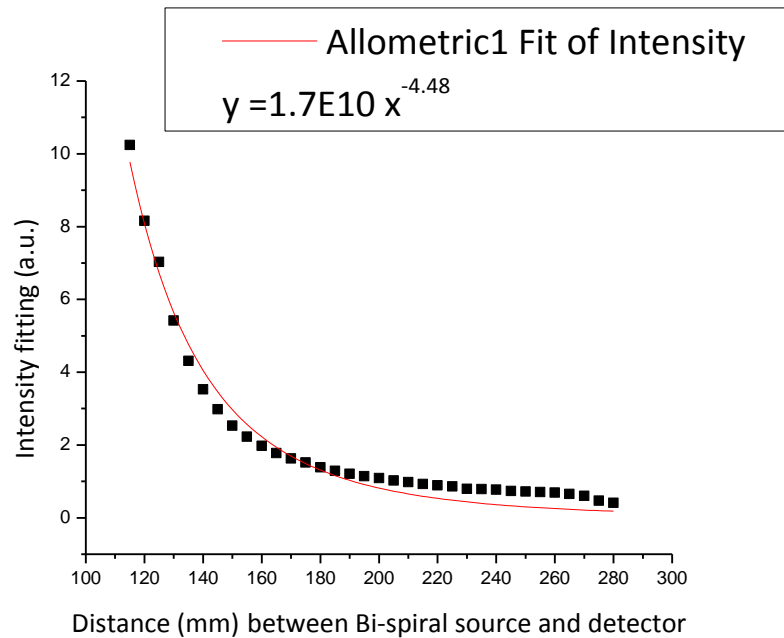


Figure 5.13: IR intensity measurements dependence distance power fitting for Bi-spiral source with Al tube wave guide

### 5.3.1.2 Hemispherical shaped reflector:

This reflector was used for its advantage of reflecting the radiation from the back side of the source with both sources. It was placed behind the source to reflect the radiation from the back side source surface toward the detector direction. IR intensity dependent frequency was studied, the distance between the IR source and the detector window was kept constant at 40.00 mm, and the results and its fitting are presented in Figure 5.14.

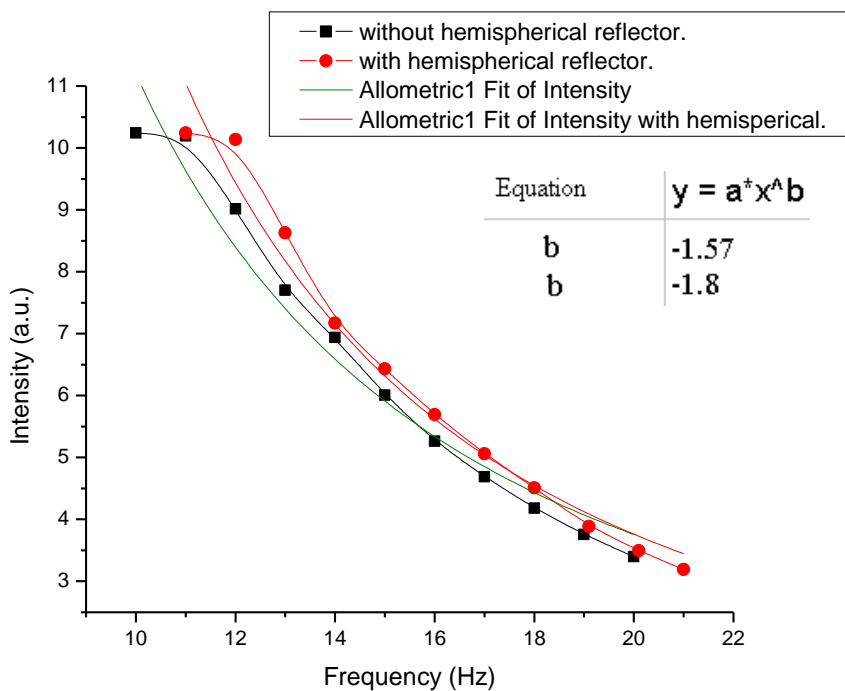


Figure 5.14: Bi-spiral source intensity versus frequency with and without hemispherical reflector at different frequencies.

Comparing the intensity values from Figure 5.14 with and without the hemispherical wave guide, it is obvious that the Bi-spiral forward emission was enhanced by using a reflector as expected.

### 5.3.1.3 Plane front surface coated mirror:

Another focusing tool was examined and the results are presented in Figure 5.15 and 5.16 respectively.

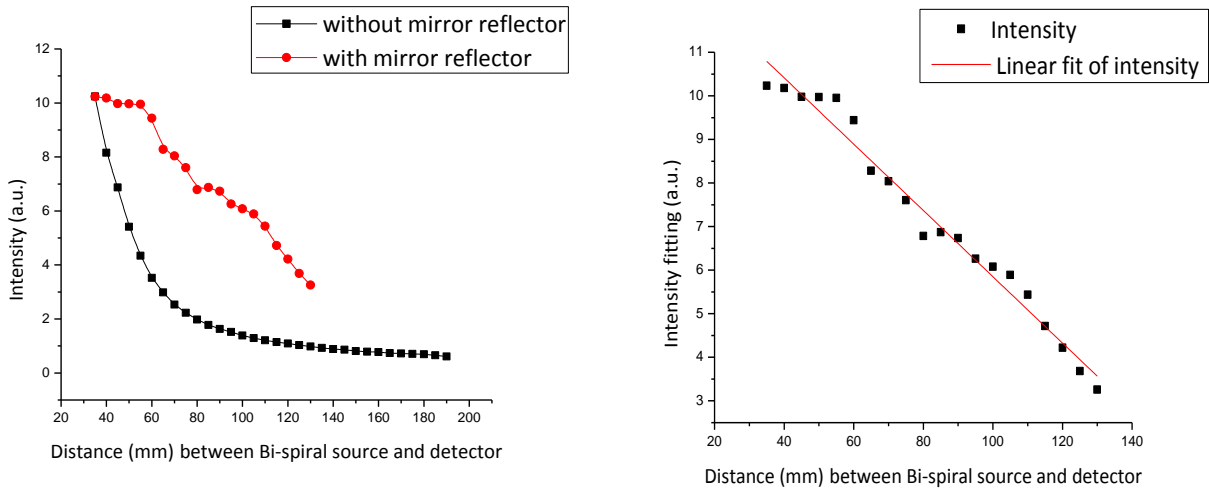


Figure 5.16: IR intensity measurements

Figure 5.15: IR intensity versus distance for Bi-spiral source without and with using plane front coated mirror.

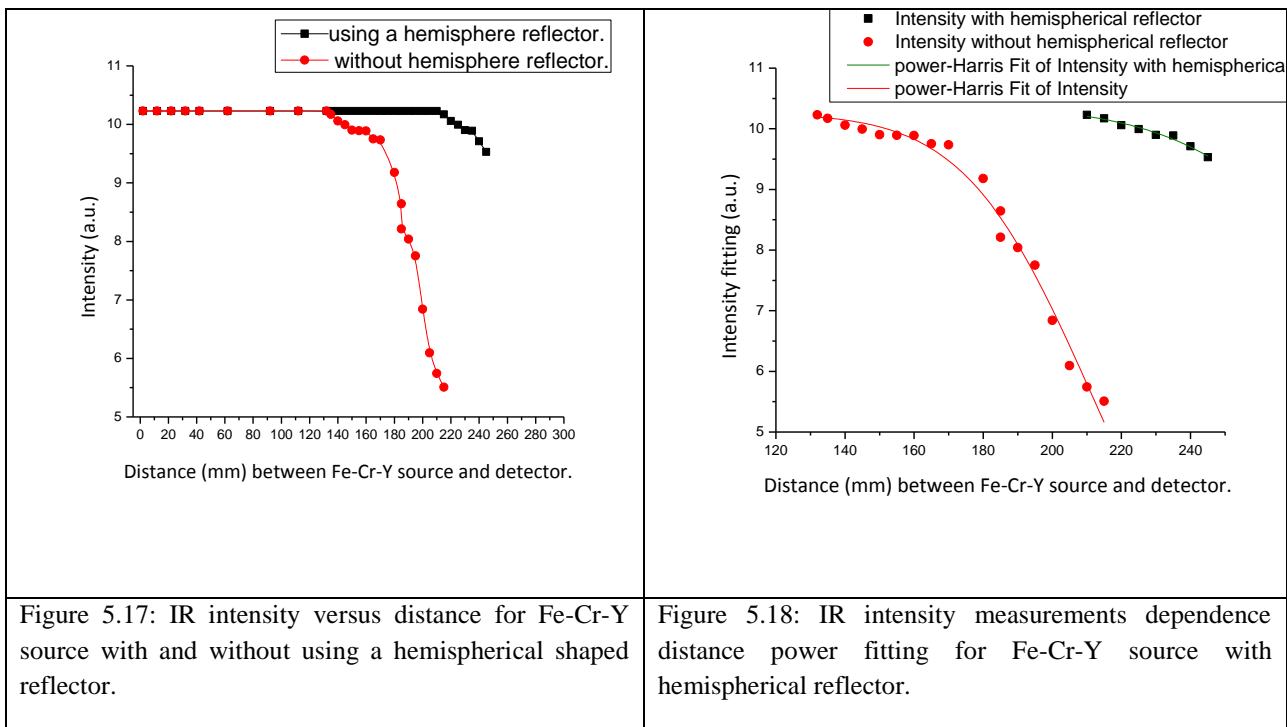
dependence distance power fitting for Bi-spiral source with plane front coated mirror placed behind

It is clear from the plotting that the Bi-spiral source radiation was enhanced when reflector is placed behind source, but in non-uniform pattern as can be seen from Figure 5.15, the IR intensity with distance using the plane mirror was linearly fitted as shown in Figure 5.16 which was unexpected, since the relationship between the intensity of the IR source and the separation distance is proportional to the inverse square separation as mentioned in equation 3.

### 5.3.2. Fe-Cr-Y source:

#### 5.3.2.1 Hemispherical shaped reflector:

The forward intensity of the Fe-Cr-Y source was enhanced after placing the hemispherical reflector behind the source recording full intensity by the detector at farther distances separation. The hemispherical reflector converge the back side IR radiation beam forward the direction of pyroelectric detector, see Figure 4.12. The results are shown in the following Figures.



The constant curve in Figure 5.20 indicates the full intensity of radiation delivered to the detector in spite of the increasing separation between them with and without using the hemispherical reflector which by the way it clearly increased the forward radiation intensity of the source. The used fitting of intensity is power-harris fit; its equation is

$$y = (a + b \times x^c)^{-1}.$$

### 5.3.2.2 Plane coated mirror:

The coated mirror performance in reflecting the backward radiation and focusing it forward the detector in order to enhance the Fe-Cr-Y source intensity was not on great deal of efficiency, the results are presented in the following Figures.

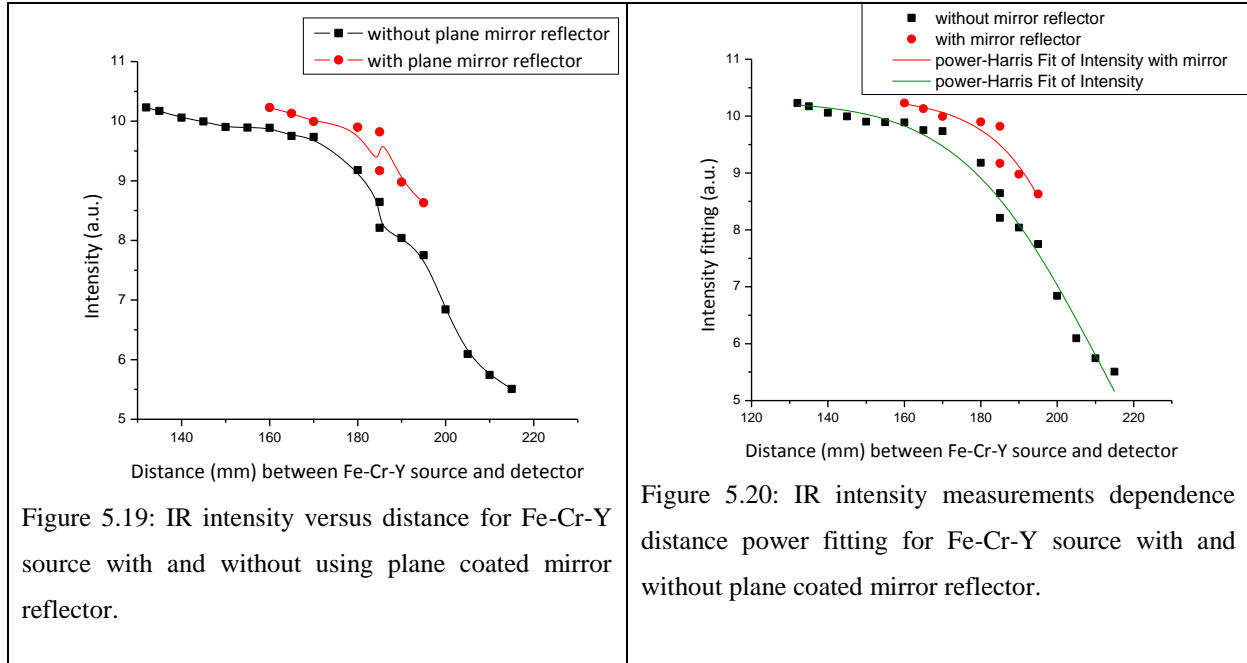


Figure 5.19: IR intensity versus distance for Fe-Cr-Y source with and without using plane coated mirror reflector.

Figure 5.20: IR intensity measurements dependence distance power fitting for Fe-Cr-Y source with and without plane coated mirror reflector.

The deviation in practical research is expected and accepted to some point.

## 5.4 Heat distribution over biological samples

### 5.4.1 Rat samples:

#### 5.4.1.1 In-vitro trial with rat sample:

Two techniques were done: first one: some sectioned pieces of white rat tissues were irradiated by Fe-Cr-Y source to study temperature distribution over them. Second one: the dead rat was not sectioned but some specific areas were radiated by the source.

##### 5.4.1.1.1 Excised pieces:

###### 1. A rat thigh

A rat thigh was sectioned and the skin layer above the thigh muscle was removed, see Figure 5.21. The sample dimensions were: length, width, and thickness respectively; 19.00, 5.00 and 0.50 mm, the sample was spread over a plexiglass plat, see Figures 4.13 and 4.15 for more clarification, and was exposed to radiation after one hour of the rat's death. Its initial temperature was equal to the environment temperature which was 11°C. Two thermocouple probes were used; one of them was fixed beneath the source directly at 0.50 mm depth of muscle sample, and the other one measured the temperature of three different locations with different time duration. The results are summarized in table 5.1.



Figure 5.21: A photo of rat's thigh

**Table 5.1: Points temperature results irradiated by IR source of thigh muscle at 0.5 mm depth.**

<b>Passed time by minutes</b>	<b>Hole No. 1</b>	<b>Hole No. 2</b>	<b>Hole No. 3</b>	<b>Hole No. 4</b>
	temperature (°C)\ Stationary probe	4.00 mm away (°C)	9.00 mm away (°C)	11.50 mm away (°C)
6.00	14	11		
14.00	15		13	
43.00	16			11

From the table it is clear that the absorption of radiation was poor; since the tissue temperature did not change. The absorption of IR radiation through tissue depend on its structure; the presence of chromophores (Cope, 1991; Marieb, 1995; Hollis, 2002; and Heelspurs, 2015), and muscles do not have much chromophores through its structure.

## 2. A piece of a rat skin

The sample was irradiated by Fe-Cr-Y source immediately after the rat death. The tissue temperature before radiation was 19°C and the environment temperature was 19°C. Temperature distribution was measured at 1 mm depth.

The results are summarized as follow:

- 1    Stationary probe: Did not measure any significant change in temperature. The temperature became 21°C after 41 seconds from the start of radiation till the end of the session (11.04 minutes)
- 2    Mobile probe: Did not record any change in the tissue temperature. The temperature kept 19°C for all 20 holes.

3. After an hour another skin sample was irradiated:

The piece dimensions were almost  $1.5 \times 1.7 \text{ cm}^2$  (see Figure 4.13 (b)). Temperature at 1.00 mm depth was probed and the total session duration was 7.57 minutes. Its temperature before radiation was 20°C. The results are summarized in Table 2 and 3:

- Stationary probe: This probe was placed directly under the source. The results are shown in table 5.2.

**Table 5.2: Points temperature results of skin irradiated by IR source at depth 1.00 mm for the station hole.**

Run #	1	2	3	4	5	6	7	8	9	10	11	12	13	
Duration for each hole (sec)	32.1	42.4	41.1	40.6	41	41.2	41.6	20.6	31.1	30.7	30.4	30.5	30.8	Session time
Mean temp (°C)	22	23	24	24	24	23	23	25	26	26	27	27	28	7.57 min

- Mobile probe: the result are shown in table 5.3

**Table 5.3: Points temperature results of skin irradiated by IR source at depth 1.00 mm for different holes.**

Run #	1	2	3	4	5	6	7	8	9	10	11	12	13	
Duration for each hole (sec)	32.1	42.4	41.1	40.6	41	41.2	41.6	20.6	31.1	30.7	30.4	30.5	30.8	Session time
Mean temp (°C)	20	21	20	20	19	20	23	21	21	21	20	20	19	7.57 min

From the previous tables it can be seen that there is no bioheat transfer for the absorbed radiation through tissue and temperature increased only directly under the radiated source, this is expected since the tissue is dead where most of life mechanisms were stopped after one hour of death.

STDEV was calculated for all points and it was zero.

Note that: Run # (1-5) represents the holes in the first row; run # (6-10) represents the holes in the second row and so on.

#### **5.4.1.1.2 Whole rat body irradiated at specific area by Fe-Cr-Y source:**

White rat weighted 305.7 gm, irradiance session started after the death within 15.00 minutes, its temperature before irradiation was 30°C. The Fe-Cr-Y source was fixed from the target sample by 1.30 cm and plane coated mirror was used as waveguide. The electrical arrangements were; current (2.21-2.70) Ampere, voltage 5.60 volts and frequency was 12 Hz. The temperature of the environment was 19°C

Upper part of rat skin not excised: the irradiated area estimated in the range  $5 \times 5$  points which equals  $96 \text{ mm}^2$  it was marked after shaving the upper part of rat skin in belly area. The total session duration was 33.00 minutes and each run's duration was 40 second. The maximum temperature recorded was 40.8°C. A contour plotting for temperature distribution over the horizontal area of the shaved skinned sample was done. Only measured temperature was for the above area of the IR source, see Figure 5.22.



Figure 5.22: A photo of the set up using gold coated mirror.

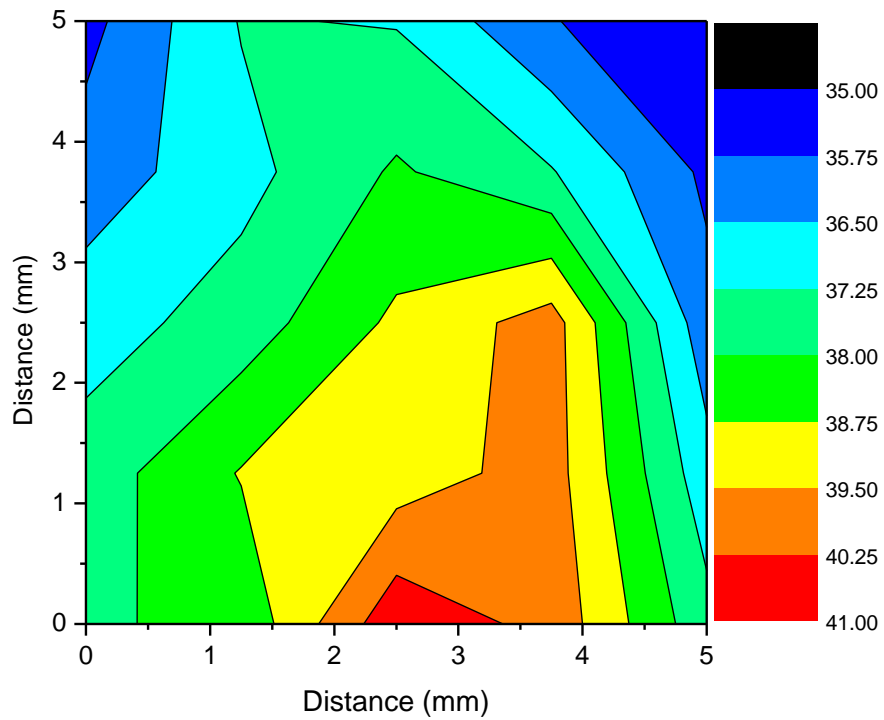


Figure 5.23: Temperature distribution over upper part of skin tissue (in vitro).

The heat is focused under the source directly and decreases as the distance from the source become farther, these results agree with Kengne, Lakhssassi and Vaillancourt concluded in (2012) about the behavior of bioheat transfer through tissue based on their model which is nonlinear bioheat equation of Penne's type. Despite the cessation of blood circulation in the rat's dead body the temperature increased from  $30^{\circ}\text{C}$  to almost  $41^{\circ}\text{C}$  which means that there is still some mechanisms still working after the death within an hour.

The marked points over the rat skin were drawn using the grid plexiglass, see Figure 4.14. The followed pattern in taken points temperature was started from point (5,1), ..., (9,1), (5,2), ..., (9,2), ..., (5,5), ..., (5,9), in column pattern which helped in studying the temperature - distance relationship and the results are summarized in table 5.4 and plotted, see Figure 5.24.

**Table 5.4: temperature-distance relationship of upper skin rat (in vitro)**

X axis (mm)\Y axis	0	3	6	9	12
0	38	38	41	40	38
2	38	39	39	40	37
4	37	38	39	40	36
6	36	37	38	37	36
8	36	37	37	36	35
<b>Total time (min)</b>	3.37	3.36	3.48	3.41	3.41

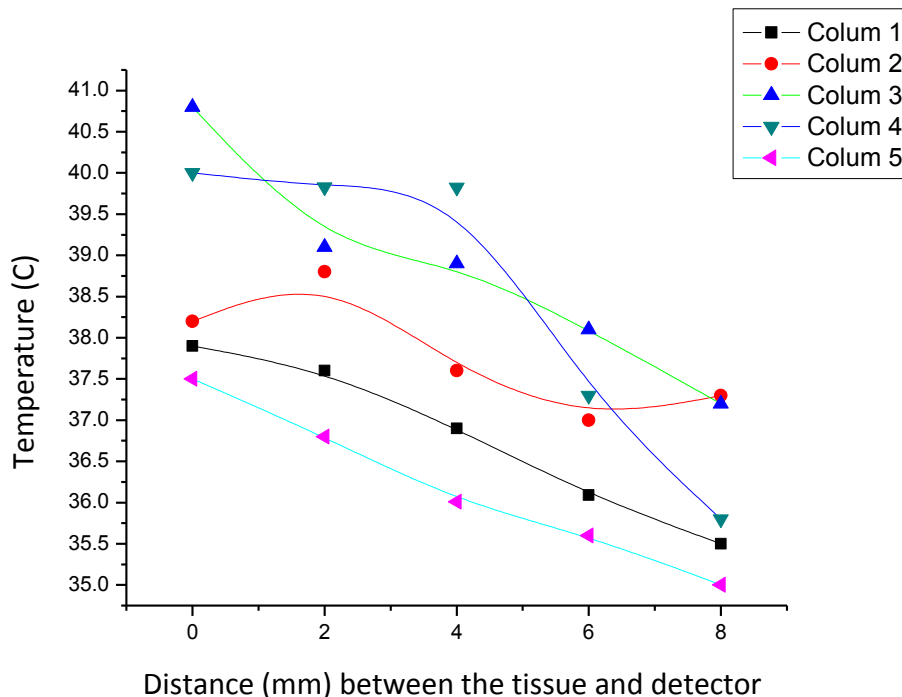


Figure 5.24: measured points temperature dependent distance (in vitro)

No doubt that Temperature-Distance relationship through biological tissue cannot be described to be linear (Kengne, Lakhssassi and Vaillancourt, 2012) or exponentially decay (Hollis,

2002) it is mainly depends on the availability of chromophores and skin color (Stadler et al., 2004)

Another type to view information:

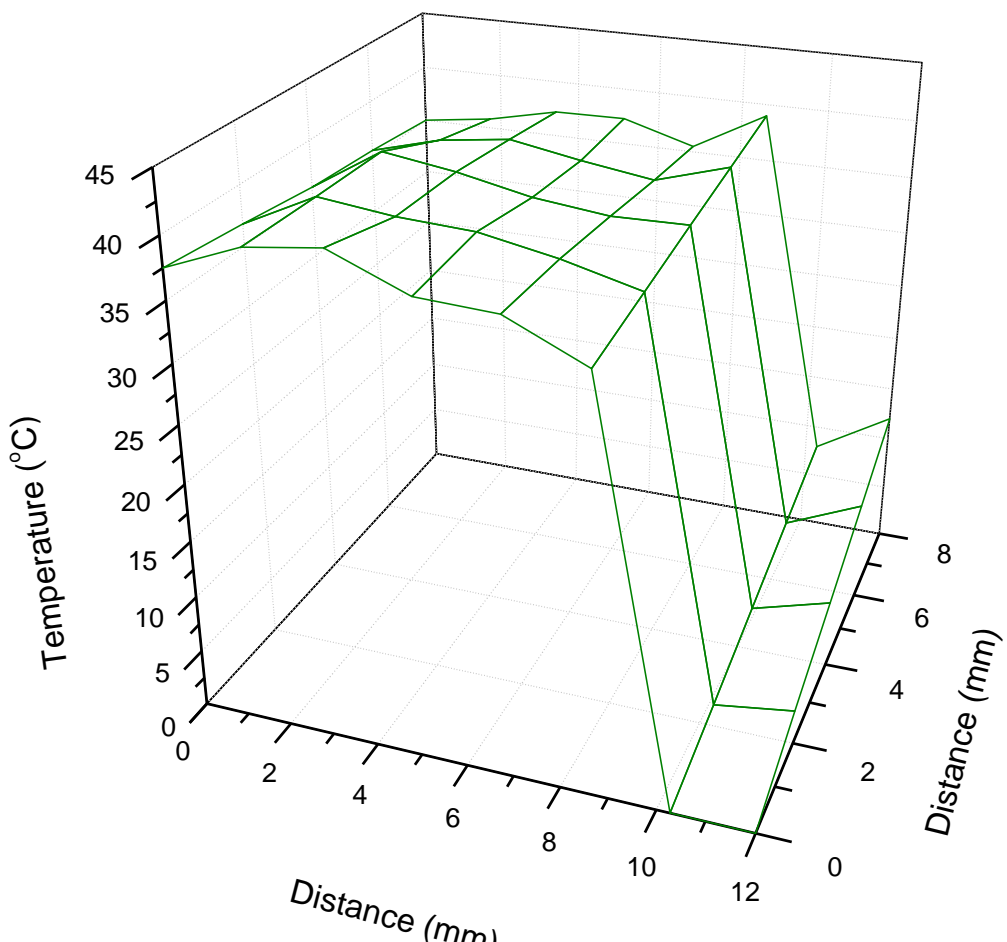


Figure 5.25: Wire frame plot for temperature distribution through the shaved marked skin (in-vitro).

### **5.4.1.1.3 Whole and excised rat body irradiated at specific area by Bi-spiral and Fe-Cr-Y source:**

A dead white rat weighted 373.0 gm was used, the session started after the death within 16.00 minutes, its temperature before irradiation was 28°C. The Bi-spiral source was fixed from the target sample by 1.70 cm. The electrical arrangements were: current 0.30 Ampere, AC voltage 1.69 Volts and frequency was 12 Hz. The environment temperature was 18°C

1. Upper part of Rat skin: the irradiated area estimated in the range  $2 \times 2$  points which equals 5 mm<sup>2</sup> it was marked after shaving the upper part of rat skin in belly area. The session duration was 17.00 minutes and each temperature reading duration was 40 second. The followed pattern in taken points temperature was started from point (0,0),..., (0,3), (1,0),..., (1,3), (2,0)...(2,3). Results are summarized in table 5.5.

**Table 5.5: Recorded point temperature for upper skinned white rat using Bi-spiral source (the station point). (In vitro)**

<b>Run #</b>	1	2	3	4	5	6
<b>Average Temperature (°C)</b>	31	31	31	31	31	31

<b>Run #</b>	7	8	9	10	11	12
<b>Average Temperature (°C)</b>	31	31	31	31	31	31

Irradiation for 17.00 minutes duration session and with only 17.00 mm separated distance between the source and the target where full irradiation intensity is delivered to the sample see Figure 5.1 which clarify the intensity-distance dependence for Bi-spiral source, and there is no significant change in temperature for the station probed nor for the mobile one; this means

that Bi-spiral source has no thermal effect on biological tissue according to the previous experiment.

2. Lower part of skin was done using Fe-Cr-Y source:

Untreated skin tissue was sectioned and kept into ice for one hour and 40.00 minutes. Each duration reading was 40 second. The temperature of the tissue before radiation was 21°C. A contour plot of temperature distribution over the inner side of white skinned rat was done, see Figure 5.26.

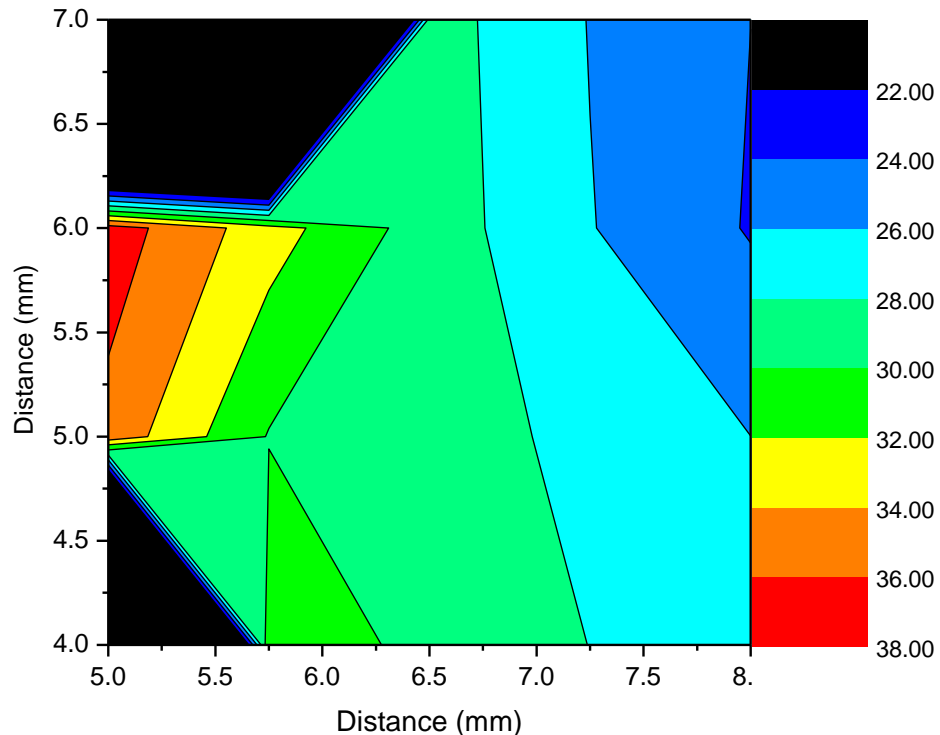


Figure 5.26: Temperature distribution over inner side of skin tissue (in vitro) using Fe-Cr-Y source

The station thermo couple probe was placed under the Fe-Cr-Y source directly; measured the temperature of the tissue at the end of session was 38°C. (The session duration was 14.00 minutes). It seems that as the time of death increases the ability of the sample to absorb heat is

weaker than living tissue; because thermoregulation in the tissue is not active any more (Stadler et al., 2004)

### 3. The Rat thigh

The sample was excised after one hour and five minutes from the rat death. Since the thigh thickness is not uniform, the same thigh was used to investigate absorption at different depths in muscle. The muscle temperature before radiation was 22°C, and placed away from the IR Fe-Cr-Y source within 5 mm the tissue was put over a plexiglass plate as was shown in Figure 5.24.

1. First run irradiation session was done after one hour and five minutes for the tissue, thigh thickness in the range of 3.64 mm and point's temperature were taken from the thigh surface and bottom respectively, and the results are summarized in table 5.6. The exposed area of radiation directly from the IR source was 28.00 mm<sup>2</sup>. The session duration was 5.00 minutes.

**Table 5.6: Recorded points temperature for upper and bottom thigh muscle of a white rat using Fe-Cr-Y source (In vitro).**

Hole No./distance from the first hole (mm)	1/ 0 mm	2/ 4.00 mm	3/ 9.00 mm
Upper side temp./ time from the first radiation (min)	41/ 1.00 min	42/ 1.66 min	34/ 3.66 min
Back side temp./ time from the first radiation (min)	38/ 2.33 min	37/ 3.00 min	36/ 4.33 min

Temperature increase from 22°C to more than 42°C by only 1.66 min for the muscle surface while at 3.64 mm depth temperature increase from 22°C to more than 37°C; this means the ability of IR broad band to affect tissue at depth greater than 3 mm of skeletal muscle (Hashmi et al., 2010; Henderson and Morries, 2015)

Number of temperature points might not be enough to plot temperature-distance relationship, because the rat's thigh did not offer many choices, but it was plotted to show the difference in absorption at different depths, see Figure 5.27.

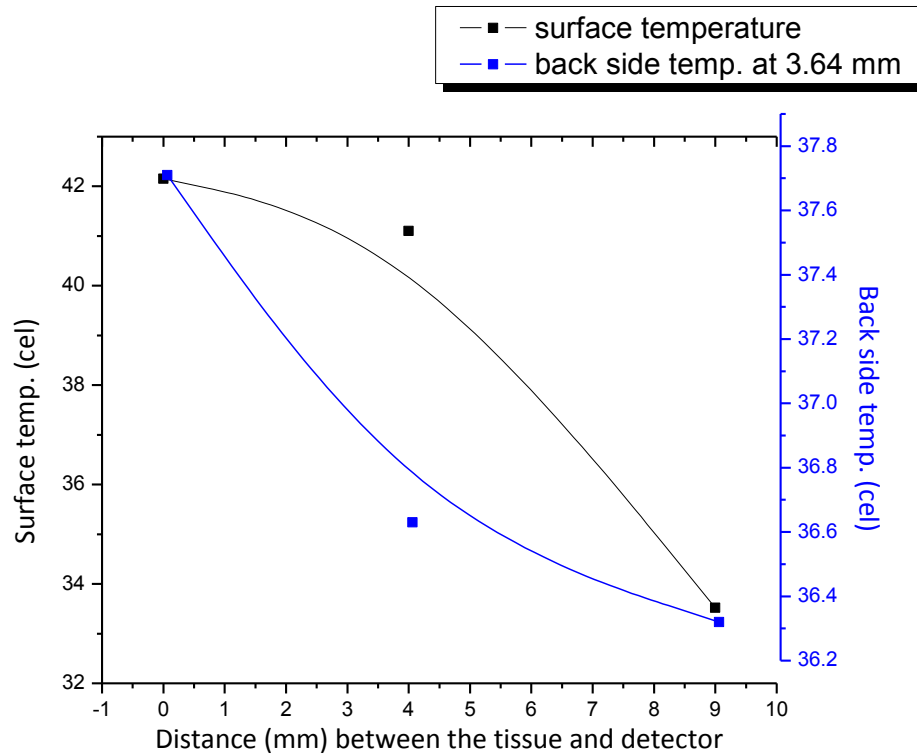


Figure 5.27: Temperature-Distance for points at same horizontal distances from the IR source, but at different depths.

2. Second run was one hour and 18 minutes for the same sample tissue; thigh side thickness was 5.00 mm, and the session duration was also 5.00 min. results are summarized in table 5.7 and the temperature-distance relationship is shown in Figure 5.28.

**Table 5.7: Recorded points temperature for upper and bottom thigh muscle of a white rat using Fe-Cr-Y source (In vitro).**

Hole No./distance from the first hole (mm)	1/ 0 mm	2/ 4 mm	3/ 9 mm
Upper side / time from the first radiation (min)	42/ 1.00 min	38/ 1.66 min	37/ 3.66 min
Lower side / time from the first radiation (min)	39/ 2.33 min	36/ 3.00 min	31/ 4.33 min

It is sure that initial temperature was affected by first run, but the results of the point's temperature are still logical; since as distance separates the IR radiating source from the target the radiation intensity suffer attenuation (Hollis, 2002; Henderson and Morries, 2015)

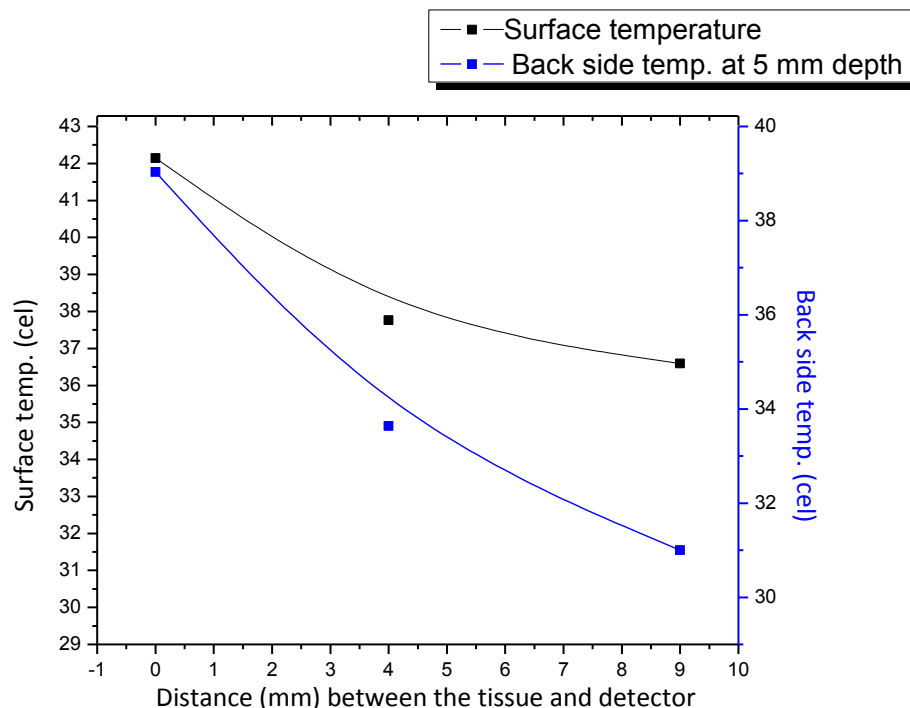


Figure 5.28: Temperature-Distance for points at the same horizontal distances from the IR source, but at different depths.

### **5.4.2 In-vivo trial using rat sample:**

The white rat weight 174.3 gm, its temperature after anesthesia was 31°C, and the environment temperature was 35°C.

#### **5.4.2.1 Upper part of skin:**

Each point's temperature duration was 39.0 second for most of them; the total session time was 11.77 minutes. The measurement pattern was taken horizontally raw by raw marked over its shaved skin. Results are summarized in table 8 and plotted, see Figure 5.29.

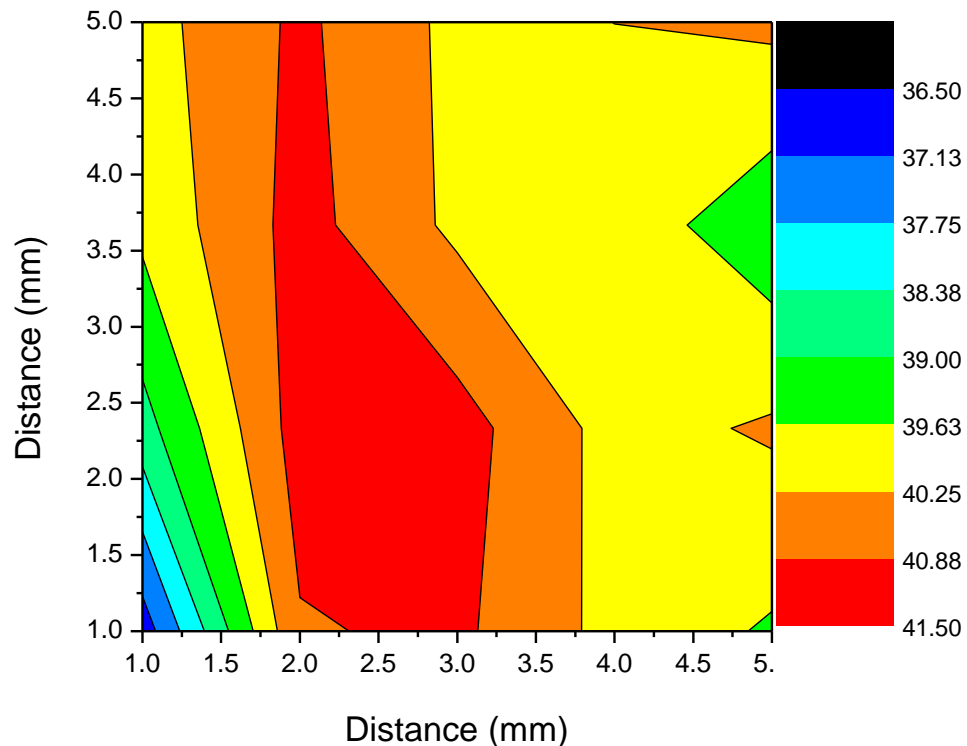


Figure 5.29: Temperature distribution over upper part of skin tissue for the first 11 minutes (in vivo).

**Table 5.8: Temperature-distance relationship of upper skin white rat for the first 11 min. (in vivo)**

X mm Y mm \	0	3.00	6.00	9.00	12.00
0	37	41	41	40	40
2.00	39	41	41	40	40
4.00	40	41	40	40	39
6.00	40	41	40	40	40

Temperature-distance was plotted for each raw, see Figure 5.30.

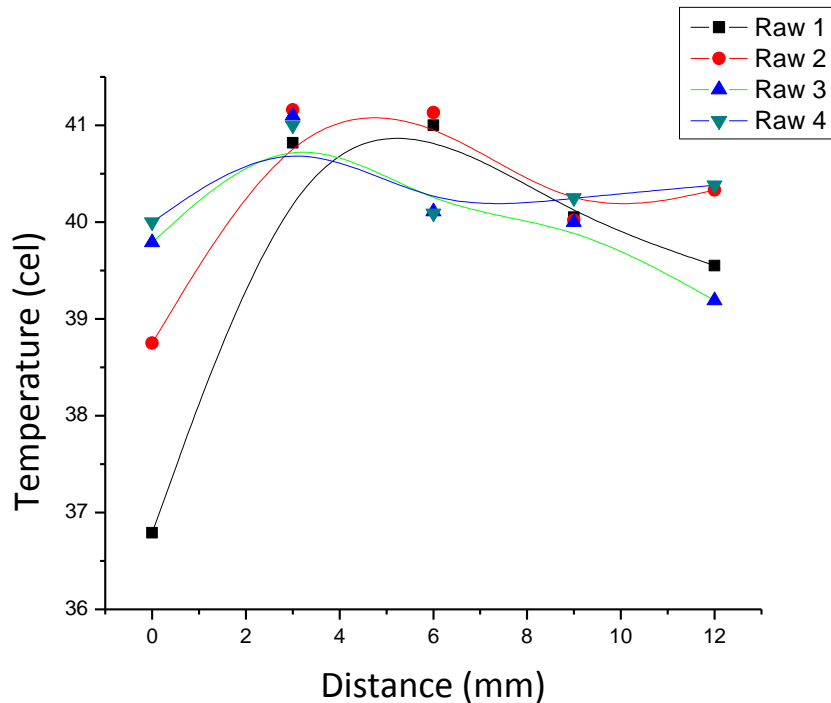


Figure 5.30: Measured temperature versus distance (in vivo) along 11.77 min session duration.

As mentioned before the relation is non-linear; since the metabolism in living tissue is temperature dependent (Kengne, Lakhssassi, and Vaillancourt, 2012), also interactions of each tissue with radiation is unique with its structure (Flammer, mozaffarieh and Bebie, 2013).

In Stadler et al. (2004) experiment in vitro temperature results recorded higher values than in vivo temperature results after irradiating the targets with  $5 \text{ J/cm}^2$  in Low level laser therapy session (LLLT), but this is not the case in this experiments; the results from (5.4.1.1.2) the highest temperature recorded after 33.00 minutes of white skinned rat was  $41^\circ\text{C}$  while in vivo trial for upper shaved skin of white rat after only 11.77 min was  $41^\circ\text{C}$  and this is opposes Stadler results.

After 11.77 minutes of radiation, the same points were followed after the first session duration. Temperature read duration range was (15.5-30.0) second. The session duration was 7.21 minutes. The results are summarized in table 5.9 and a contour plot represents the temperature distribution, see Figure 5.31. The temperature reading was taken in a column pattern.

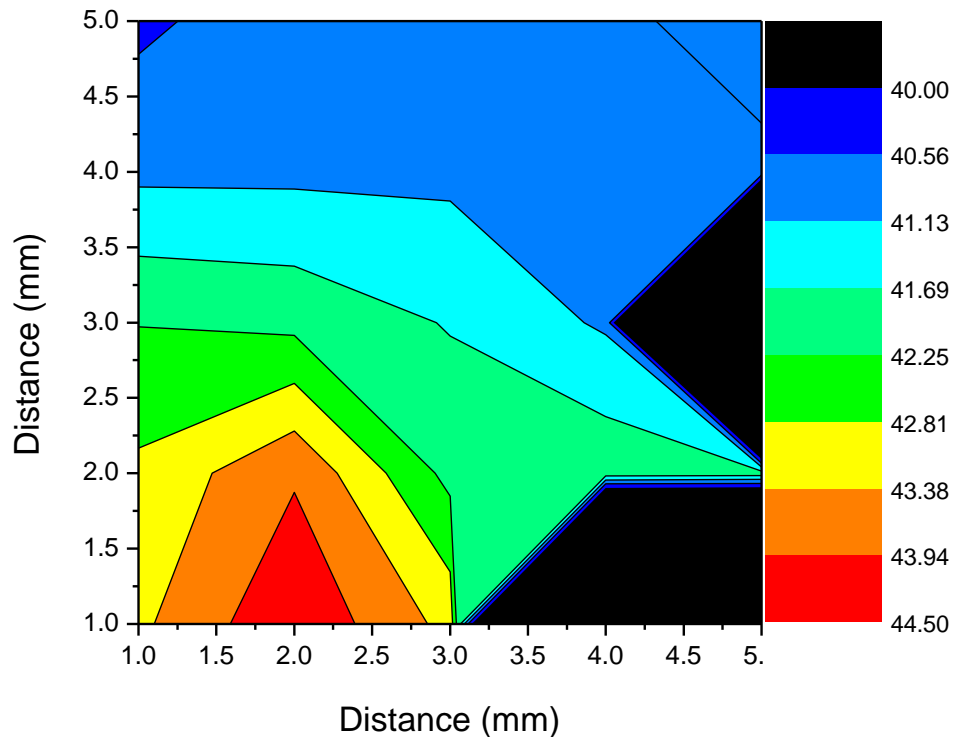


Figure 5.31: Temperature distribution over upper part of skin tissue after the pass of 11.77 minutes from irradiation (in vivo).

Table 5.9: Temperature-distance relationship of upper skin white rat after the pass of 11.77 min. of irradiation (in vivo)

X mm \ Y	0	3.00	6.00	9.00	12.00
0	43	44	43	--	--
2.00	43	44	42	42	42
4.00	42	42	42	41	--
6.00	41	41	41	41	41
8.00	40	41	41	41	41

The results were plotted column by column to investigate temperature-distance distribution, see Figure 5.32.

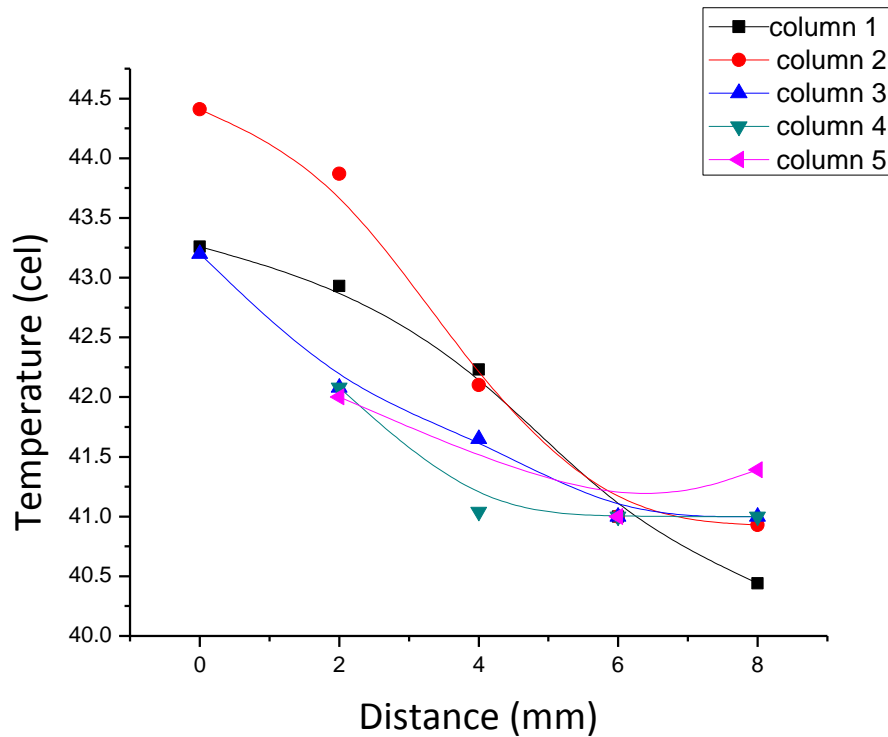


Figure 5.32: Measured temperature versus distance (in vivo) after 11.77 min of radiation

#### 5.4.2.2 Abdomen muscle:

Temperature duration of each point marked over the abdomen muscle ranged between 60.5sec and 47.7 sec completing a session of 14.51 minutes; the duration was longer from previous because muscles have less chromophores. The results from table 10 showed an increase in the temperature from the station probe beneath the source from 31°C to 37°C after almost 15.00 minutes of irradiation, this means that the duration session was not enough to affect the muscle tissue thermally, since tissue temperature must exceed 40°C (Stadler et al., 2004; Bischof, 2006; Obayashi et al., 2015). The set up arrangement was shown in Figure 4.18. A contour plot for temperature distribution is represented in Figure 5.33.

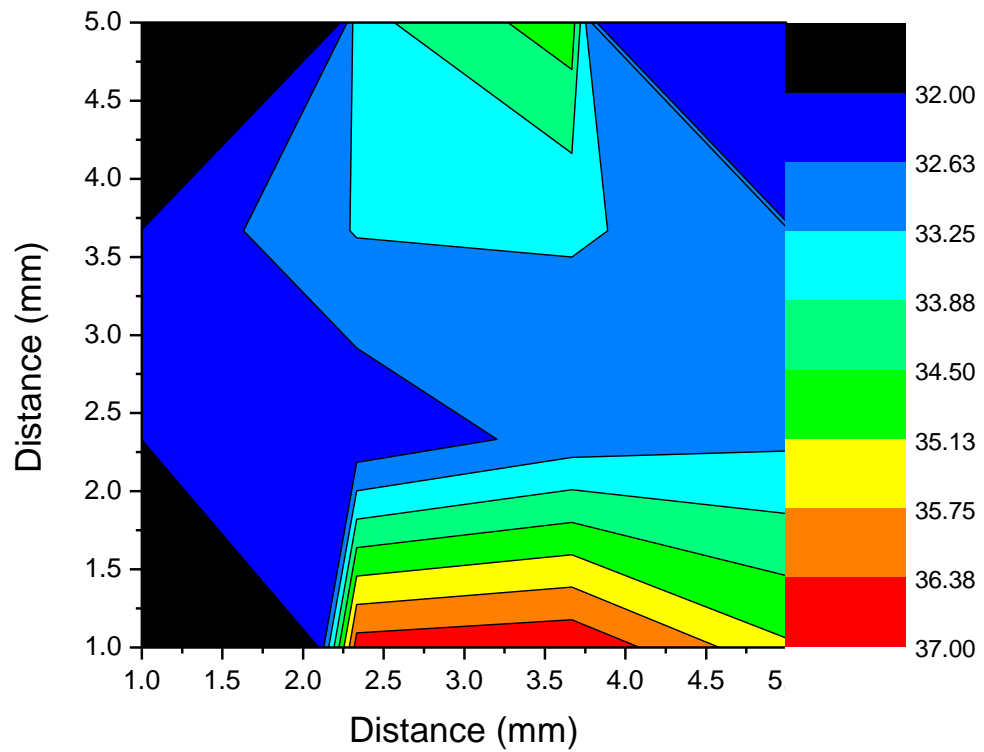


Figure 5.33: Temperature distribution over abdomen muscle

**Table 5.10: Temperature-distance relationship of abdomen muscle white rat (in vivo)**

X (mm)\Y (mm)	0	3.00	6.00	9.00
0	--	37	37	35
2.00	32	32	33	33
4.00	32	33	33	33
6.00	--	34	35	--

#### 5.4.2.3 Thigh muscle:

The results of probing the temperature at different distances from the Fe-Cr-Y source along the thigh muscle are summarized in table 5.11.

**Table 5.11: Temperature-depth relationship of a thigh muscle**

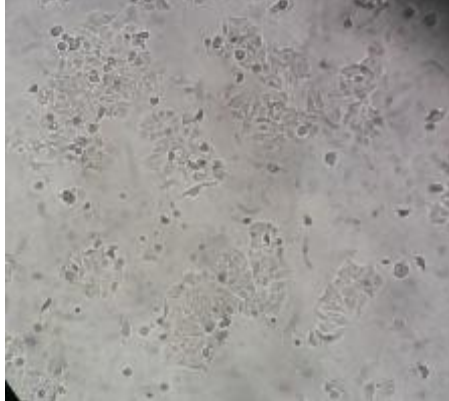
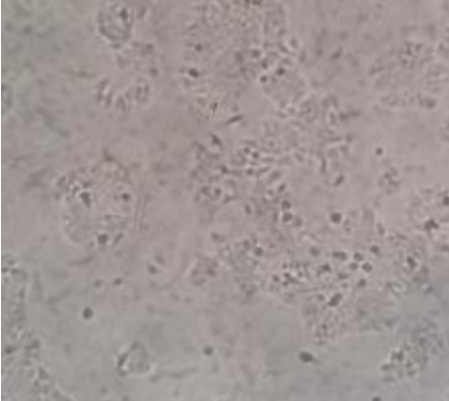
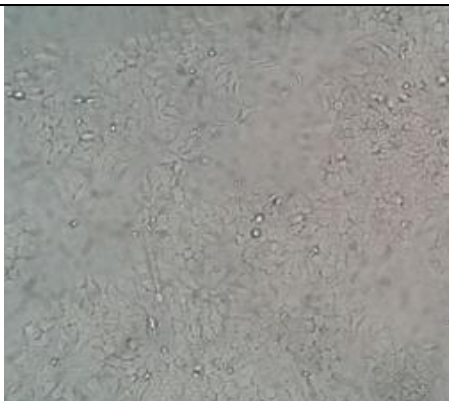
Depth (mm)	2.00- 4.00	5.00	8.00-10.00	15.00-17.00
Temperature ( $^{\circ}\text{C}$ )	37	32	32	31
Irradiation time (min)	1.85	2.66	2.41	3.87

At the end of the session; after 10.79 minutes the maximum recorded temperature was  $37^{\circ}\text{C}$  less than the temperature recorded for the rat skin, but almost the same as the abdomen muscle, this is expected since the muscles contain less chromophores.

## 5.5 Cancer cell line samples

Fe-Cr-Y source radiation was directed to cancer cell which caused a temperature increase in the media sample. To eliminate any chance that heat affected the media and changed its properties; a small experiment was done; an amount of RPMI media was exposed to irradiation by Fe-Cr-Y source for two days, each session was two hours, then it was used to grow a breast cancer sample name T-47D which was splitted into two plates one of them was used as a control which was grown in an untreated media and the other one was grown in the treated media. After 48 hrs of observations the results repealed any effect of heat on the media. See table 5.12.

**Table 5.12: Following up the development of culturing cancer cell line T-47D in treated media with IR irradiation**

	<b>Control plate</b>	<b>Treated plate</b>
<b>3<sup>d</sup> day of being cultured</b>		
<b>6<sup>th</sup> day of being cultured</b>		

### **5.5.1 First stage results:**

A group of cancer cell samples were examined out of the incubator environment in an open hood.

#### **5.5.1.1 MCF-7 cell line:**

On cultured plates specific areas were marked (position (**P**) 1, 2 and 3) in order to be monitored see Figure 5.38. Ten trials were done and each duration trial was  $\cong$  3.00 minutes for all readings and in between these trials the plate was returned back to the incubator for couple of minutes.

The temperature of the sample media before irradiation

was 30°C.

The results are summarized:

1. The average temperature of **P.1** was 32.75°C after 47:14 min.
2. The temperature of the lower area of **P.2** was 43.75°C after 29:28 min.
3. The temperature of the upper area of **P.3** was 49.84°C after 47:14 min.

After 24 hours the session was repeated.

The temperature of the sample before radiation was 26.09°C.

The results are summarized:

1. The average temperature of **P.1** was 28.42°C for 28 min.
2. The temperature of the upper area of P.3 was 42°C after 3 minutes.
3. The first 18 min. **P.2** was exposed directly to irradiation; its average temperature was only 38.45°C.



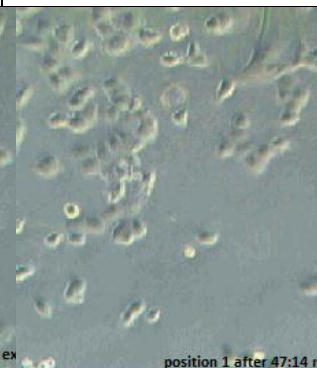
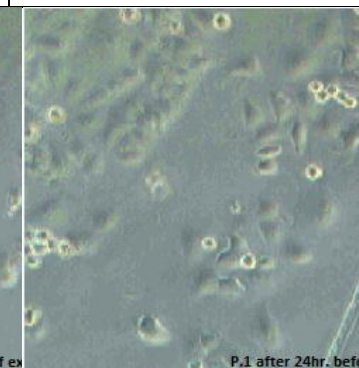
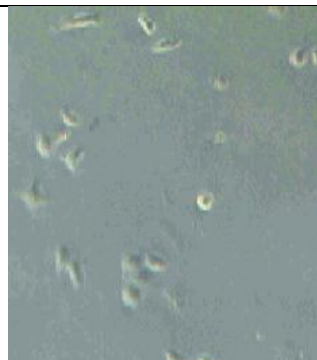
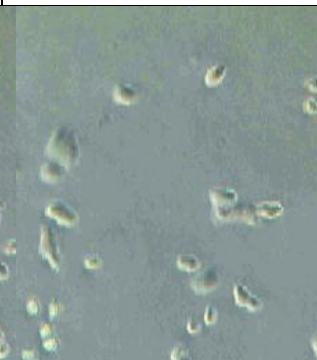
Figure 5.34: Marked 10cm cell culture dish

4. P.1 was repositioned after the first 28 min under the source directly for the next 9:32 min and the results are summarized in table 5.13.

**Table 5.13: temperature results of P1 after 2<sup>nd</sup>irradiation session. (P1 was positioned directly under the thermal source)**

40.59 C	3 min.
44.07 C	6 min
48.22 C	9 min

Photos were taken for different sessions and arranged in table 5.14.

	<b>Before 1<sup>st</sup> irradiation session</b>	<b>After 1<sup>st</sup> irradiation session</b>	<b>After 24 hrs. of 1<sup>st</sup> irradiation session</b>	<b>After 2<sup>nd</sup> irradiation session</b>
<b>Position 1</b>				
<b>Position 2</b>				

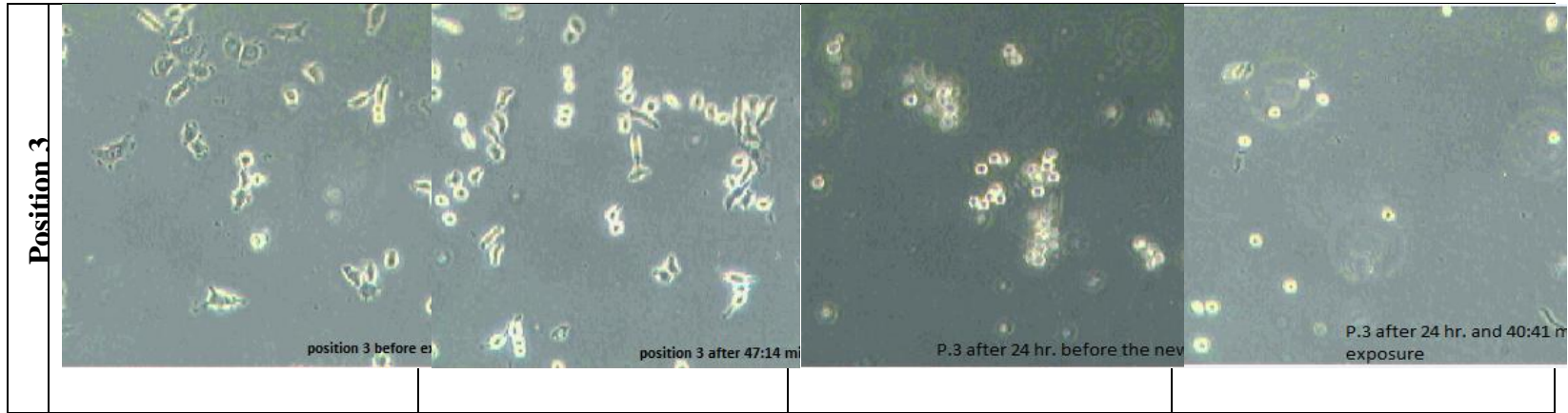


**Table 5.14: Photos of different areas of MCF-7 cell line that display IR radiation effect on them.**

Table 5.14 showed the changes that were caused by irradiating adenocarcinoma cell line sample with broad band Infrared radiation by Fe-Cr-Y source. First irradiation session; position 3 was directly beneath the source; which meant it was the closest one to the source radiation next to it positioned respectively; area 2 and 1; absorbed heat diffused through the sample media in a ascending pattern from position 3 to 1 (Kengne, Lakhssassi, and Vaillancourt, 2012), position 3 temperature was more than  $49^{\circ}\text{C}$  at the end of session 1 ( total radiation time was 47:14 min) and according to the taken photos by the inverted microscope there was no effect on the cell line in that area, it needed another 24 hours to show some effects. The breast cancer cells type is epithelial (ATCC, 2017), and epithelial cells have an adhesion dependent for survival (Martin and Leder, 2001), the cells were detached to the dish surface because of heat even though; this cannot be an evidence that the cell lines had a biological change on the contrary taken a look for all over the cultured plate indicated a growth in cells and a normal existence of death cells, it was mostly re-adhesion after while from returning it back to its suitable environment in the incubator and this is an advantage to the cancer cells (Martin and Leder, 2001; Liotta and Kohn, 2004). Heating showed that it is a potential technique for inhibition metastasis growth (Luk, Hulse, and Philips, 1980). According to Watanabe and Okada (1967) cancer cell cancer cultured in vitro in different temperature will go an exponential growth phase after several hours, so heating the samples media by IR radiation within small doses caused an increasing in the cells.

### **5.5.1.2 KHOS cell line:**

Two days of irradiation sessions by infrared radiation from Fe-Cr-Y source were done:

First day: The sample media temperature before irradiation was  $32^{\circ}\text{C}$ , four runs were done with a total duration of radiation 20 minutes each run was interspersed with a few minutes in the incubator to refresh the cell line.

1. Channel A: recorded an average temperature at the end of session  $30^{\circ}\text{C}$  with STDEV 1 and this temperature was less than the initial temperature.
2. Channel B: The average temperature that was recorded at the end of session was  $33^{\circ}\text{C}$  with STDEV 1 and this result did not exceed the initial temperature of the sample.

These results might be because the sample at first measurement was affected by the incubator temperature then its temperature begun to equalize with the environment temperature in the absence of an effective effect of heat yet from the IR source.

Second day: first thing to be measured was the sample media temperature before irradiation session which was  $33^{\circ}\text{C}$ . Five runs were done within a totally duration of radiation 30 minutes each run was interspersed with a few minutes in the incubator.

1. Channel A: recorded an average temperature  $31^{\circ}\text{C}$  with STDEV 1
2. Channel B: temperature increased markedly and achieved  $40^{\circ}\text{C}$  at the end of the session, its average temperature was  $37^{\circ}\text{C}$  with STDEV 3

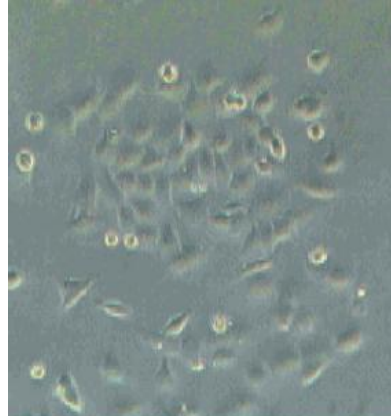
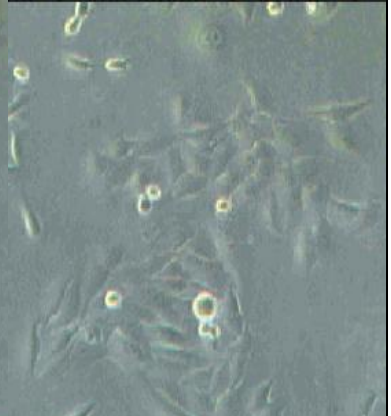
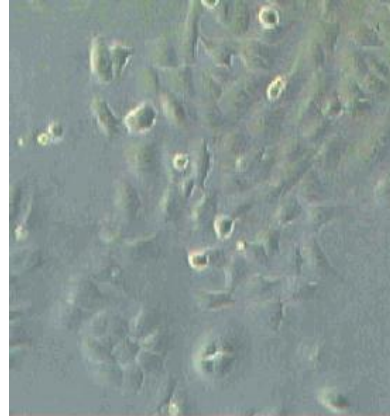
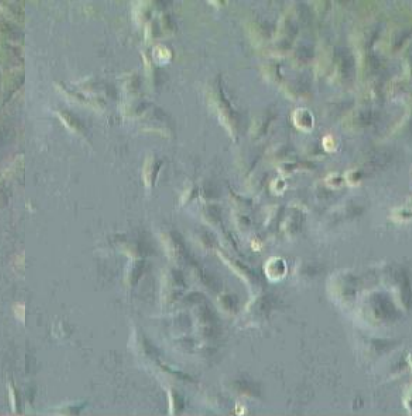
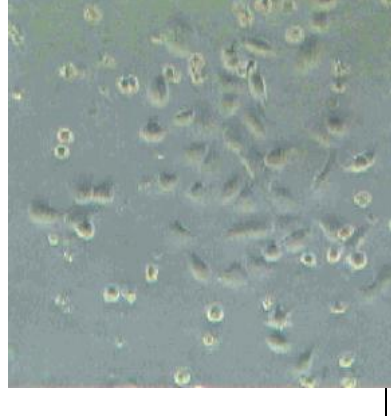
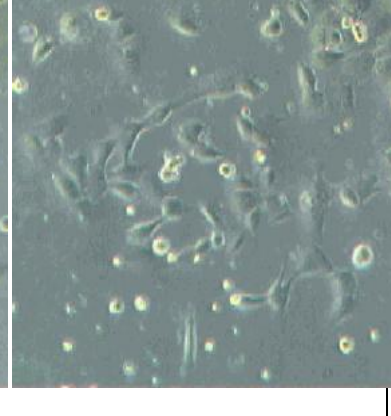
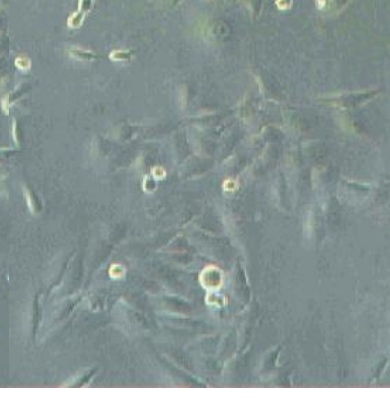
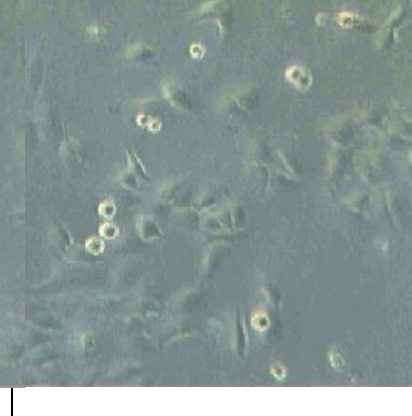
The results are summarized in table 5.15

**Table 5.15: Temperatures of two different places for bone cancer cell line.**

	Day 1		Day 2	
	Channel A	Channel B	Channel A	Channel B
Temperature of each run. ( $^{\circ}\text{C}$ )	32	32	30	33
	30	32	31	36
	29	33	32	37
	29	33	32	38
			32	40
Average temperature	30	33	31	37
STDEV	1	1	1	3

Note that Position A is farther than Position B from the emitter source.

**Table 5.16: Photos of different areas of KHOS cell line that display IR radiation effect on them.**

	<b>Before 1<sup>st</sup> irradiation session</b>	<b>After 1<sup>st</sup> irradiation session</b>	<b>After 24 hrs. of 1<sup>st</sup> irradiation session</b>	<b>After 2<sup>nd</sup> irradiation session</b>
<b>Position A</b>				
<b>Position B</b>				

It is clear that there was no effect on the cells and even more there was not enough heat to cause detachment of the cells and these results can be referred to short duration sessions.

In MCF-7 case first session duration was almost 50 minutes while KHOS duration session was 20 minutes only.

### 5.5.1.3 Caco-2 cell line:

Only one manually mobile thermocouple was used to probe 10 points temperature. The procedure was repeated 11 times first day and 6 times second day. The sample was exposed to the IR radiation to investigate the temperature distribution through the plate using marked points as shown in Figure 5.35. The pictured were taken by microscope revealed inhibition in Caco-2 cancer cell line compared to the control plate, but unfortunately this might not be due to the delivered heat from the thermal emitter, but from the long stay of the sample out of the incubator; total time radiation is 74.73 minutes. This problem was overcome by moving the whole set up into the incubator and this helped in eliminating the environment effect.



Figure5.35: a photo of colorectal adenocarcinoma cell line arrangement

Next tables (5.17 and 5.18) contain the results of two days of irradiation. Eleven trials were done first day, in each trial ten marked points 'or less than ten trials' temperature were measured, after each trial the sample was returned back to the incubator.

**Table 5.17: Average temperature results of 10 points grid marked on 10 cm cell culture dish 1<sup>st</sup> day irradiation session of Caco-2 cell line.**

		P.1	P.2	P.3	P.4	P.5	P.6	P.7	P.8	P.9	P.10	(min)
<b>Trial 1</b>	<sup>0</sup> C	31	31	30	31	30	30	31	31	30		Total time
	STD.	0	1	1	1	0	0	1	1	0		4.96
	Sec.	33.1	31.9	31.8	31.9	33	37.4	31.7	31.5	35.5		
<b>Trial 2</b>	<sup>0</sup> C	31	30	30	30	30	30	30	30	30	30	Total time
	STD.	1	0	1	1	1	1	1	1	1	1	5.59
	Sec.	27.2	31.7	34	29.5	56.2	35.1	33.6	31.9	31.6	24.6	
<b>Trial 3</b>	<sup>0</sup> C	31	30	31	30	30	30	30	31	30	30	Total time
	STD.	1	1	1	1	1	1	1	0	0	1	7.86
	Sec.	100	98.6	41.4	38.6	30.8	42	32	24.9	38.9	24.9	
<b>Trial 4</b>	<sup>0</sup> C	37	33	32	30	27	29	29	30	31		Total time
	STD.	4	1	1	1	1	1	1	1	1		7.96
	Sec.	47.6	67.4	50.4	48.2	34.5	61.4	47.3	62.9	57.6		
<b>Trial 5</b>	<sup>0</sup> C	36	33	32	31	29	29	29	28	29	28	Total time
	STD.	2	1	1	1	1	1	1	1	2	1	6.58
	Sec.	32.7	31.4	37.2	40.8	43.6	33.7	45.3	38.4	36.1	55.7	
<b>Trial 6</b>	<sup>0</sup> C	37	36	32	32	30	30	30	28	28	29	Total time
	STD.	3	2	1	1	1	1	1	1	1	1	6.77
	Sec.	29	41.2	28	33.5	49.1	51.8	48.4	38.6	44	42.5	

<b>Trial 7</b>	<sup>0</sup> C	36	34	32	32	29	30	29	29	28	30	Total time 5.94
	STD.	3	2	2	1	1	1	1	1	1	1	
	Sec.	26.6	30.6	36.6	40.9	34.1	34.9	32.3	40.8	38	41.7	
<b>Trial 8</b>	<sup>0</sup> C	33	33	32	31	30	30	30	29	29	29	Total time 9.23
	STD.	3	2	1	1	1	1	1	1	1	1	
	Sec.	63.6	49.7	52.9	56.3	55.5	63.9	40.1	46.2	80.4	45.6	
<b>Trial 9</b>	<sup>0</sup> C	37	36	31	31	30	30	29				Total time 8.18
	STD.	2	2	1	1	1	1	1				
	Sec.	48.5	50.3	42.4	55.8	50.6	51.5	192				
<b>Trial 10</b>	<sup>0</sup> C	34	32	32	32	32	31	31	32	31	31	Total time 7.34
	STD.	1	1	1	1	1	0	0	1	1	0	
	Sec.	32.9	41.4	45.5	48.1	55.1	40.2	44.7	41.6	44	47.1	
<b>Trial 11</b>	<sup>0</sup> C	32	32	32	32	31	32	32	32	32	32	Total time 4.33
	STD.	1	1	1	0	0	0	0	1	1	1	
	Sec.	27.1	23.4	26.3	24.4	24.9	26.3	25.3	26.3	27.7	28.1	

**Table 5.18: Average temperature results of 10 points marked on 10 cm cell culture dish  
2nd day irradiation session of Caco-2 cell line.**

		P.1	P.2	P.3	P.4	P.5	P.6	P.7	P.8	P.9	P.10	(min)
<b>Trial 1</b>	<sup>0</sup> C	36	33	32	30	29	30	28	28	27	28	Total time
	STD.	3	3	2	1	1	1	1	1	1	1	6.26
	Sec.	34.3	33.7	33.3	28.9	38.2	35.4	36.7	62.2	34.1	38.6	
<b>Trial 2</b>	<sup>0</sup> C	36	34	32	30	28	30	28	28	29	28	Total time
	STD.	1	2	1	1	1	1	0	1	1	1	6.00
	Sec.	27.5	31.6	34.7	32.8	40.7	34.3	48	49.6	30.4	30.6	
<b>Trial 3</b>	<sup>0</sup> C	35	32	31	30	29	29	28	27	26	28	Total time
	STD.	1	1	1	1	1	1	1	1	1	1	8.00
	Sec.	43.6	50.3	39.4	45.0	43.3	54.6	49.5	46.6	44.6	65.1	
<b>Trial 4</b>	<sup>0</sup> C	35	33	31	30	28	29	28	28	28	28	Total time
	STD.	1	2	1	1	1	1	1	1	1	1	8.88
	Sec.	41.9	50.8	51.0	58.4	72.2	55.1	51.9	48.4	58.4	44.5	
<b>Trial 5</b>	<sup>0</sup> C	36	36	32	31	30	30	29	29	28	30	Total time
	STD.	2	1	1	1	1	1	1	1	1	1	8.49
	Sec.	38.6	56.4	36.0	57.7	51.2	58.4	51.6	49.1	59.8	50.6	
<b>Trial 6</b>	<sup>0</sup> C	36	34	32	32	29	31	31	30	29	29	Total time
	STD.	2	2	1	1	1	1	1	1	1	1	7.10
	Sec.	31.6	43.1	46.6	35.8	45.9	51.0	46.4	35.1	51.1	39.6	

### **5.5.2 Second stage results:**

Since the plate's cover was removed inside the incubator for different durations of treatment; the effect of removing it was examined to eliminate any environmental effects inside the incubator on the cells growth other than heat; it was found that there was no effect of removing the plate's cover on the cells growth. Sample of T-47D cell line, which is a kind of breast cancer grown in RPMI media was splitted 1:2 one of them was used as a control, the plate cover was not taken off and the other one cover was taken off for about two hours within two days sessions.

#### **5.5.2.1 MCF-7 cell line:**

MCF-7 cell line first irradiation was on 19/2/2017: Sunday for 20 minutes. Its second irradiation was after 24 hrs for 14 minutes and the sample media temperature recorded was 39°C with STDEV 2°C. It took the sample more than 3 minutes to cool down to 31°C

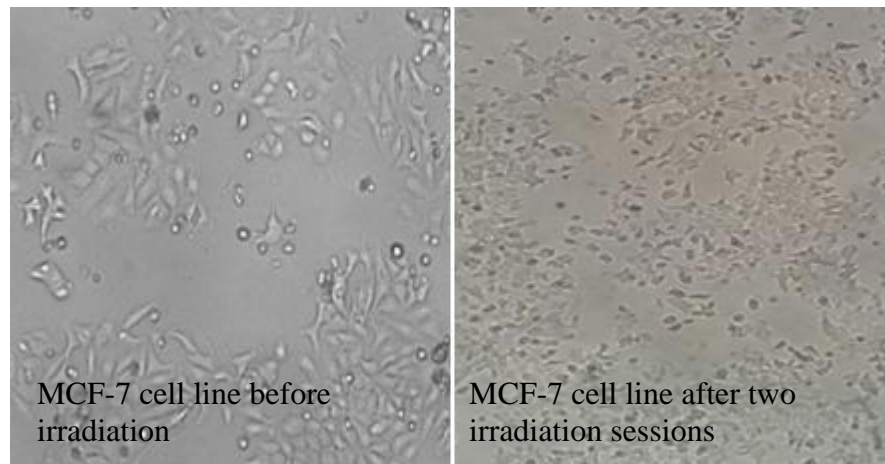


Figure 5.36: a photo of MCF-7 cell line before irradiation and at the end of sessions

### **5.6.2.2      MDA cell line:**

MDA name is adenocarcinoma (ATCC, 2017). Its first irradiation was on 20/2/2017: Monday for 16.00 minutes, its temperature reached 30°C. Its second irradiation was after 24 hrs for 15.00 minutes and the sample media temperature recorded was 37°C with STDEV 2°C. It took the sample more than 3.00 minutes to cool down to 31°C

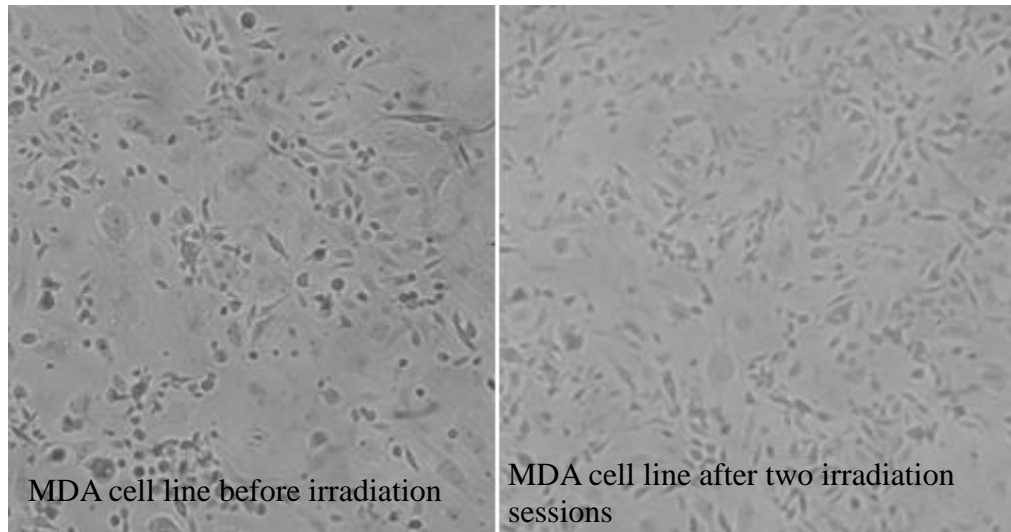


Figure 5.37: a photo of MDA cell line before irradiation and at the end of sessions

#### Another trial was done, where the session duration was longer

MDA was diluted 1:3 and the initial temperature of the media sample was 28°C inside the incubator and the procedure followed was:

- First exposure was for 2 hrs on Sunday 12/3/2017. At the end of the session; the probe under the source measured temperature 41°C and the other one measured temperature 38°C with STDEV for both equals 2°C.



Figure 5.38: a photo of untreated MDA cell line

- Second exposure was next day (after 24 hrs) also for 2 hrs on Monday 13/3/2017. At the end of the session; the probe under the source measured temperature 40°C and the other one measured temperature 37°C with STDEV for both 2

Observations by the lab technician were:

- After 24 hrs of radiation session 20% of the cells morphology was changed.
- After 48hrs it was clear that almost 80% of the cells morphology was changed.

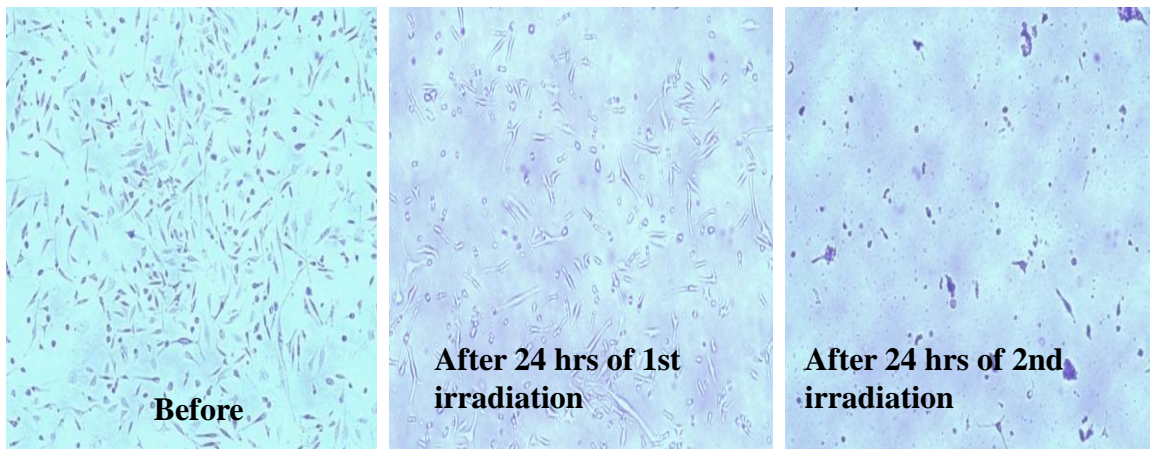


Figure 5.39: Photos of MDA cell line after 2 hrs sessions of irradiation two times

### 5.5.2.3 HT-29 cell line:

The followed procedures of HT-29 trials were done:

1. HT-29 was cultured on 28/2/2017 with percentage 1:5
2. One of them is denoted as a control plate which will not be treated.
3. Two plates were irradiated for 15.00 minutes; one of them was counted after 24 hrs of irradiation and the other was radiated twice and counted after 48 hrs.
4. Two plates were treated as the previous except for the duration session it was 30.00 minutes.

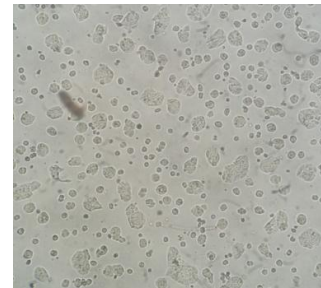


Figure 5.40: a photo of control colorectal adenocarcinoma cell line plate.

**Table 5.19: Results are summarized in the following table:**

	Plate A	Plate 2A		Plate B	Plate 2B		Control
Irradiation session NO.	First day	1 <sup>st</sup> day	2 <sup>nd</sup> day	First day	1 <sup>st</sup> day	2 <sup>nd</sup> day	

Duration session (min)	15.00	15.00		30.00	30.00	50.00	
Average Temperature (°C)	37	38		40	40	39	40
Counted living cells	407	-	714	507	-	690	598

It should be mentioned that plate 2B was irradiated for 50.00 min not 30.00 min in 2<sup>nd</sup> day.

The results were arranged in a flow chart, see Figure 5.41.

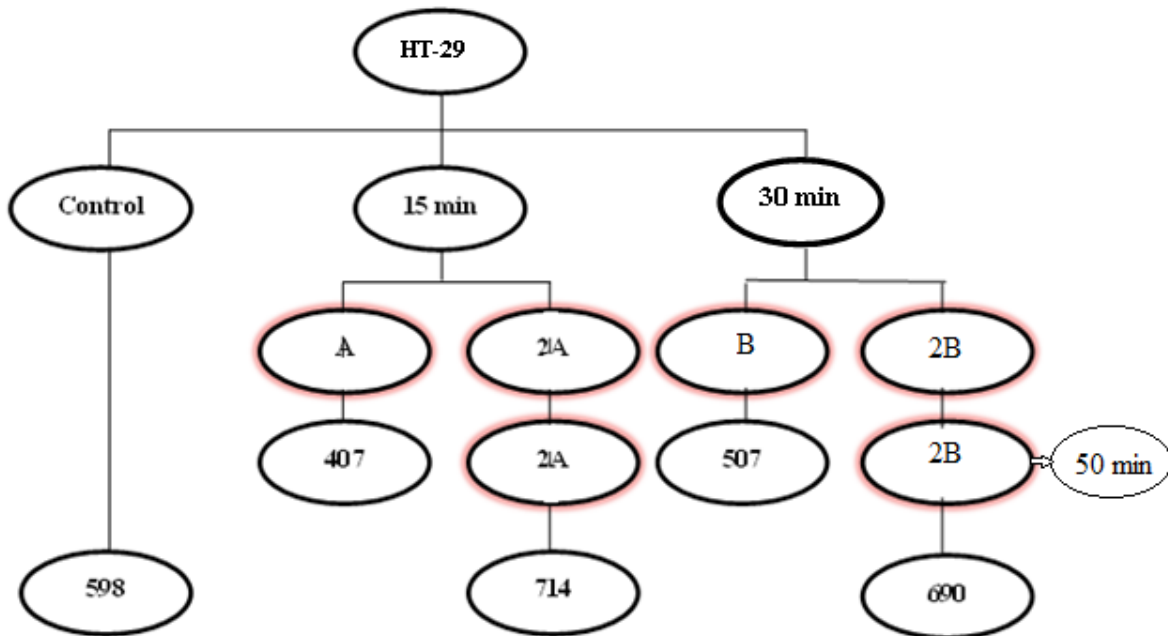


Figure 5.41: Flow chart summarizing the procedure of HT-29 trial.

Irradiating HT-29 by IR radiation for only 15.00 and 30.00 minutes only helped the cells to grow more than the cells cultured in the untreated plate which is the control plate.

#### **5.5.2.4      HCT-116 cell line:**

The followed procedures of HCT-116 trials were done:

1. HCT-116 was cultured on 19/3/2017 with percentage 1:5
2. One of them was denoted as a control plate which will not be treated.
3. Each treated plate was exposed to radiation for only one time, but for different duration and was counted after 24 hrs of irradiation.

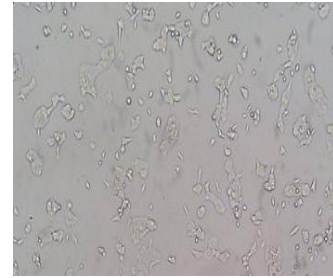


Figure 5.42: a photo of HCT-116 cell line

**Table 5.20: summarizes the procedures and the results HCT-116 cell line:**

Duration session	30 min	1 hr	2 hrs	2 hrs	Control
Average Temperature (°C)	38	38	36	36	
STDEV	1	1	2	2	
Counted living cell line	Unable to be counted (full)	447	416	Did not counted	Unable to be counted (full)

The results are shown in Flow chart form, see Figure 5.43.

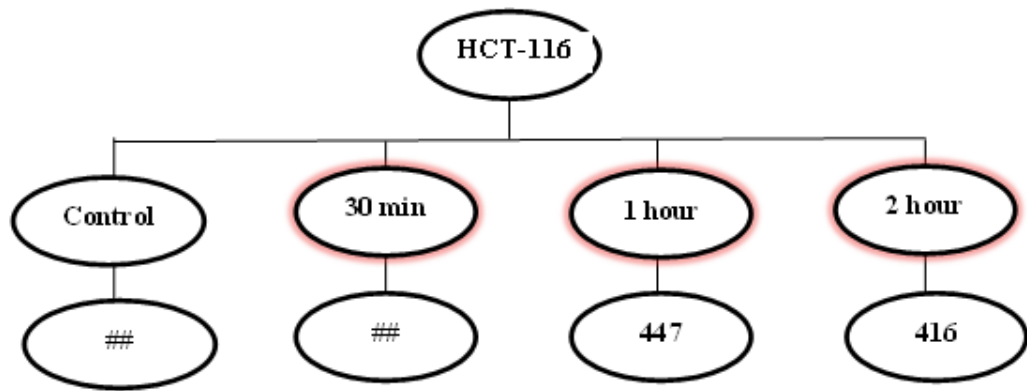


Figure 5.43: Flow chart summarizing the procedures and results of radiating HCT-116 cell line by IR radiation after 24 hours.

The second two hours radiated plate which was not counted; it was used to monitor the morphology change of the sample and kept for 72 hours. See Figure 5.44.



Figure 5.44: Photos show the changes in HCT-116 cell line after 2 hrs of irradiation

The pictures showed the inability of cancer cells to be recovered from the IR radiation intensity even after 72 hrs of radiation. 2 hrs radiations were enough to affect the growth of HCT-116 while 30.00 minutes of radiation helped the cell to accelerate their growth, see Figure 5.45.

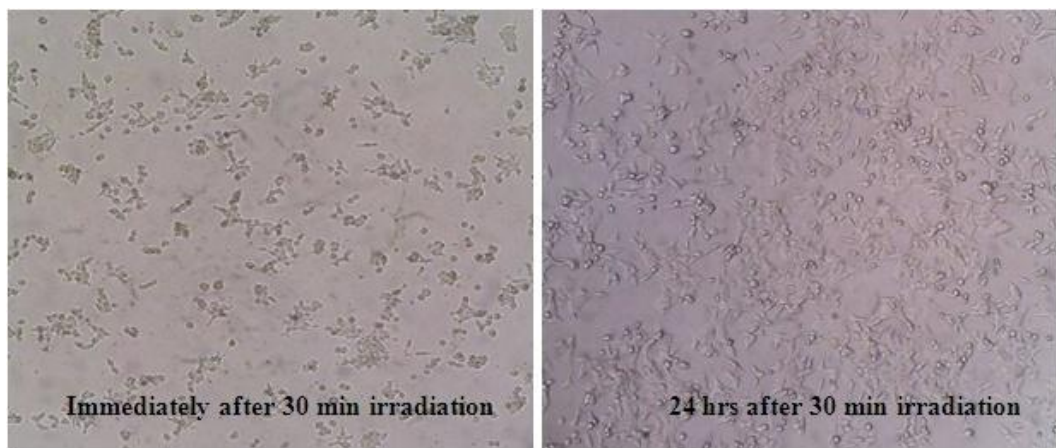
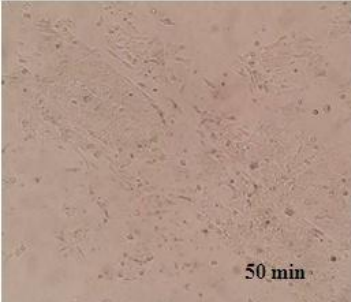
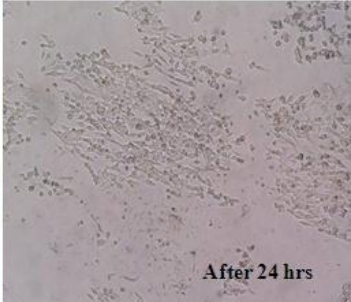
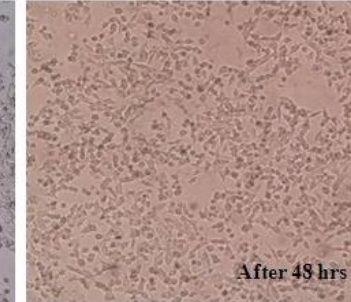
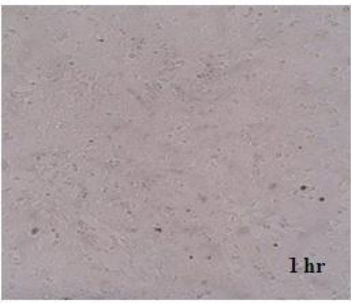
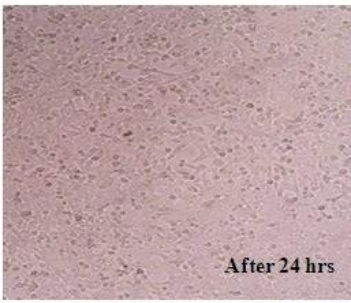
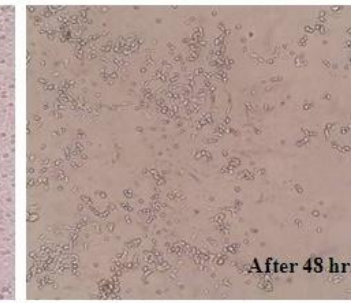
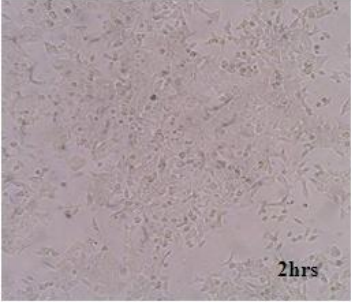
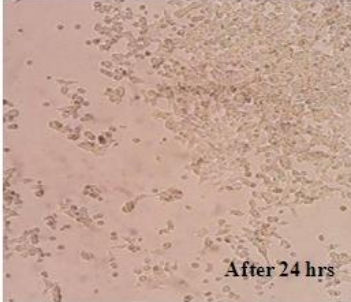
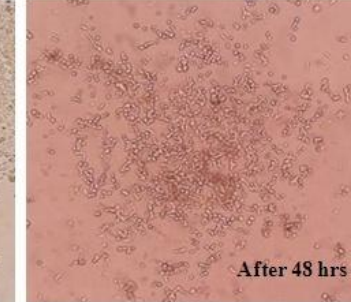


Figure 5.45: a photo of the change in HCT-116 cell line after duration 30 min of irradiation

It is can be noticed that the pictured area was filled by growing cell after 24 hrs of radiating it with IR radiation for 30.00 minutes.

For more observations another 3 plates of HCT-116 were irradiated by IR Fe-Cr-Y source for different duration sessions and pictured were taken. See table 5.21.

**Table 5.21: Following up the changes HCT-116 cell line growth after different IR radiation duration sessions.**

	Before irradiation	After 24 hours of irradiation	After 48 hours of irradiation
<b>50 min •</b>			
<b>1 hr</b>			
<b>2 hrs</b>			

## **Chapter 6**

### **Conclusions and Further work**

#### **6.1 Introduction**

This chapter summarizes the study project trials and the project development, and it includes suggestions of what can be done in the future.

#### **6.2 Conclusions**

Section 5.2 is an extension to Abu-Taha and co-workers (2013) about Miniature Infrared Sources for Spectroscopy Applications where the electrical circuit that is running the source is reused in this project for medical uses. Its intensity properties were compared with a well manufactured Bi-spiral IR source made in keel university 1997, the study proved the efficiency of the Fe-Cr-Y source. Also, there is a good possibility of creating different designed shapes. In section 5.3 the possibility of enhancing the IR radiation source in simple and inexpensive technique was studied; an aluminum waveguide tube, together with a hemispherical reflector and plane coated mirror were used in the study; the aluminum guide tube was used to deliver IR radiation efficiently to the wanted direction maintaining high radiation intensity, but in order to benefit from the back side of the source radiation a hemispherical reflector tool is the best choice. In section 5.4.1 sectioned biological samples were used to monitor their temperature during exposing them to IR radiation using Fe-Cr-Y source and Bi-spiral source, in this experiment Fe-Cr-Y source proved its ability to raise the tissue temperature more than the Bi-spiral source as shown in tables. Section 5.4.2 dealt with in vivo biological tissue of white rat's skin, abdomen muscle and thigh muscle. As discussed in the section the chromophores play the main rule in absorption IR radiation. Temperature distribution over tissue was in non-linear form and its value was greater for living tissue than dead tissue. Last section 5.5 in the results and discussion chapter; results of IR radiation effect of different cancer cell lines were presented. The same power of the source was used to irradiate different types of cancer cell lines but with different duration sessions, above 50

minutes radiation session with a power rate of 23 Watt shown suppression in the cell lines proliferation.

In conclusion a simple inexpensive IR source emitting in the range 700-15000 nm proved suitable to raise biological samples temperature. This indicates possible use to thermally kill cancer cells in tissue. This needs further work on some design and wider samples use.

### **6.3 Further work:**

The preliminary work with wideband IR absorption by a biological tissue proved successful. Further work is still needed in two parts of the work.

Firstly:

As for the IR source and its set up further design improvement is still needed to secure easy experimental measurement and data collection.

One of the main problems that faced the project is the source accessories:

1. The set up should be more compact; in order to overcome the environment intervention; the source, sample and thermocouple probes must be all in one closed unit.
2. The aluminum tube waveguide and the hemispherical reflector must be attached together in an easy way whenever it's needed to the source.
3. The interval duration (IV) of the pulse must be increased to reduce the thermal damage of the normal tissue.

Secondly:

The study has opened wide research areas in the field of IR absorption on biological samples; for example:

1. Using 3D cancer cell culture technique to investigate temperature distribution.
2. Exposing cancer cells planted into living mice to IR radiation.
3. Combining the radiations treatments with suitable drugs with different doses of IR radiation sessions.

4. Using IR radiation to study its effect in increasing the growth or inhibiting the growth of certain microorganisms, such as foot fungi.

## Appendices

### A: Bi-spiral source output depending on distance

	20-35 mm	40 mm	45 mm	50 mm	55 mm	60 mm	65 mm	70 mm	75 mm	80 mm	85 mm	90 mm	95 mm
10.24	8.12	7.04	5.36	4.31	3.55	2.97	2.55	2.22	2.00	1.80	1.60	1.53	
	8.13	7.07	5.44	4.37	3.51	2.95	2.52	2.26	2.01	1.77	1.62	1.50	
	8.14	7.00	5.42	4.31	3.52	2.95	2.48	2.22	1.98	1.75	1.65	1.51	
	8.12	7.00	5.42	4.37	3.53	2.99	2.53	2.23	1.92	1.76	1.66	1.51	
	8.16	7.00	5.33	4.36	3.53	3.01	2.55	2.22	1.98	1.78	1.60	1.50	
	8.17	7.06	5.46	4.33	3.54	3.00	2.52	2.25	1.92	1.79	1.61	1.54	
	8.20	7.01	5.48	4.32	3.53	3.02	2.54	2.22	2.01	1.78	1.60	1.52	
	8.20	7.04	5.40	4.34	3.50	2.95	2.56	2.23	1.97	1.79	1.66	1.54	
	8.18	7.03	5.41	4.35	3.51	2.97	2.54	2.24	1.99	1.76	1.65	1.52	
	8.15	6.99	5.41	4.37	3.51	2.99	2.55	2.22	1.97	1.79	1.65	1.55	
#DIV/0!	0.03	0.03	0.04	0.02	0.016	0.03	0.02	0.01	0.03	0.02	0.03	0.02	
average	10.24	8.16	7.03	5.41	4.34	3.52	2.98	2.530	2.23	1.98	1.78	1.63	1.52

100 mm	105 mm	110 mm	115 mm	120 mm	125 mm	130 mm	135 mm	140 mm	145 mm	150 mm	155 mm	160 mm	165 mm	170 mm	175 mm	180 mm	185 mm	190 mm
1.42	1.27	1.20	1.13	1.07	1.00	0.99	0.93	0.88	0.85	0.83	0.81	0.80	0.75	0.70	0.70	0.69	0.65	0.60
1.40	1.28	1.20	1.13	1.08	1.01	0.98	0.91	0.90	0.86	0.79	0.78	0.79	0.73	0.74	0.71	0.68	0.66	0.61
1.38	1.3	1.19	1.16	1.11	1.03	0.97	0.93	0.91	0.87	0.83	0.80	0.77	0.71	0.70	0.69	0.67	0.64	0.59
1.37	1.31	1.22	1.11	1.09	1.05	0.98	0.92	0.89	0.82	0.82	0.79	0.81	0.71	0.73	0.67	0.70	0.63	0.61
1.40	1.28	1.23	1.14	1.07	1.02	0.99	0.95	0.89	0.86	0.80	0.80	0.78	0.74	0.72	0.73	0.69	0.68	0.58
1.36	1.28	1.20	1.16	1.1	1.02	0.99	0.91	0.81	0.89	0.77	0.79	0.75	0.76	0.75	0.68	0.70	0.66	0.60
1.39	1.29	1.21	1.15	1.07	1.05	0.98	0.95	0.91	0.88	0.84	0.78	0.75	0.74	0.71	0.71	0.69	0.68	0.63
1.40	1.31	1.20	1.16	1.11	1.06	0.97	0.96	0.89	0.85	0.82	0.76	0.76	0.77	0.72	0.70	0.70	0.65	0.64
1.39	1.27	1.21	1.14	1.08	1.04	1.01	0.91	0.88	0.85	0.80	0.77	0.78	0.76	0.73	0.72	0.68	0.67	0.61
1.39	1.3	1.22	1.16	1.1	1.02	0.97	0.93	0.89	0.87	0.80	0.79	0.78	0.72	0.73	0.73	0.70	0.66	0.61
0.02	0.02	0.01	0.02	0.02	0.02	0.01	0.02	0.03	0.02	0.02	0.01	0.02	0.02	0.02	0.02	0.01	0.02	0.02
1.39	1.29	1.21	1.14	1.09	1.03	0.98	0.93	0.89	0.86	0.81	0.79	0.78	0.74	0.72	0.70	0.69	0.66	0.61

### B: Bi-spiral source output depending on current and frequency

20 Hz	19 Hz	18 Hz	17 Hz	16 Hz	15 Hz	14 Hz	13 Hz	12 Hz	11 Hz	10 Hz	9.1 Hz	frequency
3.3	3.2-3.3	3.2	3.1-3.2	3.0-3.1	2.9-3.0	2.7-2.9	2.4-2.6	2.4-2.2	2.1	1.9	1.7-1.8	current mA
3.30	3.25	3.20	3.15	3.05	2.95	2.80	2.50	2.30	2.10	1.90	1.75	(I) average mA
3.33	3.72	4.17	4.68	5.25	6.06	6.92	7.61	8.96	10.24	10.24	10.24	output (a.u)
3.40	3.78	4.16	4.73	5.29	6.04	6.96	7.74	9.06	9.99			
3.40	3.82	4.15	4.72	5.24	6.02	6.94	7.63	9.10	10.24			
3.40	3.82	4.16	4.70	5.27	6.00	6.93	7.66	8.92	10.23			
3.49	3.69	4.18	4.68	5.27	5.98	6.90	7.71	9.08	10.23			
3.33	3.72	4.20	4.68	5.30	6.02	6.97	7.67	9.09	10.24			
3.43	3.73	4.19	4.67	5.31	5.97	6.91	7.73	9.03	10.24			
3.41	3.74	4.20	4.69	5.20	6.04	6.99	7.73	8.95	10.16			
3.36	3.79	4.22	4.66	5.21	5.98	6.95	7.71	8.96	10.20			
3.41	3.74	4.20	4.67	5.27	5.97	6.90	7.84	8.98	10.18			
3.40	3.76	4.18	4.69	5.26	6.01	6.94	7.70	9.01	10.20			average
0.05	0.04	0.02	0.02	0.04	0.03	0.03	0.065	0.07	0.08	#DIV/0!	#DIV/0!	STDEV

### C: Fe-Cr-Y Source output depending on distance

150	145	140	135	132	112	92	62	42	32	22	12	2	distance (mm)	output (mV)
10.23	10.23	10.23	10.23	10.23	10.23	10.23	10.23	10.23	10.23	10.23	10.23	10.23	10.23	10.23
9.76	10.11	9.95	10.10											
10.05	10.04	10.01	10.20											
9.57	9.60	10.05	10.16											
9.90	10.00	10.06	10.17	10.23	10.23	10.23	10.23	10.23	10.23	10.23	10.23	10.23	10.23	10.23
0.29	0.27	0.12	0.06	#DIV/0!	STDEV									
215	210	205	200	195	190	185	185	180	170	165	160			
5.66	5.87	6.09	6.57	7.49	8.05	8.19	8.35	9.22	10.23	10.23	10.23			
5.33	5.70	6.06	7.09	7.97	8.32	8.13	8.78	9.23	9.77	10.10	9.92			
5.47	5.64	6.20	7.01	8.10	7.88	8.10	8.80	9.09	9.23	9.14	9.51			
5.57	5.76	6.03	6.70	7.45	7.91	8.43	8.27	9.00	9.71	9.54	9.89			
5.51	5.74	6.10	6.84	7.75	8.04	8.21	8.64	9.18	9.74	9.75	9.89			
0.14	0.10	0.07	0.25	0.33	0.20	0.15	0.28	0.11	0.41	0.51	0.29			

**D: Fe-Cr-Y Source output depending on degree**

Degree	output	Degree	output	56	10.23	326	10.23	Degree	output	Degree	output
0	10.23	26	10.23	58	10.23	328	10.23	296	10.14	270	3.03
2	10.23	28	10.23	60	10.23	330	10.23	298	10.16	272	3.11
4	10.23	30	10.23	62	10.23	332	10.23	300	10.23	274	3.46
6	10.23	32	10.23	64	10.23	334	10.23	302	10.23	276	4.16
8	10.23	34	10.23	66	10.23	336	10.23	304	10.23	278	4.27
10	10.23	36	10.23	68	10.23	338	10.23	306	10.23	280	5.24
12	10.23	38	10.23	70	10.23	340	10.23	308	10.23	282	6.53
14	10.23	40	10.23	72	10.1	342	10.23	310	10.23	284	7
16	10.23	42	10.23	74	10.02	344	10.23	312	10.23	286	7.93
18	10.23	44	10.23	76	10.06	346	10.23	314	10.23	288	9.92
20	10.23	46	10.23	78	9.94	348	10.23	316	10.23	290	10.05
22	10.23	48	10.23	80	8.575	350	10.23	318	10.23	292	10.06
24	10.23	50	10.23	82	7.85	352	10.23	320	10.23	294	10.1
52	10.23	82	7.85	88	4.27	322	10.23	356	10.23	86	5.29
54	10.23	84	7	90	3.46	324	10.23	358	10.23	360	10.23

## References

1. Abu-Taha, M.I, Buss, F., and Musameh, S. (2013). Some applications using simple low cost infrared light sources. *Materials Science*, 9(9), pp. 346-351.
2. Abu-Sharkh, S. (2015). Spectroscopic & Thermodynamic Investigations of the Physical Basis of Anhydrobiosis in *Caenorhabditis Elegans* Dauer Larvae. Ph.D. German: University of Dresden.
3. Abu-Rmeileh, N.E., Gianicolo, E., Brun, A. et al. (2016).Cancer mortality in the West Bank, Occupied Palestinian Territory.*BMC Public Health*, 16:76
4. Active forever.(2014). Far infrared heat therapy. [online]. Available at: <[https://www.activeforever.com/t/Press\\_Release\\_Far\\_Infrared\\_Heat](https://www.activeforever.com/t/Press_Release_Far_Infrared_Heat)>[Accessed at December 27, 2014]
5. Almeida-Lopes, L., Pretel, H., Moraes, V., et al. (2008). Effects of Continuous and Pulsed Infrared Laser Application on Bone Repair Using Different Energy Doses. Study in Rats. In: *International Conference of the World Association of Laser Therapy*. [online] Sun City, North West Province, South Africa: WALT, pp. 101-105. Available at: <http://www.biolase.com/medical/documents/bone-repair.pdf>
6. Al-Watban, F.A. and Zhang, X.Y. (2004). The Comparison of Effects between Pulsed and CW Lasers on Wound Healing. *Journal of Clinical Laser Medicine & Surgery*, 22(1), pp. 15–18.
7. Anderson R R. and Parrish J A. (1981). The Optics of Human Skin. *The Journal of Investigative Dermatology*, 70(1), pp. 13-19.
8. Ando, T., Xuan, W., Xu, T. et al. (2011). Comparison of Therapeutic Effects between Pulsed and Continuous Wave 810-nm Wavelength Laser Irradiation for Traumatic Brain Injury in Mice. *PLoS ONE*, 6(10): e26212

9. Azo materials, (2015). [online]. Available at: <[www.azom.com](http://www.azom.com)> [Accessed at June, 2016]
10. Banwell, C. N. (1972). *Fundamentals of molecular spectroscopy*, 2<sup>nd</sup> ed. McGraw-Hill.
11. BBC. (2014). Using the spectrum in medicine. [online]. Available at: <[http://www.bbc.co.uk/bitesize/standard/physics/health\\_physics/using\\_the\\_spectrum/revision/2/](http://www.bbc.co.uk/bitesize/standard/physics/health_physics/using_the_spectrum/revision/2/)>
12. Beckwith, T. and Lienhard, V.J. (1993). *Mechanical Measurements*. 5<sup>th</sup> ed. Prentice Hall. Available at: <<http://www.brighthubengineering.com>>. [Accessed at January 1, 2015]
13. Beever R. (2010). Do “Far-Infrared” Saunas have Cardiovascular Benefits in People with Type II Diabetes Mellitus? A Sequential Longitudinal Interrupted Time Series Design Study. [Online]. Available at: <<http://www.sunlighten.com/pdfs/Dr-Beever-Weight-Loss-Research.pdf>>
14. Biomedical research; in Infrared and Raman spectroscopy of BioSmart Technologies, (2014). *The History of Infrared & Infrared Technology*. [online]. Available at: <<http://www.biosmartsolutions.com/heaters/portable/history-infrared-infrared-technology>>. [Accessed December 30, 2014]
15. Buss, F. (2009). Miniature Infrared Sources for Spectroscopy Applications. M.Sc. Jerusalem: Al-Quds University.
16. Caltech. (2014). Basic concepts: Lecture #1. Available at: <<http://www.imss.caltech.edu/>> [accessed at December 31, 2014]
17. Chen, Sh., Lin Su., Lai, M. et al. (2013). Therapeutic Effects of Near-infrared Radiation on Chronic Neck Pain. *Journal of Experimental and Clinical Medicine*, 5(4), pp. 131-135.
18. Cheong, W., Prahl, S. and Welch, A. (1990). A review of Optical Properties of Biological Tissues. *IEEE Journal of Quantum Electronics*, 26(12), pp. 2166-2185
19. Colagar, A., Chaichi, M. and Khadjvand, T. (2011). Fourier transform infrared microspectroscopy as a diagnostic tool for distinguishing between normal and malignant human gastric tissue. *Journal Bioscience*, 36(4), pp. 669-677.

20. Da Silva, J., Queiroz, A., Oliveira, A. et al. (2017). *Frontiers in Bioenergy and Biofuels*. [ebook] In Tech. Available at: <<https://www.intechopen.com/books/frontiers-in-bioenergy-and-biofuels>>
21. Dash, M. and Selvi, S. (2013). Effectiveness of Infrared Rays on Wound Healing among Caesarean Section Mothers at Puducherry. *American Journal of Nursing Research*, 1(1), pp. 43-46.
22. Di Mario, F., Cavallaro, L.G., Cavestro, G.M. et al. (2006). Are there useful biomarkers for gastric cancer? *Digestive Liver Dis*, 38, pp. 308–309.
23. Duff, M. and Towey, J. (2010). Two Ways to Measure Temperature Using Thermocouples Feature Simplicity, Accuracy, and Flexibility. *Analog Dialogue*. 44(10)
24. Ezzati, A., Bayat, M. and Khoshvaghti, A. (2010). Low-level laser therapy with a pulsed infrared laser accelerates second-degree burn healing in rat: a clinical and microbiologic study. *Photomed Laser Surg*, 28(5), pp. 603-11.
25. Ezzati, A., Bayat, M., Taheri, S. et al. (2009). Low-level laser therapy with pulsed infrared laser accelerates third-degree burn healing process in rats. *Journal of Rehabilitation Research & Development*, 46(4), pp. 543–554.
26. Feinstein, (1990). Meas. Sc. Technol. 2:412. A source of information. In: Al-Jamal, A. (2007). Combined Photoacoustic and Photopyroelectric Detection. M. Sc. Palestine: Al-Quds University
27. Flammer, J., Mozaffarieh, M. and Bebie, H. (2013). *Basic sciences in Ophthalmology physics and chemistry*. [e-book] Springer. Ch2. Available at: <[www.springer.com](http://www.springer.com)>. [Accessed at November, 2014]
28. Fodor, L., Lucian, E. and Ullmann, Y. (2011). *Aesthetic Applications of Intense Pulsed Light*. [e-book] Springer. Ch2. Available at: <[www.springer.com](http://www.springer.com)>. [Accessed at November ,2014]
29. Hamamatus. Source of information. In: HAMAMATSU, (2004). Characteristics and use of Infrared detectors. [online]. Available at: [https://www.hamamatsu.com/resources/pdf/ssd/infrared\\_kird9001e.pdf](https://www.hamamatsu.com/resources/pdf/ssd/infrared_kird9001e.pdf) [ Accessed at December 2014]

30. Hashmi, J. T., Huang, Y., Sharma, S.K. et al. (2010). Effect of Pulsing in Low-Level Light Therapy. *Lasers surgery and medicine*, 42(6), pp. 450–466.
31. Hawrysz, D. and Sevick-Muraca, E. (2000). Developments Toward Diagnostic Breast Cancer Imaging Using Near\_Infrared Optical Measurements and Fluorescent Contrast Agents. *Neoplasia*, 2(5), pp. 388-417.
32. Heelspurs. (2015). [online]. *Skullbook*, ch.2. Available at: <<http://heelspurs.com/a/led/skullbook.pdf>> [accessed September 14, 2015]
33. Helguera, M. (2017). An Introduction to Ultrasound. Center for Imaging sciences. Biomedical and Materials Multimodal Imaging Laboratory. Rochester Institute of Technology. Available at: <https://www.cis.rit.edu/research/ultrasound/ultrasoundintro/ultraintro.html>
34. Henderson, T.A. and Morries, L.D. (2015). Near-infrared photonic energy penetration: can infrared phototherapy effectively reach the human brain?. *Neuropsychiatric Disease and Treatment*, 11, pp. 2191–2208.
35. Hildebrandt, B., Wust, P., Ahlers, O. et al. (2002). The cellular and molecular basis of hyperthermia. *Critical Reviews in Oncology/Hematology*, 43(1), pp. 33–56.
36. Hollis, V. (2002). Non-invasive Monitoring of Brain Tissue Temperature by Near-Infrared Spectroscopy. Ph.D. London: University of London.
37. Höningmann, H. (2013). History of phototherapy in dermatology. *Photochemical and Photobiological Sciences*, 12, pp.16-21.
38. Kalamida, D., Karagounis, I., Mitrakas, A. et al. et al. (2015). Fever-Range Hyperthermia vs. Hypothermia Effect on Cancer Cell Viability, Proliferation and HSP90 Expression. *Plos One*, 10(1): e0116021.
39. Kaur, P., Hurwitz,M.D., Krishnan, S. et al. (2011). Combined Hyperthermia and Radiotherapy for the Treatment of Cancer. *Cancers*, 3(4), pp. 3799-3823
40. Kemp William, (1987). *Organic spectroscopy*, 2<sup>nd</sup> ed. Macmillan.
41. Kengne, E., Lakhssassi, A. and Vaillancourt, R. (2012). Temperature Distributions for Regional Hypothermia Based on Nonlinear Bioheat Equation of Pennes Type: Dermis and Subcutaneous. *Applied Mathematics*, 3, pp. 217-224.

42. Keyes, R.J. (1980). *Optical and Infrared Detectors*. Springer .2<sup>nd</sup> ed. Springer-Verlag Berlin Heidleberg 1977
43. Khoshhesal, Z. (2012). *Reflectance IR Spectroscopy- Materials Science, Engineering and Technology*, ch 11. InTech. Iran.
44. Kim, S. and Jeong, S. (2014). Effects of temperature- dependent optical properties of the fluence rate and temperature of biological tissue during low-level laser therapy. *Lasers Med Sci*, 29(2), pp. 637-644.
45. Kimmitt, M.F., Walsh, J.E., Platt, C.L. et al. (1996). Infrared output from a compact high pressure arc source. *Infrared Physics and Technology*, 37(4), pp. 471-477.
46. Ku G., Fornage B., Jin X. et al. (2005). Thermoacoustic and Photoacoustic of Thick Biological Tissue Toward Breast Imaging. *Technology in Cancer Research & Treatment*, 4(5), 559-66.
47. Kurdi, S., Theerth, A. and Deva, S. (2014). Ketamine: Current applications in anesthesia, pain, and critical care. *Anesthesia Essays and Researcher*, 8(3), pp. 283-290
48. Laine, D.C., Al-Jourani, M. M., Carpenter, S. et al. (1997). Pulsed wideband IR thermal source. *IEE Proceedings - Optoelectronics*, 144(5), pp. 315 – 322.
49. Laine, D.C., and Abu-Taha, M. I. (1997). By private communications.
50. Lepock, J.R. (2003). Cellular effects of hyperthermia: relevance to the minimum dose for thermal damage. *International Journal of Hyperthermia*, 19(3), pp. 252-266.
51. Levine N. Ira, 1975. *Molecular spectroscopy*. A Wiley-inter science publication John Wiley and sons. A source of information. In: Fida M.B., (2009). *Miniature Infrared Sources for Spectroscopy Applications*. M.Sc. Jerusalem: Al-Quds University.
52. Lifepixel. (2014). [online]. *Digital Infrared Photography Primer*, ch.1. Available at: <<http://www.lifepixel.com/infrared-photography-primer>> [accessed December 30, 2014]
53. Luk, K., Hulse, R. and Phillips, T. (1980). Hyperthermia in Cancer Therapy. THE WESTERN Journal of Medicine, 132, pp. 179-185.
54. Marieb, E N. 1995. *Human Anatomy and Physiology*. 3<sup>d</sup> ed. Redwood City, California: enjamin/Cummings. Available at: Hollis, V. (2002). *Non-invasive Monitoring of Brain Tissue Temperature by Near-Infrared Spectroscopy*. Ph.D. London: University of London.

55. Matcher, S. J., Cope, M. and Delpy, D. T. (1997). In vivo measurements of the wavelength of tissue-scattering coefficients between 760 and 900 nm measured with time-resolved spectroscopy. *Applied optics*, 36(1). 386-396.
56. McDonnell, M. A., Wang, D., Khan, D. S. et al. (2003). Caspase-9 is activated in a cytochrome c-independent manner early during TNF $\alpha$ -induced apoptosis in murine cells. *Nature*. 10, pp. 1005–1015
57. Mehta, A. *Introduction to the Electromagnetic Spectrum and Spectroscopy*. [online] Pharmaxchange.info. Retrieved 2011-11-08. Available at: <<http://pharmaxchange.info/press/2011/08/introduction-to-the-electromagnetic-spectrum-and-spectroscopy/>>
58. Mise, K., Kan, N., Okino, T. et al. (1990). Effect of Heat Treatment on Tumor Cells and Antitumor Effector Cells. *Cancer Research*, 50(19), pp. 6199-6202
59. Mitsunaga, M., Nakajima, T., Sano, K. et al. (2012). Immediate in vivo target-specific cancer cell death after near infrared photoimmunotherapy. *BMC cancer*, 12:345.
60. National Cancer Institute. (2015). Available at: <<https://www.cancer.gov/>>
61. Naumann, D. (2001). FT-infrared and FT-raman spectroscopy in biomedical research. *Applied spectroscopy reviews*, 36(2&3), pp. 239-298
62. Niemz, H.M., (2004). *Laser-Tissue-Interactions*. 3<sup>d</sup>ed. Ch2. Springer
63. Obayashi, T., Funasaka, K., Ohno, E. et al. (2015). Treatment with near-infrared radiation promotes apoptosis in pancreatic cancer cells. *Onclogy Letters*, 10, pp. 1836-1840.
64. Okada, E., Schweiger, M., Arridge, S. et al. (1996). Experimental validation of Monte Carlo and finite-element methods for the estimation of the optical path length in inhomogeneous tissue. *Applied optics*, 35(19). 3362-3371.
65. Ott, T., Schossig, M., Norkus, V. et al. (2015). Efficient thermal infrared emitter with high radiant power. *Journal of sensors and sensor system*, 4, pp. 313-319.
66. Parker, F.S., (1971). Application of infrared spectroscopy in biochemistry, biology, and medicine, 18<sup>th</sup>ed. New York, Plenum Press.
67. Pidwirny, M. (2006). "The Nature of Radiation". *Fundamentals of Physical Geography*, 2<sup>nd</sup>ed.

68. Prentice, W.E. (2008). Arnheim's Principles of Athletic Training: a Competency Based Approach. New York. McGraw-Hill.
69. Putowski, M., Piróg, M., Podgórnak, M. et al. (2016). The use of electromagnetic radiation in the physiotherapy. *European Journal of Medical Technologies*, 2(11), pp. 53-58.
70. Richard, O., Rachael, C. and Zijuan L. (2014). *Infrared: theory* [online]. Available at: <[http://chemwiki.ucdavis.edu/Physical\\_Chemistry/Spectroscopy/Vibrational\\_Spectroscopy/Infrared\\_Spectroscopy/Infrared%3A\\_Theory](http://chemwiki.ucdavis.edu/Physical_Chemistry/Spectroscopy/Vibrational_Spectroscopy/Infrared_Spectroscopy/Infrared%3A_Theory)>.
71. Sankari, G., Aishuarya, T.S. and Gunasekaran, S. (2010). Fourier Transform Infrared Spectroscopy and Fluorescence emission spectroscopic investigations on Rat tissue. *Recent Research in Science and Technology*, 2(11), pp. 20-31
72. Sato, K., Choyke, P.L. and Kobayashi, H. (2014). Photoimmunotherapy of gastric cancer peritoneal carcinomatosis in a mouse model. *PLoS One*, 9(11) : e113276.
73. Sato, K., Hanaoka, H., Watanabe, R. et al. (2015). Near infrared photoimmunotherapy in the treatment of disseminated peritoneal ovarian cancer. *Molecular Cancer Therapeutics*, 14(1), pp. 141-150.
74. Scitec Instruments Ltd (2017)." Optics.org". [online]. Available at: <<http://optics.org/buyers/company/B000013176>>. [Accessed at April 17, 2017]
75. Shanthi, P. (2013). Experimental and Theoretical investigations of diffuse reflectance spectroscopy for non-invasive tissue characterization and diagnosis. [online] available at:<<http://hdl.handle.net/10603/10493>> [ Accessed at October, 2014]
76. Smith, I.T. (2002). The source issue in infrared micro spectroscopy,. Nuclear Instruments and Methods in Physics Research A483.565-570. A source of information. In: Buss, F., (2009). *Miniature Infrared Sources for Spectroscopy Applications*. M.Sc. Jerusalem: Al-Quds University.
77. Stadler, I., Lanzafame, R.J., Oskoui, P. et al. (2004). Alteration of Skin Temperature during Low-Level Laser Irradiation at 830 nm in a Mouse Model. *Photomedicine and Laser Surgery*, 22(3), pp. 227-231.

78. Tanaka, Y., Tatewaki, N., Nishida, H. et al. (2012). Non-thermal DNA damage of cancer cells using near-infrared irradiation. *Cancer science*, 103(8), pp.1467-73.
79. The International Commission on Non-Ionizing Radiation Protection (ICNIRP). "ICNIRP Statement on Far Infrared Radiation Protection". Health Physics Society. Retrieved 2011-02-12.A source of information. In: <[http://en.wikipedia.org/wiki/Heat\\_therapy](http://en.wikipedia.org/wiki/Heat_therapy)> [Accessed at November, 2014]
80. Tichauer, K. (2014). Photoimmunotherapy (PIT) busts open the doors for drug delivery. Available at: [http://www.osa.org/en-us/the\\_optical\\_society\\_blog/2014/february\\_2014/photoimmunotherapy\\_\(pit\)\\_busts\\_open\\_the\\_doors\\_for/](http://www.osa.org/en-us/the_optical_society_blog/2014/february_2014/photoimmunotherapy_(pit)_busts_open_the_doors_for/).
81. Wake, L. and Brady, R. (1993). Formulating infrared coatings for defense applications. DSTO Material Research laboratory. Australia
82. Watanabe, I. and Okada, S. (1967). Effects of temperature on growth rate of cultured mammalian cells. *The journal of cell biology*, 32, pp.309-323
83. Wiki. Wave number. Available at : <http://en.wikipedia.org/wiki/Wavenumber> [accessed at December 31, 2014]
84. William, K. (1987). *Organic spectroscopy*, 2<sup>nd</sup> ed. Macmillan.
85. Zahid, Y., Demetri, P., Michael, S.F. et al. (2008).Optical phase conjugation for turbidity suppression in biological samples. *Nature Research Journals*, 2, pp.110 – 115.
86. Zee, V. (2002). Heating the patient: a promising approach? *Annals of Oncology*, 13(8), pp. 1173–1184.

# دراسة عينات بيولوجية باستخدام الأشعة تحت الحمراء

إعداد: آية علي ابراهيم ذويب

إشراف: د. رشدي كتانه

أ. د. محمد أبو طه

## الملخص:

تقنيات الطب في وقتنا الحالي تطورت بشكل كبير إلا أنها ما زالت عاجزة أمام كثير من الأمراض والتي من بينها مرض السرطان، تنوّعه و حصانته ضد المضادات الحيوية و نموه السريع جعل السيطرة على المرض و علاجه صعباً، حتى في حالات العلاج فإن العلاج المستخدم تكون له أثار جانبية سلبية على صحة المريض أو قد يفقد المريض أجزاء من جسده ليتخلص من المرض وهذه الوسائل كلها مكلفة. توجه الطب الحديث في العقدين الماضيين نحو استراتيجية العلاج الموجّه محاولاً استهداف الخلايا السرطانية دون التأثير على الخلايا الطبيعية و الإبتعاد عن الطرق التقليدية في علاج السرطان ومن ضمنها استخدام الأشعة تحت الحمراء كمصدر مساعد أو كمصدر أساسى للعلاج ولكن كل هذه الطرق ما زالت قيد التجربة.

العثور على علاج غير مكلف للسرطان مع تأثير جانبي أقل هو الدافع لهذا المشروع. باستخدام مصدر متواوب للأشعة تحت الحمراء تم إنشاؤه في مختبر الفيزياء للبحث العلمي من مواد غير مكلفة (أبو طه، بص، مسامح. 2013) (الدائرة الكهربائية موضحة بالتفصيل في البحث) وإعادة استخدامه لدراسة مدى نجاحه ومدى تأثير الأشعة الحمراء على عينات بيولوجية مختلفة وهي: أنواع مختلفة من أنسجة جرذان بيضاء مقطعة و أخرى حية و أيضاً أنواع مختلفة من عينات خلايا سرطان تم زراعتها في مختبرات جامعة القدس.

النتائج الأولية كانت جيدة جداً و أشارت إلى كفاءة المصدر المتردد و نجاح تأثير الأشعة تحت الحمراء على العينات المستخدمة، فقد رفعت درجة حرارة بعض أنسجة الجرذ إلى 10 درجات مؤوية بحيث

سُجلت درجات حرارة أعلى من 40 درجة مئوية، أما بالنسبة للخلايا السرطانية فقد كبحت الحرارة من تسارع نمو الخلايا السرطانية و أدت إلى تغيير الشكل الخارجي لبعضها.

هذه النتائج الأولية تشير إلى إمكانية استخدام المصدر المتردد للأشعة تحت الحمراء واسعة النطاق المصنوع في مختبر البحث في المجال الطبي لتكون تقنية متحملة في علاج السرطان بتكلفة زهيدة.